1990

Identification And Characterization Of The Hexose Transporters In Rat L6 Myoblasts

Sui Rong Chen

NOTICE

The quality of this microform is heavily dependent upon the quality of the original thesis submitted for microfilming. Every effort has been made to ensure the highest quality of reproduction possible.

If pages are missing, contact the university which granted the degree.

Some pages may have indistinct print especially if the original pages were typed with a poor typewriter ribbon or if the university sent us an inferior photocopy.

Reproduction in full or in part of this microform is governed by the Canadian Copyright Act, R.S.C. 1970, c. C-30, and subsequent amendments.

AVIS

La qualité de cette microforme dépend grandement de la qualité de la thèse soumise au microfilmage. Nous avons tout fait pour assurer une qualité supérieure de reproduction.

S'il manque des pages, veuillez communiquer avec l'université qui a conféré le grade.

La qualité d'impression de certaines pages peut laisser à désirer, surtout si les pages originales ont été dactylographiées à l'aide d'un ruban usé ou si l'université nous a fait parvenir une photocopie de qualité inférieure.

La reproduction, même partielle, de cette microforme est soumise à la Loi canadienne sur le droit d'auteur, SRC 1970, c. C-30, et ses amendements subséquents.

IDENTIFICATION AND CHARACTERIZATION OF THE HEXOSE TRANSPORTERS IN RAT L6 MYOBLASTS

by

Sui Rong Chen

Department of Biochemistry

Submitted in partial fulfilment

of the requirements for the degree of

Doctor of Philosophy

Faculty of Graduate Studies

The University of Western Ontario

London, Ontario

December, 1989

ISBN 0-315-55314-6

ABSTRACT

Transport kinetic studies have demonstrated that two hexose transport systems are present in undifferentiated rat L6 myoblasts. These hexose transport systems were identified and characterized in this study using a number of different approaches. Cytochalasin B (CB), a potent inhibitor of hexose transport, was first used as a probe for these systems. CB binding studies with whole cells and membrane preparations revealed the presence of two distinct CB binding sites, CB_H and CB_L. They differ not only in their binding affinities, but also in their response to various biochemical, physiological and genetic manipulations. Based on the correlation between transport activity and the level of CB binding sites, CB_L and CB_H are thought to be associated with the high and low affinity hexose transport system (HAHT and LAHT), respectively. These CB binding components were further identified and characterized by CB photoaffinity labelling. Both mutant and glucose analogue inhibition studies suggested that the CB photolabelled components (40-60 kDa) were associated with both HAHT and LAHT. Proteolytic digestion studies indicated that the external surface of the hexose transporter was resistant to trypsin cleavage, and that the CB binding sites might be located on the cytoplasmic side of the hexose transporter. Immunoblotting studies of membrane preparations with specific antisera suggested that the 63 and 60 kDa polypeptides might be associated with HAHT and LAHT, respectively. Hexose transport mutants have proven to be indispensable in the identification and characterization of CB binding sites, CB photolabelled components and components recognized by specific antisera.

The effects of growth conditions and myogenic differentiation on hexose transport activity were also investigated. These studies revealed that the hexose transport systems were very sensitive to the growth conditions, and that myogenesis might result in the degradation or modification of HAHT.

ACKNOWLEDGEMENT

I would like to express my sincere appreciation to my supervisor, Dr. Ted Lo, for his friendship, guidance, encouragement and support during the course of this work. He is a great teacher and has taught me a valuable lesson. I would also like to thank my advisory committee, Dr. W. C. McMurray and Dr. I. G. Walker for their continual interest and helpful advice.

Thank-you to all the people of Dr. Lo's Lab, past and present, who helped and supported me over the years and made my stay in the Lab an enjoyable one. A special thanks goes to Dr. Doug Kuntz and Dr. Tony D'Amore. Trish Kudo also deserves a special thanks for her excellent proof reading on my thesis.

I would also like to thank all the staff of the Biochemistry Department for their friendship and encouragement. Special thanks goes to Mr. E. C. Jarvis, Mr. M. W. Green, Mrs. M. Coleman, Mrs. R. Webber and Miss. B. Green.

The financial support of the Muscular Dystrophy Association of Canada and the University of Western Ontario is gratefully acknowledged.

FOR LIN

TABLE OF CONTENTS

LIST OF TABLES

LIST OF FIGURES

NOMENCLATURE

α-GT	antiserum against the purified human rbc hexose transporter
α-IDIO	antiserum against the rabbit (anti-glucosamine) IgG
6-P	6-phosphate
AHDB-GlcN	6-N-(4-azido-2-hydroxyl-3,5-diiodobenzoyl)-D-glucosamine.
ATP	adenosine triphosphate
BCIP	5-bromo-4-chloro-3-indolyl phosphate
B_{max}	maximal number of binding sites
BrdUrd	5-bromo-2'-deoxyuridine
BSA	bovine serum albumin
cAMP	adenosine 3',5'-cyclic monophosphate
CB	cytochalasin B
CB_H	high affinity cytochalasin B binding site
CB_L	low affinity cytochalasin B binding site
CE	cytochalasin E
cPBS	complete phosphate-buffered saline containing 0.9 mM $CaCl_2$ and 0.5 mM $MgCl_2$, pH 7.4
dGlc	2-deoxy-D-glucose
DPM	disintegrations per minute
EDTA	ethylene diamine tetraacetic acid
EGTA	ethylene glycol tetraacetic acid
FDNB	1-fluoro-2,4-dinitrobenzene
FGF	fibroblast growth factor
HAHT	high affinity hexose transport system
HAHTer	transporter for HAHT
HDMF	high density microsomal fraction

HEPES	4-(2-hydroxyethyl)-1-piperazine-ethane sulfonic acid
HT	hexose transport
HTer	hexose transporter
IAPS-forskolin	3-iodo-4-azidophenethylamido-7-O-succinyldeacetylforskolin
IGFs	insulin-like growth factors
IgG	immunoglobulin G
IODO-GEN	1,3,4,6-tetrachloro-3α,6α-diphenylglycoluril
K_d	dissociation constant
kDa	kilodalton
K_i	inhibition constant
K_m	Michaelis-Menten constant
LAHT	low affinity hexose transport system
LAHTer	transporter for LAHT
LDMF	low density microsomal fraction
MeGlc	3-O-methyl-D-glucose
M_r	relative molecular mass
Na^+, K^+-ATPase	ouabain-insensitive Na^+, K^+-ATPase
NBMPR	6-[(4-nitrobenzyl)thiol]-9-ß-D-ribofuranosylpurine
NBT	nitro blue tetrazolium
NEM	N-ethylmaleimide
PAGE	polyacrylamide gel electrophoresis
PBS	phosphate-buffered saline (137 mM NaCl/2.7 mM KCl/ 8.1 mM Na_2HPO_4/1.5 mM KH_2PO_4, pH7.4)
pCMBS	p-chloromercuribenzenesulfonic acid
PMSF	phenylmethylsulfonyl fluoride
rbc	red blood cell

ß-ME	ß-mercaptoethanol
SDS	sodium dodecyl sulfate
TCA	trichloroacetic acid
TGF-ß	transforming growth factor-ß
TRIS	tris (hydroxymethyl) aminomethane
UV	ultraviolet
V_{max}	maximal rate

CHAPTER 1

INTRODUCTION

1.1 THE STRUCTURE AND FUNCTION OF BIOLOGICAL MEMBRANES

A considerable amount of biochemical research has been directed towards understanding biological membrane structure and function over the past decades. It is now generally recognized that membranes are dynamic biological systems, and a molecular understanding of their cellular functions is the key to elucidating various important biological events (Bohinski, 1987). Cell membranes or plasma membranes are found in all living cells; they separate the cell interior from the external environment, and give cells their individual integrity. Moreover, in mammalian cells, there are many other unique intracellular membranes which separate subcellular compartments, such as the nucleus, lysosome, mitochondria, smooth and rough endoplasmic reticulum, Golgi apparatus, etc. from the cytosol. These membranes are not static boundaries. They are also involved in important cellular functions, such as substrate translocation, cell-cell recognition and adhesion, differentiation, energy conversion processes, hormone-receptor action, communication between cells and their environment, the antigenic specificity of cell types, etc. (Stryer, 1988).

Biological membranes are composed primarily of proteins, lipids and carbohydrates. The ratio of protein to lipid varies considerably among different membranes, ranging from 1:4 to 4:1. While lipids comprise about 75% of the mass of the myelin membrane, proteins are the major component in the inner mitochondrial membrane, comprising about 75% of the mass of the membrane. Generally, about 40-60% of the mass of the plasma membranes is comprised of proteins. Carbohydrates, in the form of glycolipids and glycoproteins, account for

0.5-10% of the mass of a membrane (Guidotti, 1972).

The modern concept of membrane structure was first described over six decades ago by Gorter and Grendel (1925). To date the most accepted view of the ultrastructure of biological membranes is embodied in the Fluid Mosaic Model of Biological Membranes (Singer and Nicolson, 1972). According to this model, a membrane consists essentially of a two-dimensional matrix made up of a phospholipid and glycolipid bilayer, interrupted and coated by proteins. The lipid bilayer is viewed both as a highly selective permeability barrier and as a solvent for integral proteins. Specific protein-lipid interactions are thought to be essential for the functioning of some proteins. The components in the matrix are held together mainly by non-covalent forces among which the hydrophobic and hydrophilic interactions are most important in stabilizing the bilayer. Another important feature of this model is the ability of membrane proteins and lipids to move laterally within the plane of the lipid bilayer (lateral diffusion), unless they are restricted by specific interactions. On the other hand, movement across the membrane (transverse diffusion) occurs very slowly. This gives rise to two important properties of biological membranes, ie. fluidity and asymmetry. Membrane fluidity is controlled by fatty acid composition and by cholesterol level. Membrane fluidity is essential for the formation of functional distinct domains which is the critical step in hormone-receptor action, endocytosis, etc. (Le and Doyle, 1984). Compositional asymmetry gives rise to structural and functional asymmetry. The inner surface of the membrane is mainly associated with intracellular events, whereas the outer surface of the membrane is primarily associated with cellular communication (Stryer, 1988).

Although the membrane matrix is formed by lipids, the biological specificity of the cell membrane is primarily mediated by specific proteins interacting with the lipid bilayer. Membrane proteins can be generally classified as peripheral or

integral proteins, depending on their association with lipid bilayer (Le and Doyle, 1984). Peripheral proteins are usually associated with the hydrophilic surface of the lipid bilayer by ionic interaction with proteins or with the polar head group of phospholipids or by covalent or non-covalent interactions with oligosaccharide components of glycolipids or glycoproteins. They can be dissociated from the membrane by mild treatments, such as changes in ionic strength, heavy metals, etc. Peripheral proteins are soluble in a neutral aqueous buffer once they are released from the membrane. Some examples of these proteins are actin, spectrin and fibronectin. On the other hand, integral proteins are associated with the membrane by hydrophobic interaction. They can interact with the hydrophobic core of the lipid bilayer to a different extent. Dissociation of these proteins from membranes requires much more drastic treatments, such as the use of detergents and organic solvents. They are often highly insoluble in neutral aqueous buffer in the absence of detergents or lipids. Some examples of these proteins are glycophorin, hexose transporter (HTer) and various receptor proteins. Recently, a new class of membrane proteins referred to as the amphitropic proteins was proposed (Burn, 1988; Ferguson and Williams, 1988; Jennings, 1989). Amphitropic proteins are soluble cytoplasmic proteins that can interact covalently with specific lipids. They can exist either in a soluble cytoplasmic form or in a membrane bound form under appropriate conditions. These proteins are attached to the membrane via a specific lipid. Cleavage of the specific lipid from the proteins will result in their release from the cell membrane. They can be solubilized by removal of the bound lipids, or dissociation of the lipid bilayer. Some of the best studied amphitropic proteins include protein kinase C and cytoskeletal proteins, such as α-actinin, ankyrin and vinculin.

1.2 TYPES OF MEMBRANE TRANSPORT PROCESSES

The lipid bilayer is a highly impermeable barrier to most polar molecules. However, cells must take up essential nutrients, excrete metabolic wastes and regulate intracellular ion concentrations in order to grow and keep the internal environment relatively constant. To achieve these functions, cells have evolved a large variety of transport systems. Depending on the substance and the membrane involved, transport of molecules across a membrane may occur via one of the three general processes: passive transport, active transport or group translocation (Kaback, 1973). In passive transport, a substrate moves across a membrane from high concentration to low concentration. No metabolic energy is required. Depending on the involvement of membrane proteins, passive transport can be further classified into simple diffusion which occurs without any direct involvement of membrane proteins, and facilitated diffusion in which the substrate reacts reversibly with specific membrane protein(s). Some examples of simple diffusion are the transport of water or some lipid soluble substances. Hexose transport (HT) into human erythrocytes is a typical example of facilitated diffusion. In active transport, a substrate is accumulated against a concentration gradient. Specific membrane protein(s) and metabolic energy are required. Many amino acids and sugars are transported into bacteria via this mechanism. Group translocation is a process in which the transported substrate is chemically modified during the transport process. Such a process requires metabolic energy. An example of this type is the phosphoenolpyruvate phosphotransferase system in bacteria. In this system, sugar is transported across the membrane, and is simultaneously phosphorylated to form sugar phosphate (Postma and Lengeler, 1985).

1.3 HEXOSE TRANSPORT

1.3.1 Hexose Transport in Human Erythrocytes

Glucose is an important substrate for most types of cells. It is translocated across the membrane by a specific transport system. The existence of such a system was first recognized in human red blood cells by the observation that the kinetics of glucose movement across the cell membrane was very different from that predicted by Fick's law over five decades ago (Bang and Ørskov, 1937). It was later demonstrated that the movement of glucose across the membrane was saturable and specific, and had features incompatible with simple diffusion. This suggested the existence of a specific component involved in facilitating HT (LeFevre, 1948). Many detailed studies on the saturation kinetics, sugar specificity, inhibition and other aspects of the HT have since been reported (LeFevre, 1953, 1961; Miller, 1969; Barnett et al., 1973; Jung, 1973).

One of the interesting observations from these studies is the asymmetry of the human rbc HT system (Widdas, 1980). Different transport affinities were observed for efflux and influx (Batt and Schachter, 1973). The counterflow phenomenon (Rosenberg and Wilbrandt, 1957) in which the transport of one sugar is inhibited by a different concentration of another sugar across the membrane, demonstrated the necessity for at least two sugar binding sites in the transporter. Furthermore, glucose with alkyl groups at the C6 or C1 position inhibits transport only from one side of the membrane (Barnett et al., 1975). This suggests that the reaction with the external and internal sites of the transporter involves different ends of the glucose molecule. In addition, phloretin is more effective in inhibiting glucose efflux than influx (Wilbrandt, 1954). Cytochalasin B (CB), a fungal metabolite, also inhibits HT asymmetrically (Taverna and Langdon, 1973a; Bloch, 1973). More direct evidence of this asymmetric behaviour of the transport system comes from proteolytic digestion studies. Mild trypsinization of intact cells or

resealed right-side-out ghosts caused significant loss of membrane proteins, but retained the CB binding and HT activity (Jung and Rampal, 1977; Avruch et al., 1973; Carter et al., 1973). On the other hand, when trypsin was accessible to the inner surface of the membrane, CB binding was largely abolished. Thus, it seems there is structural as well as kinetic asymmetry in the human erythrocyte HT system. Based on transport kinetic studies, several kinetic models for the mechanism of HT in human rbc have been suggested, viz. the simple aggregate-rearrangement model (Singer, 1977), the carrier model (Regen and Morgan, 1964) and the alternating conformation model (Vidaver, 1966).

1.3.2 Identification and Isolation of Hexose Transporter

In order to understand the molecular mechanism of HT, it is essential to identify and to isolate the transport components. By far the best studied HTer is that of the human erythrocytes, which are readily available and highly pure membranes can be easily prepared. The chemical compositions and molecular structure of this membrane have also been well studied. Different approaches have been used to identify and to isolate the human rbc HTer. Some of the most widely used ones include membrane vesicle transport kinetics, specific binding, affinity labelling and reconstitution studies.

One of the earlier studies in identifying the human rbc HT system involved measuring transport activity of purified membrane vesicles. Highly purified, resealed ghosts were shown to have HT properties virtually identical to those of intact cells, in spite of the rather drastic alteration in membrane structure (Jung, 1971). Removal of peripheral proteins (such as bands 1, 2, 5, and 6) from human rbc ghosts by alkaline (pH 11.5) treatment had no effect on HT. This suggested that these peripheral proteins were not involved in HT (Zoccoli and Lienhard, 1977).

Affinity labels have been used to identify membrane receptors and transporters. Sugar derivatives, transport inhibitors and protein modifying reagents

are the most widely used affinity labels. For example, a 100 kDa protein in human rbc plasma membrane was found to be covalently labelled by glucosyl isothiocyanate (Taverna and Langdon, 1973b) and by maltosyl isothiocyanate (MITC) (Mullins and L' ngdon, 1980). The incorporation of both glucosyl isothiocyanate and MITC could be inhibited by D-glucose or CB. In addition, a broad band centred around 55 kDa was differentially labelled by impermeable maleimide in the presence and absence of glucose or CB (Batt et al., 1976). A similar polypeptide was also labelled by 1-fluoro-2,4 dinitrobenzene (FDNB) (Lienhard et al., 1977; Shanahan and Jacquez, 1978; Jung and Carlson, 1975).

The best studied affinity label for HTer is CB. It is a potent inhibitor of HT (Taverna and Langdon, 1973a). It binds to the HTer very tightly, with a dissociation constant around 10 M. Three classes of CB binding sites with different affinities have been detected in human rbc plasma membrane (Jung and Rampal, 1977). Only the high affinity CB binding site (site 1) was inhibited by D-glucose (Pinkofsky et al., 1978). Kinetic and proteolytic digestion studies revealed that site I is accessible from the inner surface of the membrane (Basketter and Widdas, 1977; Jung and Rampal, 1977). The high affinity CB binding c' .ponent was further purified and identified as a major broad band in the band 4.5 region (Sogin and Hinkle, 1978; Baldwin et al., 1979). This suggests that band 4.5 may be involved in HT. The molecular mechanism by which CB inhibits HT is currently not clear. Both non-competitive and competitive inhibition mechanisms have been suggested (Taverna and Langdon, 1973a; Taylor and Gagenja, 1975). Upon irradiation with intensive UV light, CB is covalently linked to the band 4.5 region (40-70 kDa) of human erythrocyte plasma membrane (Carter-Su et al., 1982; Shanahan, 1982). The reaction is inhibited by high concentrations of D-glucose, but not by L-glucose. Recently, the same region (band 4.5) has also been labelled by forskolin, an activator of adenylate cyclase (Seamon et al., 1981) and also an

inhibitor of HT (Shanahan et al., 1987; Sergeant and Kim, 1985). The above studies showed that the HTer in human erythrocytes was likely to be associated with band 3 and/or band 4.5 region(s). It was suggested that the 55 kDa polypeptide might be a proteolytic fragment of higher molecular weight components, such as band 3 (Phutrakul and Jones, 1979; Mullins and Langdon, 1980). However, recent studies have shown that this is not the case. Antibodies raised against the solated 55 kDa polypeptide only recognized a broad band centred at 55 kDa, indicating that the 55 kDa polypeptide was not a fragment from some native higher molecular weight proteins (Baldwin and Lienhard, 1980; Sogin and Hinkle, 1980).

Another approach to identify the human erythrocyte HTer involves solubilization and isolation of the membrane components, incorporation of these solubilized membrane components into an artificial phospholipid bilayer, such as liposome or planar lipid bilayer, and followed by measurement of specific transport or binding activity. It was found that sonicated soybean phospholipid liposome reconstituted with erythrocyte membrane protein fractions exhibited stereospecific uptake of D-glucose (Kasahara and Hinkle, 1976, 1977). This transport process was inhibited by CB, phloretin, $HgCl_2$ and other HT inhibitors. The active fraction was further separated in SDS-PAGE, and a broad band centred at 55 kDa (band 4.5) was identified in a Coomassie-blue-stained SDS polyacrylamide gel. However, a 100 kDa polypeptide (band 3) was also identified using a similar reconstitution technique (Shelton and Langdon, 1983). Some of the major problems with the reconstitution studies are the low specific activity, contamination and irreproducibility. Only about 1% of the transport rate by intact erythrocytes was observed with the purified, reconstituted band 4.5 protein (Kasahara and Hinkle, 1977; Baldwin et al., 1981).

1.3.3. Structure and Function of Hexose Transporter

CB binding. CB photolabelling and immunoblotting studies revealed that the

human rbc HTer was heterogeneously glycosylated and migrated as a very broad band (40-70 kDa) on SDS-PAGE (Wang, 1987). Treatment of the HTer with endoglycosidases gives rise to a more discrete band of about 46 kDa (Gorga et al., 1979). This protein is a transmembrane protein, with an extracellular domain resistant to proteolysis and a cytoplasmic domain susceptible to trypsin cleavage (Baldwin et al., 1980). The CB binding site and the antibody-binding sites for most of the available antisera are located on the cytoplasmic side of the membrane (Davies et al., 1987; Cairns et al., 1984; Haspel et al., 1985).

Recent molecular cloning studies have greatly advanced the understanding of the structure and function of the HTer. Using a rabbit polyclonal anti-(human rbc HTer) antibody, a full length cDNA clone for the HTer was isolated from the HepG2 expression library, and sequenced (Mueckler et al., 1985). The identity of the cDNA clone was further confirmed by structural analysis of the purified human erythrocyte HTer. These studies also demonstrated that the HepG2 and erythrocyte HTers are highly homologous.

A diagrammatic representation of the membrane disposition model of the HTer is shown in Fig 1.1 (from Mueckler et al., 1985). Based on the hydropathy analysis of the amino acid sequence deduced from the nucleotide sequence of the cDNA clone, it was proposed that this protein of 492 amino acids (54,117 dalton) might cross the membrane 12 times in the form of largely hydrophobic α-helices. Several of these membrane spanning domains contained hydroxy and amide side chains which could be involved in the formation of either a glucose binding site or a pore through the membrane. The model also indicates there is a large hydrophilic domain located on the cytoplasmic side of the membrane and a smaller exofacial domain containing the carbohydrate moiety. Both the amino and carboxyl termini are predicted to be on the cytoplasmic side of the membrane. This model has at least partially been confirmed by the vectorial proteolytic digestion studies.

Fig. 1.1 Schematic Representation of the Membrane Disposition Model for the Hexose Transporter as Proposed by Mueckler et al. (1985).

The 12 putative membrane-spanning domains are shown as numbered rectangles. The single-letters within the putative membrane-spanning domains (rectangles) indicate the uncharged polar residues; H, histidine; N, asparagine; Q, glutamine; S, serine and T, threonine. Circled (+) and (-) signs denote acidic (Glu, Asp) and basic (Lys, Arg) amino acid residues, respectively. The position of the N-linked oligosaccharide is predicted at Asn 45 and shown as a "tree". The arrows indicate the position of known trypsin cleavage sites in the native erythrocyte HTer. T indicates the trypsin cleavage site.

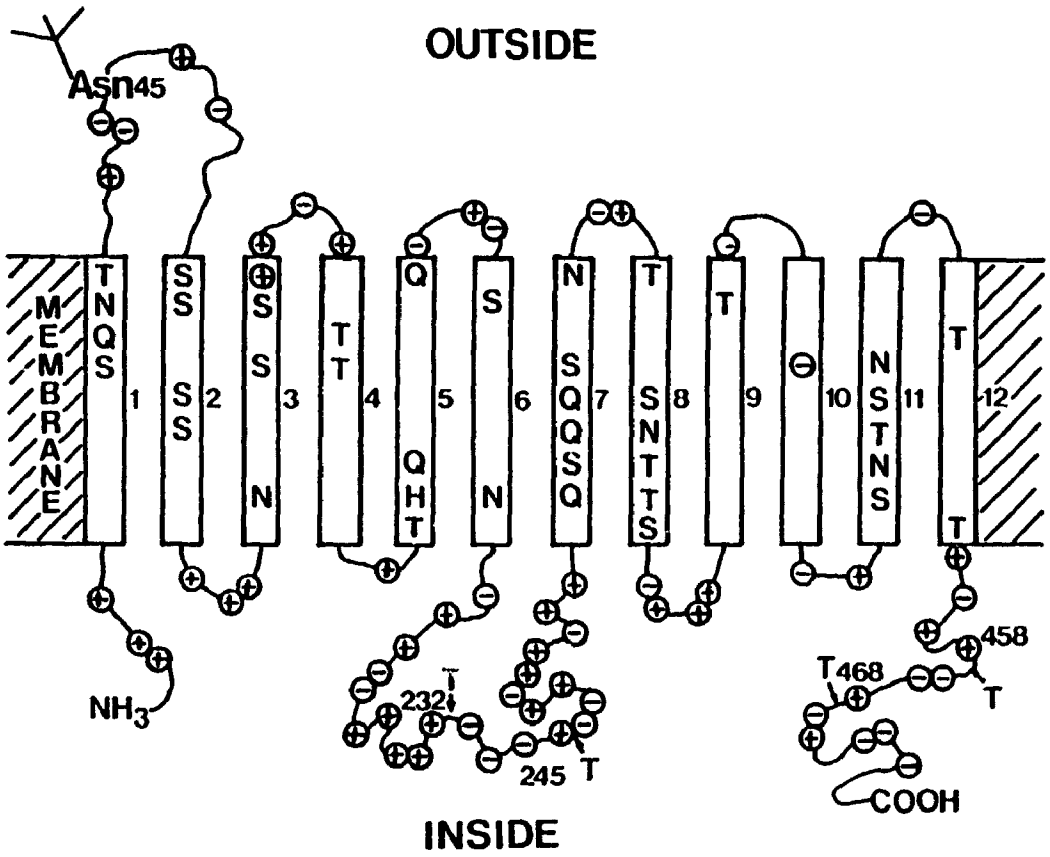
OUTSIDE
Asn45
MEMBRANE
TNQS 1
SS SS 2
SS N 3
TT 4
Q QHT 5
S N 6
N SQQSQ 7
T SNTTS 8
T 9
10
NSTNS 11
T T 12
NH3
T232i
245 T
T468
458
T
COOH
INSIDE

There are no trypsin cleavable sites exposed on the exofacial surface of the membrane. This is in agreement with the finding that trypsin only acts on the cytoplasmic portion of the transporter.

1.3.4 Hexose Transporters of Other Mammalian Cells

HTers in other mammalian cells have also been identified by CB binding, CB photolabelling and by anti-(human rbc HTer) antibodies. HTers in the following types of cells have been identified: rat adipocytes (Lienhard et al., 1982; Shanahan et al., 1982), chick embryo fibroblasts (Pessin et al., 1982; Salter et al., 1982), murine fibroblasts (Haspel et al., 1986), skeletal muscle (Klip et al., 1983b), human fibroblasts (Horner et al., 1987), human placenta (Ingermann et al., 1983; Johnson and Smith, 1982), rat brain (Birnbaum et al., 1986) and rat heart (Wheeler, 1988). In most cases, they have molecular weights ranging from 40-60 kDa.

The HTers in mammalian cells are found to be tissue specific. Using anti-(human rbc HTer) antibodies, the distribution of HTer-like proteins in various cells and tissues has been examined (Haspel et al., 1985; Wadzinski et al., 1987, 1988; Wang, 1987). The anti-(human rbc HTer) antibody was found to cross-react differentially with HTer-like proteins in different cells or tissues. The cross-reactivity with HTer-like proteins in rat brain is 5-10 times higher than those in skeletal muscle and adipocytes. HTer-like proteins in fetal rat erythrocytes and adult kidney were found to be highly heterogeneous; they migrated as a broad band (40-70 kDa) on SDS-PAGE. On the other hand, HTer-like proteins in adult rat brain, diaphragm, adipocytes and skeletal muscle were more homogeneous, appearing as a discrete band (40-60 kDa) on SDS-PAGE (Wang, 1987). Treatment with endoglycosidases changed the electrophoretic mobilities of HTer-like proteins in fetal rat erythrocytes, but not in rat brain, murine fibroblasts and human fibroblasts (Wang, 1987; Horner et al., 1987; Haspel et al., 1986).

Another interesting observation is that more than one form of HTer-like

proteins is present in some cells. In rat adipocytes, two ^{3}H-CB photolabelled components with isoelectric points of 5.6 and 6.4 were found in the low density microsomal fraction (LDMF), whereas only one component with an isoelectric point of 5.6 was observed in the plasma membrane (Horuk et al., 1986). The distribution of these components between the plasma membrane and LDMF was affected by insulin. Two ^{3}H-CB photolabelled components (52 and 46 kDa) were also observed in chick embryo fibroblasts (Pessin et al., 1984). The labelling of these components was elevated by glucose starvation. In addition, antibodies directed against synthetic peptides corresponding to sequences deduced from the cDNA of both the human hepatoma HepG2 and rat brain HTers did not recognize all of the CB photolabelled components in rat adipocytes. This suggests the presence of different types of HTer-like proteins in these cells (Oka et al., 1988).

Aside from HepG2 expression library, cDNA clones for the HTer have also been isolated from other expression libraries, such as rat brain (Birnbaum et al., 1986), liver (Fukumoto et al., 1988), adipocytes and heart (James et al., 1989). Using these cDNA clones, the levels of the HTer mRNA were found to vary considerably from tissue to tissue (Mueckler et al., 1985; Birnbaum et al., 1986; Flier et al., 1987; Fukumoto et al., 1988; Thorens et al., 1988; James et al., 1989). For example, while the mRNA encoding for the HepG2 HTer was abundant in rat brain, kidney and several other tissues, it was present in low levels in rat adult liver, adipose tissues, skeletal muscle and human small intestine (Birnbaum et al., 1986; Flier et al., 1987; Fukumoto et al., 1988; Kayano et al., 1988). At least three distinct types of mRNAs encoding for HTer-like proteins are thought to be present in mammalian cells. One type is found in the HepG2 cells and rat brain. The second is present in the liver and kidney. The third is expressed in adipocytes, heart and skeletal muscle. Some tissues contain more than one type of HTer mRNAs. Thus it seems likely that there is a family of structurally related HTer-

like proteins in mammalian cells (Kayano et al., 1988).

A question that arises from the above observations concerns the identity of these HTer-like proteins. A comparison of the sequences of HTer-like proteins in different tissues revealed that approximately 40% of the amino acid residues were identical (Fukumoto et al., 1988). It should also be pointed out that there was a 40% sequence homology between the human rbc HTer and the arabinose-H^+ symporters of Escherichia coli (Maiden et al., 1987; Baldwin and Henderson, 1989). Thus, while there is increasing evidence that a family of HTer-like proteins may exist in mammalian cells (Kayano et al., 1988), it is not certain whether all of these proteins are indeed involved in HT. The most convincing proof of the identity of the cDNA clone came from the observation that the HepG2 gene encoding for the human rbc HTer could be expressed functionally in Escherichia coli (Sarkar et al., 1988). However, few such studies on the identity of cDNA clone have been reported.

1.3.5 Regulation of Hexose Transport

Considerable efforts have also been focused on the regulation of transport, especially on the insulin-mediated activation of HT. Two mechanisms, conceptually, could give rise to a stimulation of HT by insulin. One involves an increase in the number of functional transporters in the plasma membrane; whereas the other suggests a change or modulation of the intrinsic activity of the transporter. Based on the CB binding and reconstitution studies, two groups have independently proposed that insulin stimulates the translocation of intracellular HTers to the plasma membrane (recruitment hypothesis) (Suzuki and Kono, 1980; Cushman and Wardzala, 1980). However, the mechanism by which insulin modulates the translocation of the transporters to the plasma membrane is still unknown. Recently, changes in the intrinsic activity of the HTer by insulin have also been reported (Whitesell and Abumrad, 1985; Kahn and Cushman, 1987; Joost et al.,

1988). There is increasing evidence to suggest that the insulin-mediated stimulation of HT may involve both mechanisms, ie. changes in the intrinsic transport activity and also in the number of the transporters on the plasma membrane.

1.4 RAT L6 MYOBLASTS

While HT and its regulation by insulin in muscle have been studied for over four decades (Lundsgaard, 1939; Levine et al., 1949), the most often studied insulin-sensitive HT system is that of adipose tissue. This is probably because homogeneous adipose cells can be readily prepared, whereas there are many technical difficulties in getting good muscle samples or in perfusion studies (Morgen et al., 1964). It is also difficult to perform quantitative transport studies with pieces of tissues. Primary cultures or permanent cell lines were found to serve as powerful tools in studying muscle HT. Aside from the time required for their isolation from tissues, primary cultures are often contaminated by other cell types. Reproducibility between different isolates is often problematic. Furthermore, primary cultures have only a very limited life span. This makes the isolation and characterization of mutants difficult. The use of a permanent cell line has several advantages. The population of cells is very homogeneous, as there are no contaminating cell types. The cell line can be maintained in the laboratory for an extended period, which is essential for mutant analysis. Mutants offer a unique and useful means for identifying and characterizing transport systems.

The Rat L6 myoblast cell line is a permanent cell line, originally isolated by Yaffe (1968) from rat embryonic skeletal muscle. It has widely been used as a model system to study muscle differentiation. During myogenesis, both morphological and biochemical differentiation occur. In morphological differentiation, mononucleated myoblasts proliferate, align, differentiate and fuse to form multinucleated myotubes. In biochemical differentiation, the synthesis of muscle specific proteins, such as creatine phosphokinase, acetylcholine receptors,

skeletal muscle myosin, actin etc. is elevated (Sanwal, 1979). Down regulation of the synthesis of other proteins has also been observed (Devlin and Emerson, 1978).

The molecular mechanism of myogenesis is still a subject of intense investigation. Several important events are thought to be involved. These include cell-cell recognition and adhesion, cessation of DNA synthesis, synthesis of mRNA for muscle-specific proteins and membrane fusion (Wakelam, 1985; Pearson, 1981; Medford et al., 1983; Jaynes et al., 1986). A large number of factors and culture conditions have been found to affect myogenic differentiation. Growth factors, such as FGF and TGF-ß were found to inhibit differentiation; whereas IGFs stimulated the process of differentiation (Florini and Magri, 1989). Agents, such as phorbol esters and bromodeoxyuridine, also inhibit fusion (Cohen et al., 1977; Rogers et al., 1975). Such differentiation inhibitors, stimulators and culture conditions have proven to be useful probes for studying various biochemical and morphological changes during myogenic differentiation.

1.5 OBJECTIVES

One of the main objectives of research in our laboratory is to elucidate the molecular mechanism and regulation of the HT systems in myoblasts. Previous transport kinetic studies revealed that two HT systems are present in undifferentiated rat L6 myoblasts. They differ in their transport affinity, substrate specificity, responses to various biochemical, physiological and genetic manipulations (Table 1.1). It was the long range goal of this research to understand the structure and function of these HTers. More specifically, my project was to identify and to characterize the HTers in rat L6 myoblasts; and to examine the regulation of HT during myogenesis.

As indicated earlier, while many HTer-like proteins have been identified in mammalian cells, only a few of them have been shown to be indeed involved in

Table 1.1 Properties of the Two Hexose Transport Systems in Rat L6 Myoblasts

(1) High Affinity Hexose Transport System (HAHT)
(a) K_m = 0.6 mM
(b) Responsible for the uptake of 2-deoxyglucose and D-glucose
(c) An active transport process
(d) Sensitive to sulfhydryl reagents
(e) Derepressed in glucose-starved cells
(f) Defective in transport mutants
(2) Low Affinity Hexose Transport System (LAHT)
(a) K_m = 3.6 mM
(b) 3-OMG is the preferred substrate
(c) Facilitated diffusion
(d) Insensitive to sulfhydryl reagents
(e) Not affected by glucose-starvation
(f) Not altered in transport mutants

HT. In the light of this observation, we believed that HT mutants would serve as a useful tool in identifying HTers.

Based on its high binding affinity and binding specificity, an attempt was made to use ^{3}H-CB as an affinity ligand for identifying the transporter. We started our CB binding studies with whole cells. These studies allowed us to compare the transport and Cb binding properties directly and to obtain a general perspective of the transport systems. A comparison of CB binding properties of whole cells and of purified membrane fractions provided valuable information on the effects of various cellular metabolites and other aspects of the transport systems. After establishing a specific and efficient binding assay, the binding properties and effects of glucose analogues and glucose starvation on the CB binding in a mutant and its parental cells were subsequently determined (Chapter 2). Purified membrane preparations from a transport mutant and its parental cells demonstrated the location and distribution of the transport components and effects of substrate metabolites on CB binding. We have also determined the binding properties and effects of glucose analogues and proteolysis on CB binding (Chapter 3). Further identification of the HTer was carried out by CB photolabelling studies with both whole cells and membrane fractions prepared from transport mutants and their parental L6 cells (Chapter 4).

Another approach to identify the HTer was to use antisera raised against the purified human HTer and against the rabbit anti-glucosamine IgG. The rationale for using anti-idiotypic antibodies (second antibody) was that these antibodies should recognize the antigen binding site (or idiotype) of the first IgG molecule which was raised against a specific ligand. Thus, the antigen binding site of these anti-idiotypic antibodies would constitute an internal image of the specific ligand. It follows that these anti-idiotypic antibodies should also recognize the ligand binding site of the proteins. Attempts were made to identify proteins that cross-

reacted with the anti-(human rbc HTer) and/or anti-(rabbit anti-glucosamine IgG) antibodies by immunoblotting studies (Chapter 5). In these experiments, both whole cells and purified membrane preparations from the HT mutant and its parental L6 cells were used.

Another aspect of our research involved the regulation of HT. A review of the literature revealed that most of the HT studies were carried out in either myoblasts or myotubes. Little is known about the regulation of the transport systems during myogenic differentiation. Thus, the objective of this final phase of the study was to gain some understanding of how these HT systems responded to myogenic differentiation (Chapter 6). These studies may also shed some light on the physiological roles of these two transport systems.

CHAPTER 2

CYTOCHALASIN B AS A PROBE FOR THE TWO HEXOSE TRANSPORT SYSTEMS IN UNDIFFERENTIATED RAT L6 MYOBLASTS

I. WHOLE CELL STUDIES

2.1 INTRODUCTION

HT has been characterized in a variety of eukaryotic cells (Baldwin and Lienhard, 1981; Olefsky, 1978; Czech, 1976a,b,; Pessin et al., 1982; Griffin et al., 1982). An examination of the transport affinity, substrate specificity and sensitivity to sulfhydryl reagents reveals that more than one HT system may be operating in these cells. For example, two HT systems are detected in chick embryo fibroblasts (Christopher et al., 1976a,b; Pessin et al., 1984), rat adipocytes (Olefsky, 1978; Foley et al., 1980), and mouse 3T3 cells (Colby and Romano, 1975). A number of affinity ligands have been used to identify the HTers. These range from monoclonal antibodies to a variety of sugar analogues (Weber and Eichholz, 1985; Allard and Lienhard, 1985; Taverna and Langdon, 1973a,b; Lin and Spudich, 1974; Fannin et al., 1981; Kay, 1985). Of these, cytochalasin B (CB) is the best characterized reagent (Czech, 1976a,b). It is a very specific and potent inhibitor of HT in human erythrocytes, adipocytes, and chick embryo fibroblasts (Pessin et al., 1982; Czech, 1976a,b). Although it binds to three different sites in human rbc and in rat adipose cells (Lin and Spudich 1974; Czech, 1976b, Jung and Rampal, 1977, Wardzala et al., 1978; Carter-Su and Okamoto, 1985), only one site is sensitive to the HT substrates, while the other two sites can be blocked by cytochalasin E (CE). The hexose-sensitive CB binding site is therefore thought to be associated with the HTer.

A combination of biochemical and genetic approaches was recently used to examine HT in undifferentiated rat L6 myoblasts (D'Amore and Lo, 1986a,b,c;

D'Amore et al., 1986a,b; Klip et al., 1982). Kinetic studies with whole cells revealed the presence of two HT systems with different transport affinities and specificities (D'Amore and Lo, 1986a,b; D'Amore et al., 1986a,b). D-glucose and 2-deoxy-D-glucose (dGlc) are transported preferentially by the high affinity hexose transport system (HAHT), whereas 3-O-methyl-D-glucose (MeGlc) is transported primarily by the low affinity hexose transport system (LAHT) (Table 1.1). Similar to chick embryo fibroblasts, HAHT is sensitive to low concentrations of sulfhydryl reagents, whereas LAHT is not (Christopher et al., 1976b; D'Amore and Lo, 1986b). HAHT also differs from LAHT in its dependence on membrane electrical potential (Table 1.1). Plasma membrane vesicle studies also show that D-glucose and dGlc are transported against a concentration gradient, whereas MeGlc only equilibrates across the plasma membrane (D'Amore and Lo, 1986a; Cheung and Lo, 1984). These two systems also differ in their response to glucose starvation (D'Amore and Lo, 1986a; D'Amore et al., 1986a). Finally, mutants defective only in HAHT have been isolated, thus suggesting that the transporters may be coded by different genes (D'Amore et al., 1986b) (Table 1.1). This study presents our attempts in establishing the relationship between the CB binding sites and the HT systems.

2.2 MATERIALS AND METHODS

2.2.1 Materials

2-Deoxy-D-[2,6-^{3}H]-glucose (38.7 Ci/mmol), 3-O-[1-^{3}H]methyl-D-glucose (2.1 Ci/mmol) and [4-^{3}H(n)]-cytochalasin B (15.5 Ci/mmol) were purchased from Amersham Canada Ltd. ^{3}H-D-glucose was from New England Nuclear. Scinti Verse E was from Fisher Scientific Co. Cytochalasins, glucose analogues, transport inhibitors and other chemicals were from Sigma Chemical Co. All chemicals were obtained from commercial sources and were of the highest available purity.

2.2.2 Cell Lines and Culture Media

Yaffe's L6 rat skeletal myoblast line (Yaffe, 1968) was maintained in Alpha medium (Flow Laboratories) supplemented with 10% horse serum (Flow Laboratories) and 50 μg/ml of gentamycin (Gibco) as previously described (Lo and Duronio, 1984a,b). Transfers were routinely made every three days (prior to fusion) using 0.1% trypsin to detach cells from plates. The glucose starvation medium (or referred to as the fructose medium) was comprised of essentially the same ingredients, except that glucose was replaced with 0.1% fructose, and the horse serum was previously dialysed extensively against complete phosphate buffered saline (cPBS).

2.2.3 Whole Cell Transport Assay

Transport assays were carried out as described previously (Lo and Duronio, 1984a,b) with minor modifications. Unless otherwise stated, cells were grown for two days in six-well Costar plates (35 x 15 mm), seeded with 1 x 10^5 cells. Medium was aspirated and each well was washed with 10 ml of cPBS. 900 μl of the uptake buffer (cPBS containing 1 mg/ml bovine serum albumin) was added to each well. Transport studies were carried out at 23 °C and were initiated by the addition of 100 μl of the radioactive substrate. At appropriate times, the uptake was terminated by washing the cells rapidly (less than 15 sec.) twice with 10 ml ice cold cPBS. In the case of MeGlc uptake, washes were always with cold cPBS containing 1 mM mercuric chloride to prevent sugar efflux. Unless otherwise stated, 1 min. uptake assays were performed; samples were taken at 15, 30, 45 and 60 sec. after the addition of the radioactive substrates. The effect of CB was tested by simultaneous addition of CB with the radioactive substrate. Cells were solubilized in 1 ml of 0.1% Triton X-100; 0.8 ml aliquots were counted in 10 ml of scintillation fluid. Two wells on each plate were trypsinized and used to determine the average cell number per well. Background radioactivities were determined by adding 10 mM

D-glucose, and were subtracted from the crude data.

2.2.4 CB Binding Assay by the Oil Phase Separation Method

The oil phase separation method is actually a modification of the method used by Klip (Klip et al., 1982) in studying hexose uptake in L6 cell suspension. Cells were grown on tissue culture dishes (20 x 140 mm) in the glucose or fructose medium, and harvested before reaching confluence. After dissociation from each plate by incubating with 5 ml citrate saline (134 mM KCl, 15 mM trisodium citrate, pH 7.8) at 37 °C for 15-20 min., cells were pelleted by centrifugation at 1000 x g for 5 min. The cell pellet was suspended in cPBS at a density of 2 x 10^7/cells/ml, and kept at 4 °C to minimize cell damage. Just before the binding assay, cells were incubated at 37 °C for 5 min.; 100 μl of this suspension was then incubated with an equal volume of cPBS containing ^{3}H-CB (0.01 - 2.5 μM), and 10 μM CE for 6 min. at 37 °C. Sugar analogues or inhibitors were included in this binding buffer whenever necessary. The sugar concentration in the binding buffer was adjusted to 0.6 M with sorbitol. The reaction mixture was then transferred to an Eppendorf micro test tube containing 1 ml dibutyl phthalate and centrifuged immediately at 4 °C for 2 min. The cell pellet was separated from the unbound ^{3}H-CB by the oil phase separation method. After carefully aspirating off the liquid, the cell pellet was solubilized in 100 μl 0.5 M NaOH for 4 hrs or longer, and counted in 10 ml scintillation fluid supplemented with 0.7% of glacial acetic acid. Background radioactivities for each assay were determined by adding unlabelled CB (10 μM) or phloretin (0.5 mM). In order to determine the response of specific CB binding sites to D-glucose, the latter was not included in the background radioactivity determinations. A detailed examination of the effect of D-glucose on CB binding is presented in Chapter 3. All CB binding was carried out in duplicate. Each experiment was repeated two or three times. Unless otherwise stated, figures show results of representative experiments, and background counts have been

subtracted from the crude data. The above procedures provide quite reproducible data.

2.2.5 CB Binding Assay by the Filtration Method

The conditions and reaction mixture for the ^{3}H-CB binding assay were similar to those described above. Instead of separating the free ^{3}H-CB by centrifugation, the reaction mixture was filtered immediately through a 0.4 μm polycarbonate membrane (Biorad) which was then washed three times with 2 ml ice cold cPBS. The filters were dried, dissolved, and counted in scintillation fluid.

2.2.6 Measurement of Intracellular Free Sugar and Sugar Phosphate

Intracellular free sugar and sugar phosphate were determined as previously described (D'Amore and Lo, 1986a), with some modifications. Cells were incubated with 400 mM of the radioactive sugar analogues (dGlc or D-glucose) in the presence of CE (10 μM) and non-radioactive CB (0.5 μM), under the CB binding conditions. After 6 min. of incubation, cells were separated from the reaction mixture by the oil phase separation procedure. The cell pellet was immediately washed with 200 μl ice cold cPBS. The internalized substrate was then released by treatment with 1 ml of ice cold 10% (w/v) trichloroacetic acid (TCA). After centrifugation, the TCA-soluble materials were extracted three times with one volume of ethyl ether to remove the TCA. After removal of ether by heating at 60 °C for 10 min., 200 μl of this extract was then loaded onto a 1.7 x 14 cm column of Dowex 1-X8 (200-400 mesh, Cl^- form) resin (Biorad) (D'Amore and Lo, 1986a). It should be noted that the column was not saturated under these conditions (data not shown). The unphosphorylated sugar was first eluted with 40 ml of water, and the sugar phosphate retained on the column was then eluted with 40 ml of 0.1 M HCl plus 0.1 M NaCl; 2 ml fractions were collected. The amounts of free sugar and sugar phosphate were then determined.

2.2.7 Estimation of Intracellular Space

The intracellular space under the CB binding conditions was determined as described previously (D'Amore and Lo, 1986a) with some modifications. Cells were incubated with 400 mM radioactive MeGlc under conditions similar to those used in CB binding experiments by the oil phase separation method. The amounts of MeGlc internalized at different times were determined. At equilibrium, the amount present inside the cells was 51.6 nmol/10^5 cells. This indicated an intracellular volume of 1.29 pl/cell. We have previously obtained a value of 1.86 pl/cell for cells in suspension (Lo, 1979). The observed decrease in cell volume is probably due to the very high sugar concentration used under the CB binding conditions.

2.3 RESULTS

2.3.1 CB is a Potent Inhibitor for Both Hexose Transport Systems

CB has been shown to be a potent inhibitor of HT in rat L6 myoblasts (Czech, 1976b; Lo and Duronio, 1984a,b). In view of our recent demonstration of the presence of two HT systems (D'Amore and Lo, 1986a,b), experiments were carried out to examine the effect of CB on these two transport processes (Fig. 2.1). Kinetic studies with the low concentration range of 2-deoxy-D-glucose (dGlc), or D-glucose were used to monitor the response of HAHT; whereas 3-O-methyl-D-glucose (MeGlc) was used to study the properties of LAHT (D'Amore and Lo, 1986a,b). Fig. 2.1A, 2.1B, and 2.1C are Dixon plots showing the effects of CB on dGlc, D-glucose and MeGlc uptake by glucose-grown L6 myoblasts. Fig. 2.1A and 2.1B show that dGlc and D-glucose uptake are affected similarly by CB, with apparent K_i values of around 0.16 ± 0.013 μM. Fig. 2.1C shows that LAHT can be inactivated by very low concentration of CB; the apparent K_i value is around 16 ± 1.4 nM. Thus the low affinity transport activity is not likely a result of non-carrier mediated simple diffusion. These studies also indicate that the two HT

Fig. 2.1 CB Inhibition of dGlc, D-glucose and MeGlc Uptake.

Panel A, B and C are Dixon plots of the inhibition of dGlc, D-glucose and MeGlc uptake by CB, respectively. Transport studies were carried out as described in the text. The concentrations of dGlc used were 0.06 mM (▼), 0.12 mM (□), 0.25 mM (▽) 0.50 mM (●) and 1.00 mM (△). The concentrations of D-glucose used were 0.06 mM (▼), 0.08 mM (□), 0.12 mM (▽), 0.25 mM (●) and 1.00 mM (△). The concentrations of MeGlc used were 1.00 mM (▼), 1.25 mM (□), 1.70 mM (▽), 2.5 mM (●) and 5.00 mM (△). The rate of uptake (V) is expressed as pmol/10^5 cells/min.

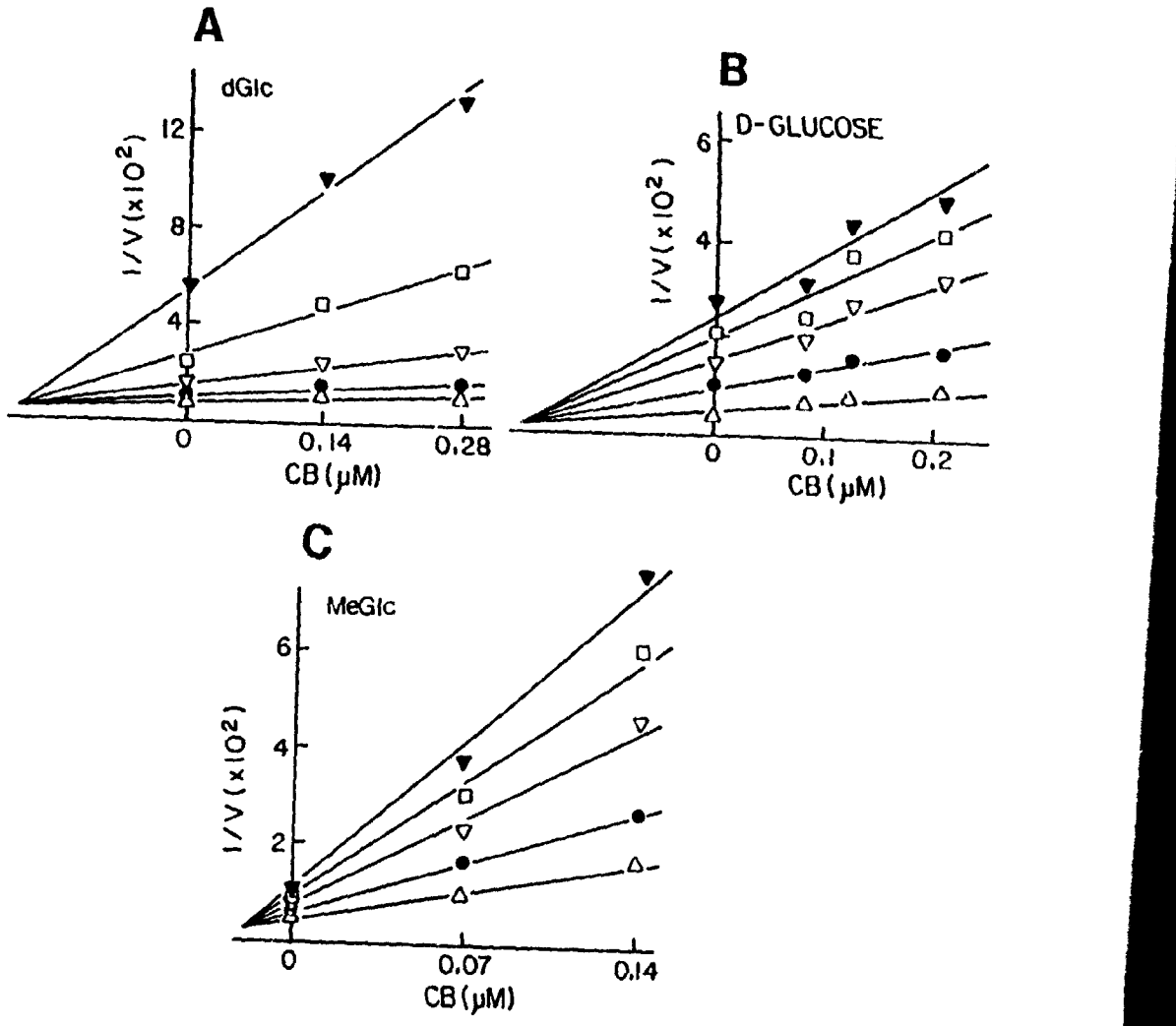
A
dGlc
1/V(x10²)
12
8
4
0
0.14
0.28
CB(μM)
B
D-GLUCOSE
1/V(x10²)
6
4
0
0.1
0.2
CB(μM)
C
MeGlc
1/V(x10²)
6
4
2
0
0.07
0.14
CB(μM)

systems respond differently to CB inhibition.

2.3.2 Assay for the Binding of CB to Rat L6 Myoblasts

The above transport studies suggest that the two HTers may have their own specific CB binding sites. This possibility was tested directly by binding studies using radioactive CB. Although CE and CB can bind to similar proteins, CE differs from CB in its inability to recognize the HTer (Carter-Su and Okamoto, 1985). Therefore, CE is always included in the CB binding assay to block CB binding sites which are not related to the HTer. The effect of CE on CB binding to whole cells is shown in Fig. 2.2. Similar binding activity was found when CE concentrations varied from 5-50 μM . Thus CE-sensitive CB binding sites can be sufficiently inhibited by 5 μM CE.

Two different CB binding assays have been used by various workers (Klip and Walker, 1983). These included removal of unbound ^{3}H-CB from the reaction mixture by filtration or by centrifugation. Fig. 2.3A shows that the oil phase separation method not only yields higher specific binding, but the amount of ^{3}H-CB bound is also directly proportional to the cell number. However, this is not the case with the filtration method; the lower binding at higher cell density is probably due to the slower rate of filtration during sample application and washing. Table 2.1 also shows that the oil phase separation method is much more sensitive in detecting specific CB binding; about 77% higher specific CB binding was observed in the control experiments, and that this binding is much more sensitive to hexose analogues, such as MeGlc and dGlc. Only a negligible inhibitory effect was observed when the filtration method was used. Similar results were also reported by other workers (Klip et al., 1983b) Table 2.1 also shows that phloretin, a very potent HT inhibitor (D'Amore and Lo, 1986a), is just as effective as 10 μM CB in blocking specific CB binding.

Fig. 2.3B shows the optimal conditions for measuring ^{3}H-CB binding by the

Fig. 2.2 Effect of CE on CB Binding to Glucose-grown L6 Myoblasts as Determined by the Oil Phase Separation Method

The amount of ^{3}H-CB bound to glucose-grown L6 myoblasts in the presence of 0.5 μM radioactive CB and different concentrations of CE was determined by the oil phase separation method as described in the text. Data presented indicate total binding. The specific activity of the radioactive CB was 2.40 x 10^{3} d.p.m./pmol.

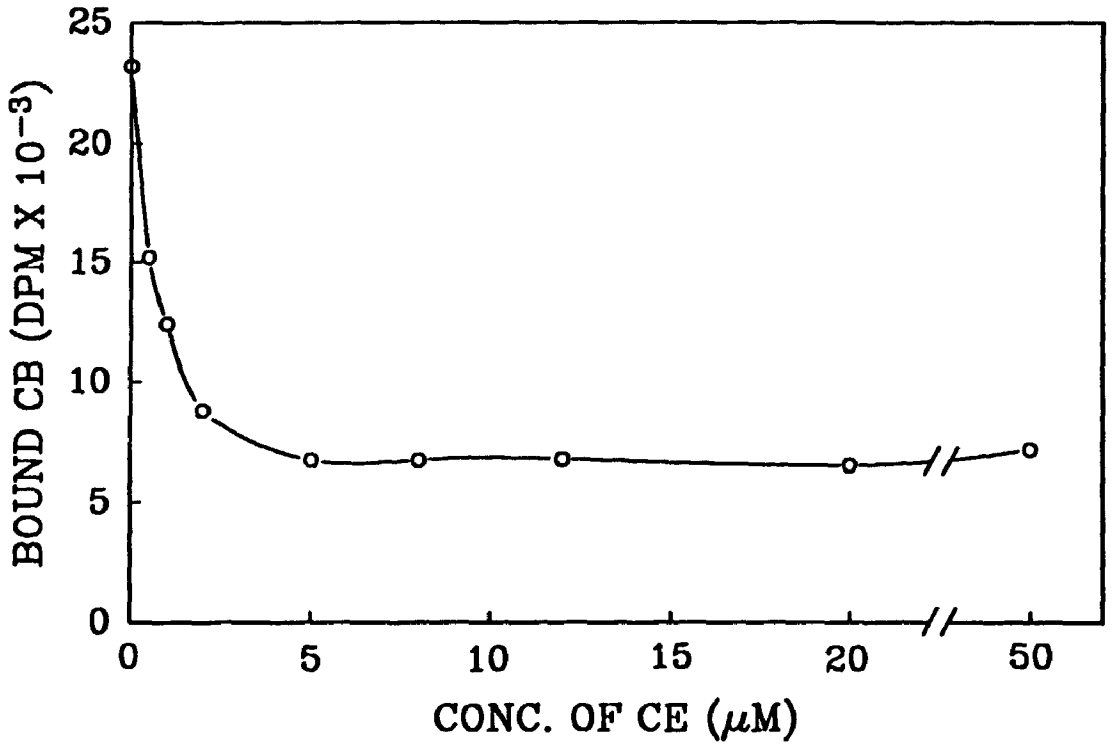
BOUND CB (DPM X 10^{-3})
25
20
15
10
5
0
0
5
10
15
20
50
CONC. OF CE (μM)

Fig. 2.3A A Comparison of the Filtration and Oil Phase Separation Methods in Measuring CB Binding.

Glucose-grown L6 myoblasts were incubated with 0.5 μM ^{3}H-CB in the presence of 10 μM cytochalasin E (CE). Data presented indicate specific binding in which the background radioactivity at each point has been subtracted from the crude data. The filtration (△) and the oil phase separation (○) methods are described in the text. The specific activity of the radioactive CB was 2.40 x 10^3 d.p.m./pmol.

Fig. 2.3B Effect of Temperature on CB Binding as Determined by the Oil Phase Separation Method.

The amount of CB specifically bound at various times was determined, as described in the text, after incubating glucose-grown L6 myoblasts at 4°C (△) and 37 °C (○) in the presence of 0.5 μM radioactive CB and 10 μM CE. The specific activity of the radioactive CB was 2.40 x 10^3 d.p.m./pmol.

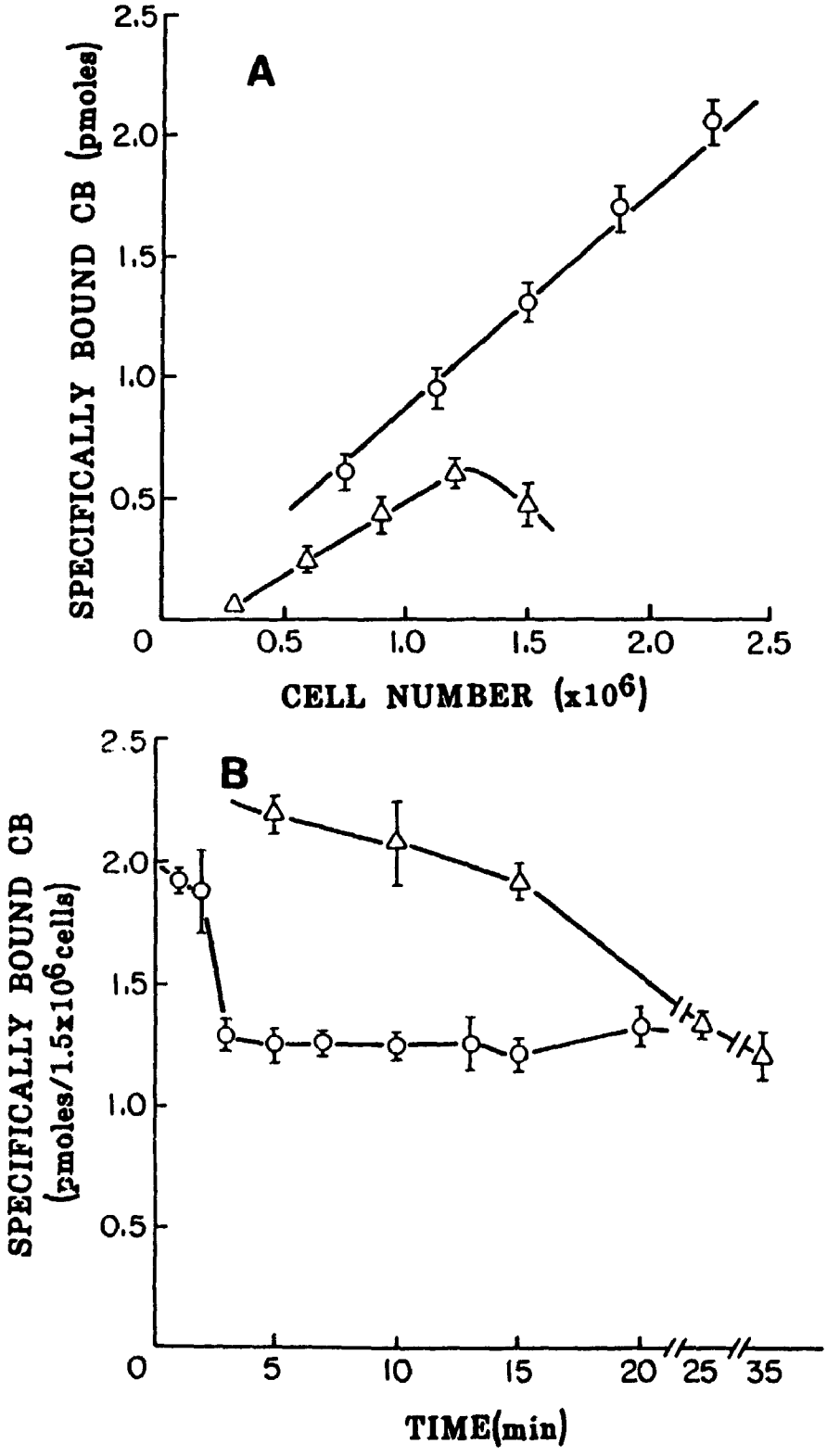
A
SPECIFICALLY BOUND CB (pmoles)
2.5
2.0
1.5
1.0
0.5
0
0.5
1.0
1.5
2.0
2.5
CELL NUMBER (x10^6)
B
SPECIFICALLY BOUND CB
(pmoles/1.5x10^6cells)
2.5
2.0
1.5
1.0
0.5
0
5
10
15
20
25
35
TIME(min)

Table 2.1 A Comparison of the Two Methods for CB Binding

	CYTOCHALASIN B BOUND			
	Oil phase separation method		Filtration method	
Addition	(pmol x $10^2/10^6$ cells)	%	(pmol x $10^2/10^6$ cells)	%
Control	85 ± 0.9	100	48 ± 1.4	100
Sorbitol (0.2 M)	82 ± 2.5	97	N.D.	N.D.
Sorbitol (0.6 M)	84 ± 0.3	99	N.D.	N.D.
L-glucose (0.4 M)	81 ± 1.6	95	50 ± 1.2	104
MeGlc (0.4 M)	53 ± 1.3	62	47 ± 1.6	98
dGlc (0.4 M)	50 ± 4.0	59	43 ± 2.2	90
Phloretin (0.5 mM)	0 ± 1.0	0	0 ± 0.4	0

Experiments were carried out as described in the text. The ^{3}H-CB and CE concentrations used in this study were 0.5 μM and 10 μM, respectively. The specificity of the radioactive CB was 2.40 x 10^3 d.p.m./pmol. Abbreviation: N.D., not determined.

oil phase separation method. As indicated in "Materials and Methods", the sugar concentration of the reaction mixture was adjusted to 0.6 M with sorbitol, which has no effect on CB binding (Table 2.1). Since a constant sugar concentration was maintained in all assays, alteration in CB binding could not be attributed to changes in osmolarity. Fig. 2.3B shows the effect of temperature on CB binding. The amount bound at 4 °C was initially much higher than that at 37 °C; and it continued to decrease even after 15 min. On the other hand, the amount bound at 37 °C remained constant after 3 min of incubation. Thus it seems additional CB binds transiently to the cells at low temperatures. However, such transient binding is not as apparent at 37 °C. In the following studies, CB binding assays were carried out at 37 °C for 6 min.

2.3.3 CB Binding to Glucose-grown Rat L6 Myoblasts

Having established the method and optimal conditions for CB binding, binding studies were carried out with glucose-grown L6 myoblasts. Fig. 2.4 is a Scatchard plot of the binding data. Since the background radioactivity at each CB concentration has been subtracted from the raw data, the data presented indicate specific binding. Fig. 2.4 shows a biphasic CB binding curve for the glucose-grown L6 myoblasts. The slope of the binding curve at low CB concentrations (SL-1) is significantly higher than that at high CB concentrations (SL-2). This indicates the presence of a high and a low affinity CB binding site in rat L6 myoblasts. These binding sites will be referred to as CB_H and CB_L, respectively. Since different parts of the binding curve represented varying extents of contribution by the two CB binding sites, their binding affinities were therefore determined by the vectorial analysis of a curved Scatchard plot as described by Munck (Munck, 1976), and also by a Scafit program written for microcomputers to analyze multicomponent Scatchard plots (Biomedical Computing Technology Information Center, Vanderbilt Medical Center). Similar values were obtained by both approaches. The first

Fig. 2.4 Effects of dGlc and MeGlc on CB Binding to Glucose-grown L6 Myoblasts

CB binding to glucose-grown L6 myoblasts was determined by the oil phase separation method as described in the text. The concentrations of ^{3}H-CB used ranged from 10 nM to 2.5 μM. Data presented represented the amount of CB specifically bound to the cells, the amount of non-specific background radioactivity at each CB concentration had been subtracted. The control experiment contained 400 mM sorbitol (●). (△) and (○) indicate the inhibition of specific CB binding by 400 mM dGlc and 400 mM MeGlc, respectively.

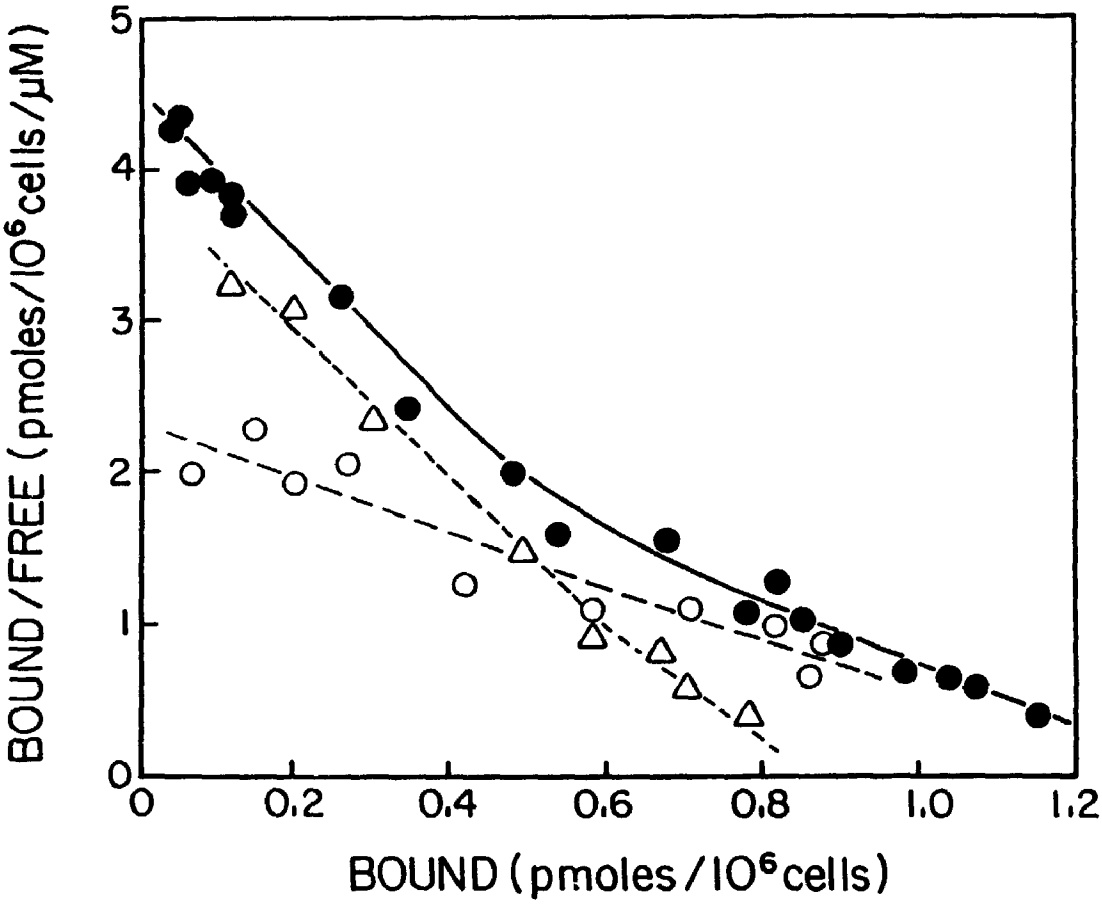
BOUND/FREE (pmoles/10⁶cells/μM)
BOUND (pmoles/10⁶cells)
0
1
2
3
4
5
0
0.2
0.4
0.6
0.8
1.0
1.2

approach gave K_d values of 0.11 and 1.07 μM, and Bmax values of 0.40 and 1.07 pmol/10^6 cells for CB_H and CB_L, respectively. Analysis by the Scafit program yielded K_d values of 0.11 and 0.95 μM, and Bmax values of 0.39 and 1.05 pmol/10^6 cells for CB_H and CB_L, respectively. Thus the two sites differ significantly in their CB binding affinity.

If two CB binding sites are indeed present, one may also be able distinguish them by differential inhibition (Clark and Peck, 1979). To this end, the effects of specific HT substrates were tested. Fig. 2.4 shows that while SL-1 is slightly affected, SL-2 is considerably reduced by 400 mM dGlc. This suggests that CB_L is more sensitive to dGlc than CB_H. When cells were incubated with 400 mM dGlc under the CB binding conditions, the intracellular concentrations of dGlc and dGlc 6-P were found to be 322 mM and 45 mM, respectively. It was found that CB binding to the plasma membrane is inhibited by dGlc, but not by dGlc 6-P (see Chapter 3). This demonstrates that dGlc is responsible for the inhibition of CB binding to whole cells rather than dGlc 6-P. It should also be noted that this inhibition is observed when the dGlc concentration is at least 100,000 times higher than that of CB. On the other hand, MeGlc exerts quite a different effect on CB binding (Fig. 2.4). SL-1 is lowered considerably by 400 mM MeGlc, whereas SL-2 is hardly affected. Thus CB_H seems to be more sensitive to MeGlc than CB_L. The above observations indicate that CB binding to CB_L and CB_H can be preferentially affected by the substrates of HAHT and LAHT, respectively.

2.3.4 CB Binding to Glucose-starved Rat L6 Myoblasts

We have recently demonstrated that only HAHT was stimulated during glucose starvation (D'Amore and Lo, 1986a; D'Amore et al., 1986a). If the CB binding sites are associated with their respective transporters, the corresponding changes may be observed. Fig. 2.5A shows that the CB binding curve for glucose-starved cells has a much higher Bmax value. This binding curve is similar to SL-2

Fig. 2.5 Effect of Glucose Starvation on the CB Binding Sites.

Panels A and B are Scatchard plots of CB binding to glucose-grown and glucose-starved cells. The CB binding curves were determined as described in Fig. 2.4 and in the text. Panel A indicates the CB binding curves of glucose-grown (●), and glucose-starved (○) L6 cells. Panel B shows the effect of dGlc and MeGlc on CB binding to glucose-starved L6 cells. (●) denotes CB binding to glucose-starved cells. (□) denotes the CB binding to glucose-starved cells in the presence of 400 mM dGlc, whereas (△) denotes that in the presence of 400 mM MeGlc.

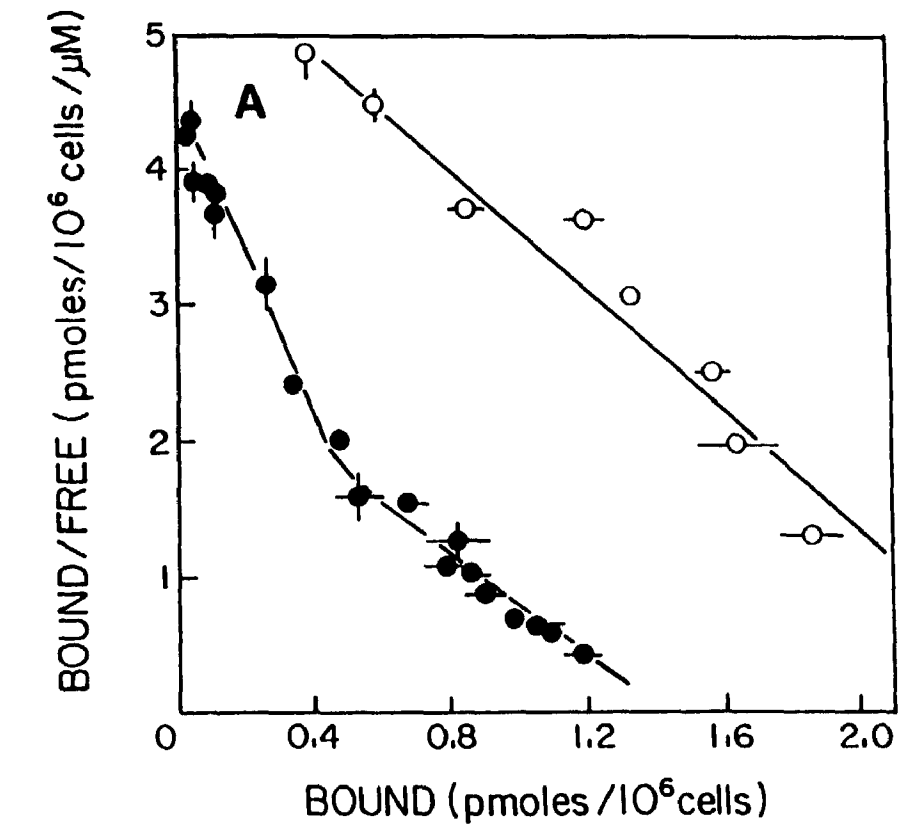
A
BOUND/FREE (pmoles/10⁶ cells/μM)
BOUND (pmoles/10⁶cells)
0
0.4
0.8
1.2
1.6
2.0
1
2
3
4
5

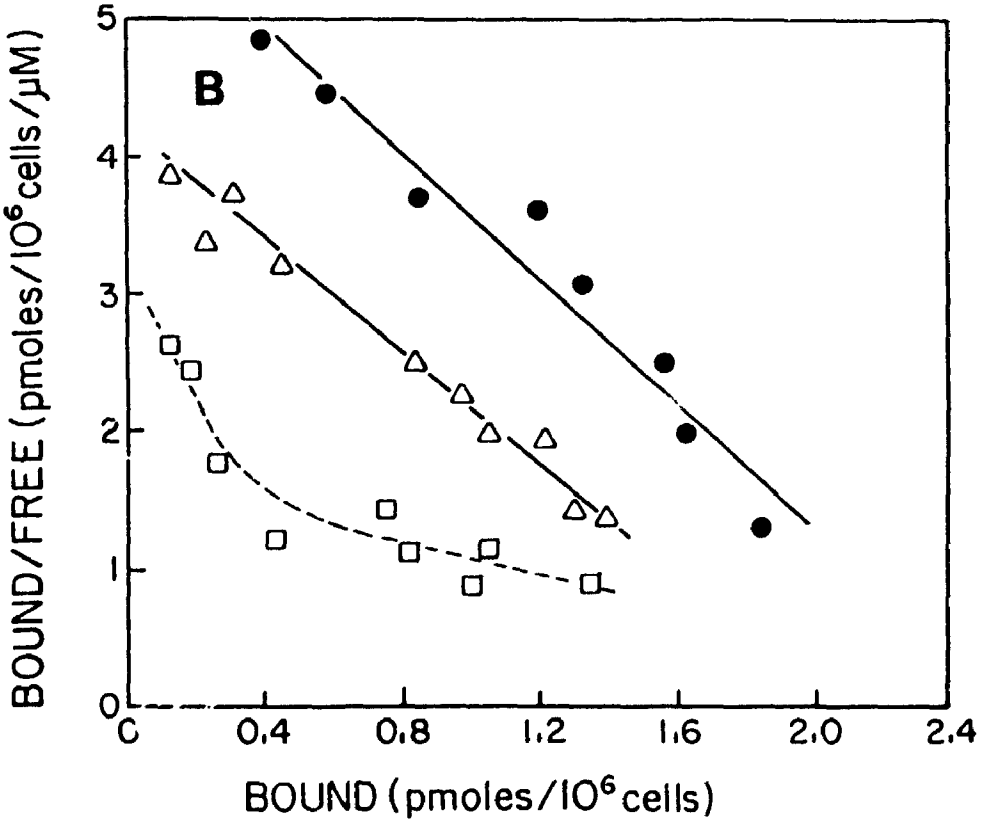
B
BOUND/FREE (pmoles/10⁶cells/μM)
BOUND (pmoles/10⁶cells)
0
0.4
0.8
1.2
1.6
2.0
2.4
1
2
3
4
5

of glucose-grown cells not only in its slope, but also in its sensitivity to dGlc (Fig. 2.5B). In fact, the presence of CB_H becomes apparent only when CB_L is inhibited by dGlc. At a CB concentration of 0.8 μM, 50% reduction of CB binding can be brought about by 420 mM dGlc. On the other hand, 400 mM MeGlc lowers the amount of CB bound without altering the binding affinity (Fig. 2.5B), Thus CB_L seems to be present at a much elevated level in glucose-starved cells. After correcting for the inhibitory effect of 400 mM dGlc, the level of CB_H is similar to that in glucose-grown cells. Thus CB_L seems to respond in a similar manner as HAHT to glucose starvation.

2.3.5 CB Binding to a Hexose Transport Mutant

A more definitive indication of the association of CB binding sites with the HTers comes from studies with a HT mutant. Transport kinetic studies reveal that mutant D23 is defective in HAHT (D'Amore et al., 1986b and Table 2.2). Table 2.2 also shows that the residual high affinity HT activity in this mutant can still be activated, albeit to not as great an extent by glucose starvation. Thus this mutant still contains residual level of HAHT. LAHT remains unaltered in this mutant.

Fig. 2.6A shows that the slope of the CB binding curve for glucose-grown mutant D23 is quite similar to SL-1 of glucose-grown L6; the presence of CB_L is not readily apparent here. The binding capacity of this mutant is similar to that of CB_H in glucose-grown L6. Fig. 2.6B indicates that glucose-starvation does not exert much effect on CB binding to the mutant. CB binding to this mutant is also found to be more sensitive to MeGlc than to dGlc (Fig. 2.7). Thus CB_L is either absent or present in very low concentrations, and CB_H is the predominant CB binding site in this mutant. A comparison of the transport and CB binding properties of this mutant suggests that CB_L and CB_H are associated with HAHT and LAHT, respectively.

Table 2.2 Kinetic Properties of the Two Hexose Transport Systems in Mutant D23 and its Parental L6 Cells.

		dGlc (HAHT)		McGlc (LAHT)	
Cell type	Growth condition	Km (mM)	Vmax	Km (mM)	Vmax
L6	Glucose	0.6 ± 0.1	235 ± 15	3.5 ± 0.5	357 ± 20
	Fructose	0.6 ± 0.1	396 ± 10	3.5 ± 0.3	596 ± 38
D23	Glucose	0.6 ± 0.1	90 ± 7	3.7 ± 0.5	328 ± 32
	Fructose	0.7 ± 0.1	138 ± 13	3.1 ± 0.4	344 ± 40

HT studies were carried out as indicated in the text. Km and Vmax (pmol/10^5 cells/min) values were determined from double reciprocal plots of the initial rates of uptake. Data on the transport properties of rat L6 myoblasts were taken from the reference of D'Amore & Lo, 1986c.

Fig. 2.6 CB Binding to Hexose Transport Mutant D23 and its Parental L6 Cells.

Panels A and B are Scatchard plots of CB binding to glucose-grown and glucose-starved cells, respectively. Experiments were carried out as described in Fig. 2.4 and in the text. (○) denotes CB binding curve of mutant D23, and (●) denotes that of its parental L6 cells.

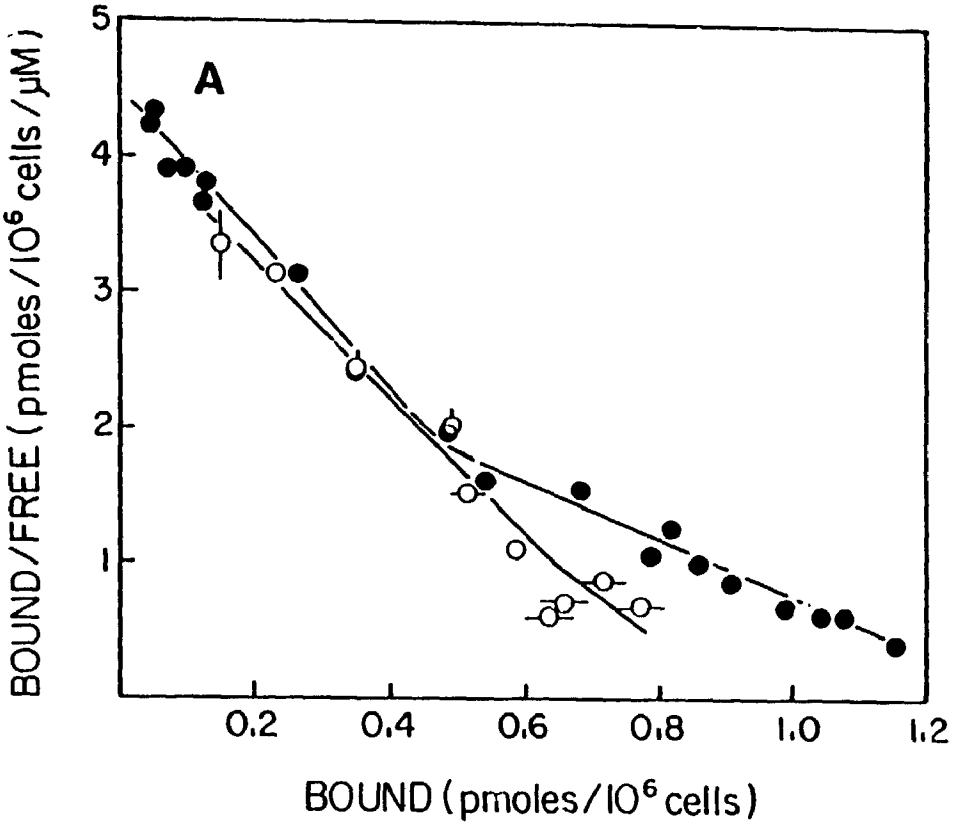
A
BOUND/FREE (pmoles/10⁶ cells/μM)
BOUND (pmoles/10⁶ cells)
0.2
0.4
0.6
0.8
1.0
1.2
1
2
3
4
5

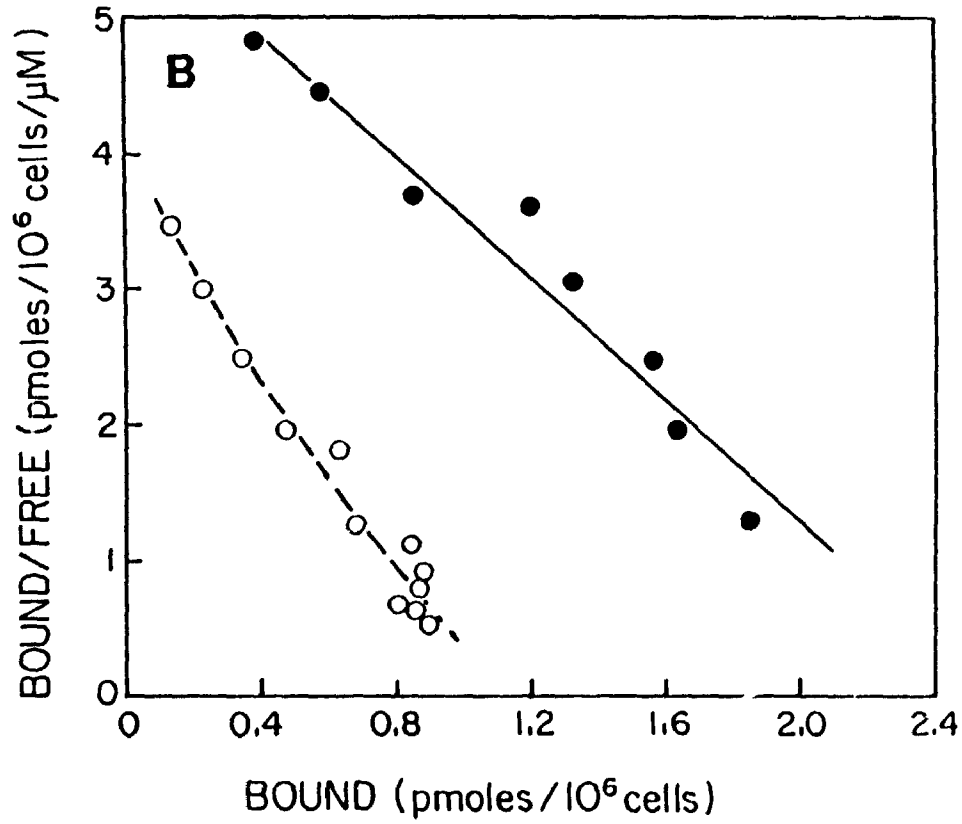
B
BOUND/FREE (pmoles/10⁶ cells/μM)
BOUND (pmoles/10⁶ cells)
0
0.4
0.8
1.2
1.6
2.0
2.4
0
1
2
3
4
5

Fig. 2.7 Effects of dGlc and MeGlc on CB Binding to Glucose-grown Mutant D23

This Scatchard plot was determined as described in Fig. 2.4 and in the text. (●), (◦), and (□) denote CB binding in the presence of 400 mM sorbitol, 400 mM dGlc and 400 mM MeGlc, respectively. The dash line represents the CB binding curve of glucose-grown L6 myoblasts.

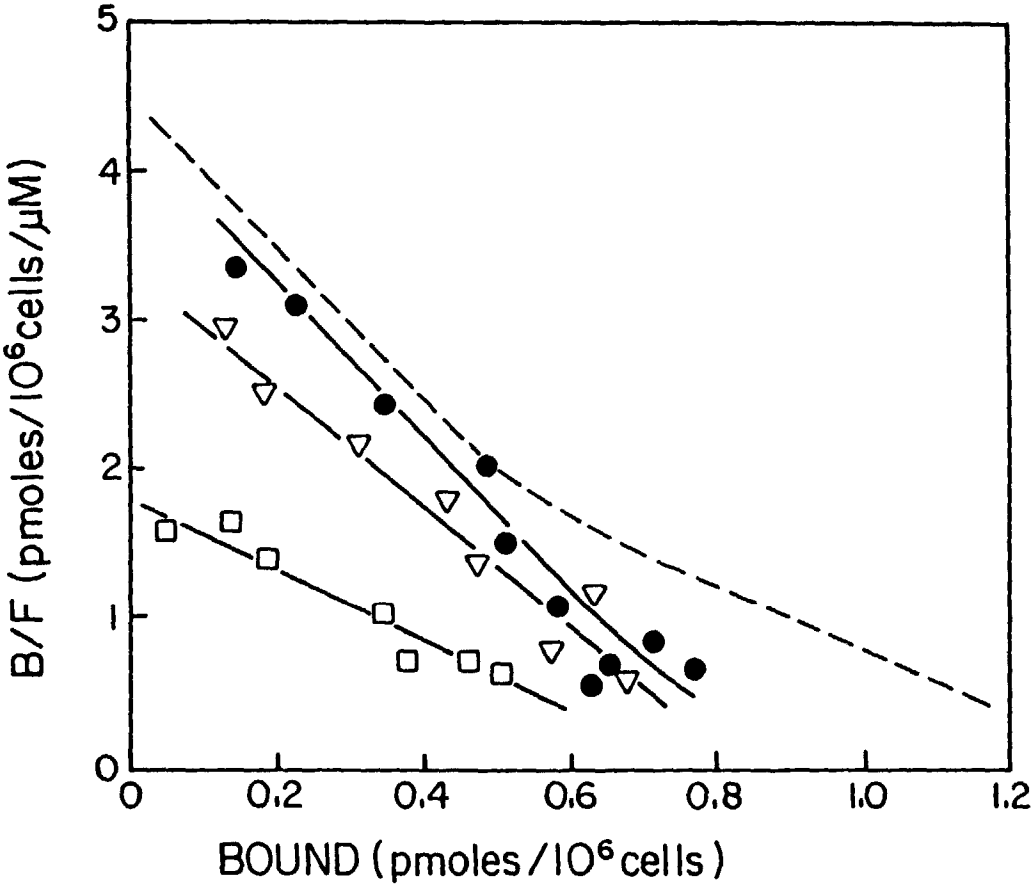
B/F (pmoles/10⁶cells/μM)
BOUND (pmoles/10⁶cells)
0
1
2
3
4
5
0
0.2
0.4
0.6
0.8
1.0
1.2

2.4 DISCUSSION

The mechanism and regulation of HT have been studied quite extensively in human erythrocytes, adipocytes, and chick embryo fibroblasts (Baldwin and Lienhard, 1981; Olefsky, 1978; Czech, 1976a,b; Pessin et al., 1982; Griffin et al., 1982). In these studies, CB has been used to identify and to quantitate the HTer (Foley et al., 1980; Simpson and Cushman, 1986; Mullins and Langdon, 1980; Cushman and Wardzala, 1980). In fact, it has recently been used to photolabel the HTer (see Chapter 4). One of the unresolved problems in these studies is the uncertainty of the molecular weight of the human rbc HTer. Depending on the affinity labels and the reconstitution procedures used, the molecular weights of the HTers in human rbc and adipocytes are found to be around 40-70 kDa and 90-100 kDa (Kay, 1985; Mullins and Langdon, 1980; Shelton and Langdon, 1983; Carruthers and Melchiors, 1984; Malchoff et al., 1985). Thus one cannot identify the HTer on the basis of its apparent molecular weight alone. The second problem is the very high transport substrate concentration required to produce close to 50% inhibition of CB binding. It is therefore questionable whether CB is actually competing with the transport substrate for the same site on the transporter (see Chapter 3). The above complications do make it difficult to demonstrate unequivocally that CB is indeed binding to the HTer(s).

We have recently demonstrated the presence of two HT systems in undifferentiated rat L6 myoblasts (D'Amore and Lo, 1986a,b,c; D'Amore et al., 1986a,b). These two systems differ not only in their transport affinity and substrate specificity, but also in their expression under different growth conditions. Mutants defective only in HAHT have also been isolated (D'Amore et al., 1986b). These mutants are not altered in LAHT and have the normal levels of enzymes involved in glucose metabolism. These mutants can therefore serve as unique tools in examining the relationship between the CB binding sites and the HTers. CB binding

studies with these mutants will provide information on the identity and properties of the specific CB binding site.

CB was a potent inhibitor for both rat myoblast HT systems, with LAHT being much more sensitive (Fig. 2.1). Thus either the two transporters possess their own CB binding sites or the binding of CB to one site may exert different effects on the two transport systems. CB binding studies were therefore carried out to resolve these possibilities. Considerable efforts have been spent in this investigation in determining the most effective CB binding assay, and the optimal conditions for measuring CB binding. The oil phase separation assay was found to be the most efficient and sensitive method for measuring CB binding to whole cells (Table 2.1 and Fig 2.3). CB binding studies with whole cells have several distinct advantages. (i) Whole cell binding studies require only a relatively small number of cells, whereas a much larger number of cells is required for the preparation of plasma membrane (Cheung and Lo, 1984). (ii) Whole cell studies allow a direct comparison of the transport and the CB binding properties. (iii) Unless purified plasma membrane vesicles are used, crude membrane preparations do not have a distinct advantage over whole cells, as they still contain a substantial amount of microsomal and mitochondrial contamination. (iv) A comparison of the CB binding properties of whole cells with that of purified plasma membrane preparations may provide additional information as to the effects of various metabolites. It is important to note that both whole cell and plasma membrane studies yield essentially similar information on the intrinsic properties of the CB binding sites (see Chapter 3).

The following pieces of evidence suggest that two specific CB binding sites are present in undifferentiated rat L6 myoblasts. (i) Scatchard analysis of the binding data revealed the presence of two specific CB binding sites in glucose-grown L6 cells (Fig. 2.4). The Kd values of CB_H and CB_L were 0.11 ± 0.02 and 1.01 ± 0.03 μM, respectively; while their respective Bmax values were 0.40 ± 0.07

and 1.06 ± 0.09 pmol/10^6 cells. (ii) The two CB binding sites can be differentially inhibited by specific substrate analogues. CB_H is preferentially inhibited by MeGlc, whereas CB_L is preferentially inhibited by dGlc (Fig. 2.4). (iii) Glucose starvation increased the level of CB_L without significantly affecting CB_H (Fig. 2.5). (iv) Using identical assay conditions, only one CB binding site can be detected in transport mutant D23 (Fig. 2.6); this suggests that the two CB binding sites are coded or regulated by different genetic elements. In conclusion, the two CB binding sites not only differ in their binding affinity, but their levels can also be differentially altered by various biochemical, physiological and genetic manipulations. Since all the binding assays were performed and analyzed under identical conditions, it was unlikely that our observations were artifacts arising from the method of analysis. CB binding studies with purified plasma membrane also indicate the presence of two CB binding sites (see Chapter 3). It can be calculated from the Bmax values that CB_H and CB_L are present to the extent of 2.4 x 10^5 and 6.4 x 10^5 binding sites per glucose grown L6 myoblast, respectively. It is interesting to note that about 3.3 x 10^5 binding sites/cell are found in human erythrocytes (Klip et al, 1982).

The next question concerns the identity of these two specific CB binding sites. Both biochemical and genetic evidence indicates that CB_L is associated with HAHT. (i) CB_L can be preferentially inhibited by dGlc, the preferred substrate of HAHT (Fig. 2.4). (ii) Glucose starvation activates not only HAHT, but also CB_L (Fig. 2.5). (iii) The mutant defective in HAHT is also defective in CB_L (Fig. 2.6 and Table 2.2). (iv) Glucose starvation fails to generate the expected increase in either CB_L or HAHT in this mutant (Fig. 2.6 and Table 2.2). The above correlations strongly suggest that CB_L may be associated with HAHT.

One of the advantages of using mutant D23 is that it allows one to examine the properties of LAHT without much of the interference of HAHT. Fig. 2.6 shows

that CB_L can hardly be detected in glucose-grown mutant D23. It follows from this observation that CB binding to this mutant should reflect fairly closely the intrinsic properties of CB_H. Fig. 2.6 shows that the CB binding affinity and capacity of this mutant are quite similar to those of CB_H in glucose-grown L6 cells. It is interesting to note that Km and Vmax values of LAHT in glucose-grown mutant D23 are also similar to the corresponding values in L6 cells (Table 2.2). Similar to L6 cells, the levels of CB_H and LAHT remain unaltered in both glucose-grown and glucose-starved mutant D23. Furthermore, MeGlc is more effective in inhibiting CB binding to CB_H in this mutant than dGlc. In other words, CB_H is preferentially inhibited by the substrate of LAHT. Thus this study demonstrates the close correlation between CB_H and LAHT.

CHAPTER 3

CYTOCHALASIN B AS A PROBE FOR THE TWO HEXOSE TRANSPORT SYSTEMS IN UNDIFFERENTIATED RAT L6 MYOBLASTS II. PLASMA MEMBRANE STUDIES

3.1 INTRODUCTION

The HT systems in human erythrocytes, rat adipocytes, chick embryo fibroblasts and rat myoblasts have been examined primarily through the use of intact whole cells (Wheeler and Hinkle, 1985; Gliemann and Rees, 1983; Kalckar and Ullrey, 1984; D'Amore and Lo, 1986a,b,c; D'Amore et al., 1986a,b). Purified plasma membrane vesicles have also been employed to further define the properties of these transport systems (Cheung and Lo, 1984; Mesmer et al., 1986). CB has been used as an affinity ligand for the detection and quantitation of the HTers (Simpson and Cushman, 1986; Jung et al., 1986; Jung and Rampal, 1977; Klip and Walker, 1983; Oka and Czech, 1984; Lienhard et al., 1982). In most of these studies, either crude or semi-purified membrane preparations were used.

Whole cell CB binding studies revealed that rat L6 myoblasts possess two specific CB binding sites which differ considerably in their binding affinity and capacity. These two sites can be differentially inhibited by substrates of the two rat L6 myoblast HT systems. Furthermore, these two specific CB binding sites are also differentially expressed in glucose-starved cells, and in a HT mutant. The above biochemical, physiological, and genetic evidence strongly suggests that both HAHT and LAHT possess their own CB binding sites.

CB binding studies with whole cells are not without problems. First, one is uncertain of the location of the CB binding sites, especially when two such sites have been detected in whole cells. It is possible that one site is associated only

with the plasma membrane, while the other site is associated with the microsomal fractions. Whole cell binding studies do not allow one to examine such a possibility. Second, whole cell studies are complicated by the presence of various metabolic events, such as protein turnover, protein phosphorylation, DNA and RNA syntheses. Furthermore, one is never sure of the effect of various substrate metabolites on CB binding. In fact, it has been reported that different forms of HTers are present in plasma membrane and the low density microsomal fraction in rat adipocytes (Carter-Su and Okamoto, 1985; Horuk et al., 1986), and that the distribution of the HTers in these membrane fractions can be affected by various physiological and metabolic events (Simpson and Cushman, 1986; Karnieli et al., 1981). In this chapter, we attempted to locate the CB binding sites and to determine the effects of metabolites of glucose or glucose analogues on CB binding using purified membrane fractions.

3.2 MATERIALS AND METHODS

3.2.1 Materials

[^{3}H]-D-glucose was purchased from New England Nuclear. [4-^{3}H(n)]-cytochalasin B (15.5 Ci/mmol) was purchased from Amersham Canada Ltd. Scinti-Verse E (scintillation fluid) was from Fisher Scientific Co. Cytochalasins, glucose analogues and other chemicals were from Sigma Chemical Co. All chemicals were obtained from commercial sources and were of the highest available purity.

3.2.2 Preparation of Plasma Membrane Fractions.

Plasma membrane fractions were prepared from undifferentiated rat L6 myoblasts as described previously (Cheung and Lo, 1984), with some modifications. Briefly, rat L6 myoblasts were grown in 245 x 245 x 20 mm tissue culture plates (Nunc, Denmark) at 37 °C with 5% CO_2. Cells were washed twice with PBS containing PMSF (0.5 mM), EDTA (1 mM), leupeptin (2 μg/ml), and pepstatin A

(1 μg/ml). Cells were then harvested by scraping and centrifugation at 700 x g for 10 min. at 25 °C. All remaining steps were carried out at 4 °C. Cells were homogenized by 15-20 strokes with a tight fitting (pestle A) Dounce homogenizer in ice cold buffer A [0.25 M sucrose, 10 mM Hepes (pH 7.0), 1 mM EDTA, 0.5 mM PMSF, 2 μg/ml leupeptin, and 1 μg/ml pepstatin A]. The extent of cell breakage was monitored with a phase contrast microscope. Unbroken cells and nuclei were removed by centrifugation at 700 x g for 5 min. After centrifugation at 33,000 x g for 15 min., the supernatant was kept for the preparation of microsomal fractions; whereas the pellet was resuspended in ice cold buffer A and layered over a discontinuous sucrose density gradient, containing 3 ml of 35%, 29%, and 24 % (W/W) sucrose in buffer B [Hepes (10 mM), PMSF (0.5 mM), EDTA (1 mM), leupeptin (2 μg/ml) and pepstatin A (1μg/ml), pH 7.4]. This was then centrifuged at 33,000 rpm for 2 hrs. in a Beckman SW40 rotor. The interfaces between buffer A and 24% sucrose (fraction A), 24% and 29% sucrose (fraction B), and 29% and 35% sucrose (fraction C) were collected, diluted with buffer B and centrifuged at 33,000 x g for 20 min. The pellets were resuspended in the same buffer and stored at -80 °C. Both fractions A and B exhibit 5-7 fold enrichment of the ouabain-sensitive Na^+, K^+-ATPase (plasma membrane marker enzyme) specific activity over the initial cell free extract. These two fractions have negligible activities of hexokinase, lactate dehydrogenase, succinate-dependent cytochrome c reductase and NADPH-dependent cytochrome c reductase (Cheung and Lo, 1984).

3.2.3 Preparation of Microsomal Fractions

Microsomal membranes were prepared as described by Carter-Su and Okamoto (1985), with some modifications. Cell free homogenates were prepared as described above. The high density microsomal fraction (HDMF) was pelleted by centrifuging the 33,000 x g supernatant at 48,000 x g for 20 min. The pellet was

then resuspended in 10 mM Hepes buffer, pH 7.0. The specific activity of Na^+, K^+-ATPase in this fraction was 30-40% of that in the plasma membrane. The low density microsomal fraction (LDMF) was harvested by further centrifuging the 48,000 x g supernatant at 250,000 x g for 1 hr. The Na^+, K^+-ATPase activity of LDMF was about 2-5% of the plasma membrane activity. In other words, this preparation was relatively free of contamination by the plasma membrane.

3.2.4 CB Binding to Membrane Preparations

Equilibrium CB binding was initiated by the addition of membrane preparation (suspended in 10 mM phosphate buffer, pH 7.4, and 1 mM EDTA) to the binding assay buffer. The latter contained 10 mM phosphate buffer (pH 7.4), cytochalasin E (CE), and ^{3}H-CB. Sugar analogues or inhibitors were included in this buffer whenever necessary. The total volume of the reaction mixture was 160 μl. The final membrane protein concentration was between 0.5 and 1.2 mg/ml, and the final concentrations of CE and CB were 15 μM, and 0.011 - 3.0 μM, respectively. The reaction mixture was incubated at 4 °C for 90 min. in polycarbonate microcentrifuge tubes (7 x 20 mm, Beckman). This was then centrifuged at 436,000 x g for 40 min. at 4 °C in a Beckman TL-100 ultracentrifuge. Centrifugation at such high centrifugal force was found to be essential to obtain a tightly packed pellet. The amount of unbound (i.e. free) CB was determined by sampling 60 μl of the resulting supernatant. In order to remove the residual ^{3}H-CB, the tubes were washed four times with ice-cold 180 μl of sucrose-phosphate buffer [0.25 M sucrose, 10 mM sodium phosphate (pH 7.4), 1 mM EDTA]. The pellet was dissolved overnight in 80 μl of 0.5 M NaOH, and counted for radioactivity in scintillation fluid containing 0.7% glacial acetic acid. The background radioactivities were determined by the inclusion of 30 μM of unlabelled CB and 100 μM of phloretin. Since the effect of D-glucose on the two CB binding sites was to be examined, D-glucose was not used to determine the background

radioactivity. Unless otherwise stated, all the results presented represent specific binding, background radioactivity having been subtracted from the crude data. All CB binding studies were carried out in duplicate. Data presented illustrate results of representative experiments, and each experiment was repeated at least twice and usually three or more times. Results were found to be very consistent in all cases.

3.2.5 CB Binding to Intact Whole Cells.

CB binding to whole cells was carried out by the oil-phase separation method as described in Chapter 2

3.2.6 Treatment of Intact Whole Cells and Membrane Preparations With Trypsin

Glucose-grown L6 myoblasts were treated with 1 mg/ml of trypsin in citrate saline at 37 °C for 20 min. Trypsinized cells were diluted with cPBS and centrifuged at 1,000 x g for 5 min. Cell pellets were suspended in cPBS and used for CB binding studies as described for the whole cells.

Plasma membrane was treated with trypsin (0-500 μg/ml) in 10 mM phosphate buffer, pH 7.4, containing 1 mM EDTA at 37 °C for 1 h. CB binding was initiated by adding buffer containing 15 μM CE, 0.5 μM ^{3}H-CB (final concentration). The reaction mixture was incubated at 4 °C for 90 min., the remaining steps having been described in the previous section.

3.2.7 Protein and Marker Enzyme Assays

Protein determinations were made by the method of Lowry (Lowry et al., 1951) with bovine serum albumin as the standard. The plasma membrane marker enzyme, ouabain-sensitive Na^+, K^+-ATPase was determined in a 0.1 ml mixture containing 30 mM imidazole (pH 7.5), 11 mM NaCl, 15 mM KCl, 5 mM NaN_3, 0.5 mM EGTA, 4 mM $MgCl_2$, 3 mM ATP, and 10-30 μg protein with and without 1 mM ouabain. Reactions were carried out in triplicate at 37 °C for 30 min. and stopped by adding 0.1 ml silicotungstic acid as described previously (Lindberg and Ernster, 1956). Inorganic phosphate content was determined by the standard

procedure (Martin and Doty, 1949). Enzyme activity was calculated by the difference in ATPase activity in the presence and absence of ouabain.

3.2.8 Other Procedures

For other methods and materials, see Chapter 2.

3.3 RESULTS

3.3.1 Assay for the Binding of CB to Rat L6 Myoblast Plasma Membrane

As discussed in Chapter 2 in whole cell CB binding studies, CE was used to block the CB binding sites associated with the HTer. The effect of CE on the binding of CB to plasma membrane was also examined. Fig. 3.1A shows that similar amounts of CB were bound to plasma membrane at CE concentrations ranging from 10 to 100 μM. Thus most of the CE-sensitive CB binding sites in plasma membrane can be blocked by 10 μM of CE.

Washing of whole cells was found to cause significant loss of specific CB binding activity (Fig. 2.3A). The effect of washing on CB binding to plasma membrane under the present binding conditions was also examined (Fig. 3.1B). While the background radioactivity was decreased about 30%, no significant change was observed in the specifically bound CB after 3-6 washings. Presumably, the washing step in this assay removed mainly the CB attached to the side of the tube or to the surface of the pellets.

3.3.2 CB Binding to Purified Plasma Membrane From Rat L6 Myoblasts.

In order to define the location of the CB binding sites and to carry out binding studies in the absence of various metabolic events, CB binding was carried out with purified membrane fractions. Plasma membrane was isolated from glucose-grown rat L6 myoblasts as described in "Methods and Materials". In most of the following studies, fractions A and B were pooled to examine the CB binding properties of the plasma membrane. Fig. 3.2 shows the binding of CB to purified

Fig. 3.1 Effects of CE and Washing on CB Binding to Purified Plasma Membrane from Glucose-grown L6 Myoblasts.

CB binding to plasma membrane was carried out as described in the text. Panel (A) indicates totally bound ^{3}H-CB to plasma membrane in the presence of various concentrations of CE. Panel (B) shows the effect of washing on the amounts of specifically (○) and non-specifically (●) bound ^{3}H-CB. The concentration of CB used was 0.5 μM, and the specific activity of ^{3}H-CB was 1.0 x 10^{4} d.p.m./pmol.

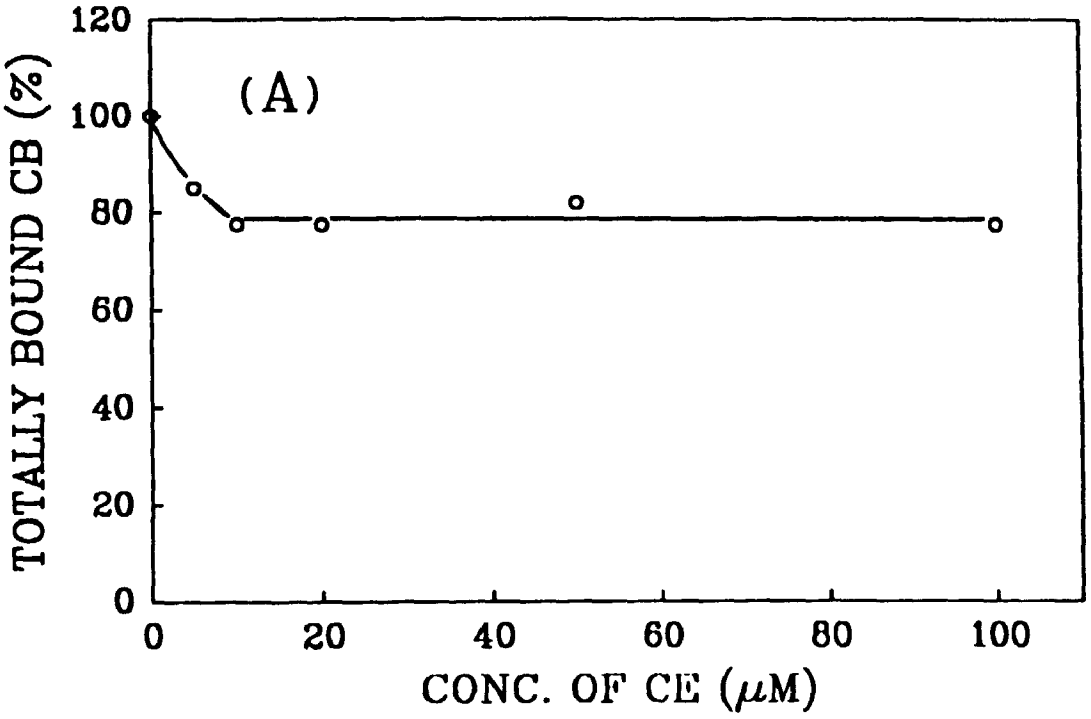
(A)
TOTALLY BOUND CB (%)
120
100
80
60
40
20
0
0
20
40
60
80
100
CONC. OF CE (μM)

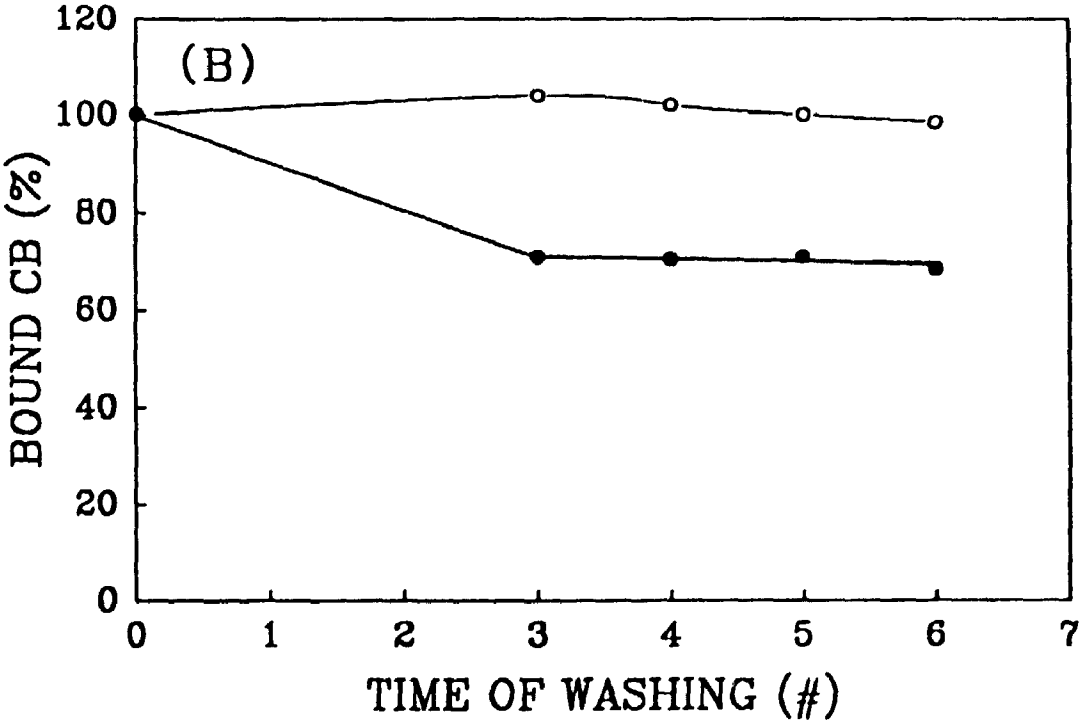
(B)
BOUND CB (%)
120
100
80
60
40
20
0
0
1
2
3
4
5
6
7
TIME OF WASHING (#)

Fig. 3.2 CB binding to Purified Plasma Membrane from Glucose-grown Mutant D23 and its Parental L6 Cells.

Preparation of plasma membranes and CB binding assays were carried out as described in the text. CB binding was determined at concentrations ranging from 11 nM to 3.0 μM. Data presented represented binding to specific sites. The amount of non-specific binding (background radioactivity) had been subtracted from the raw data. (○) and (●) represent binding to plasma membrane prepared from glucose-grown mutant D23 and its parental L6 cells. Values presented are the means of duplicate estimates from one typical experiment. The average error was around 3%.

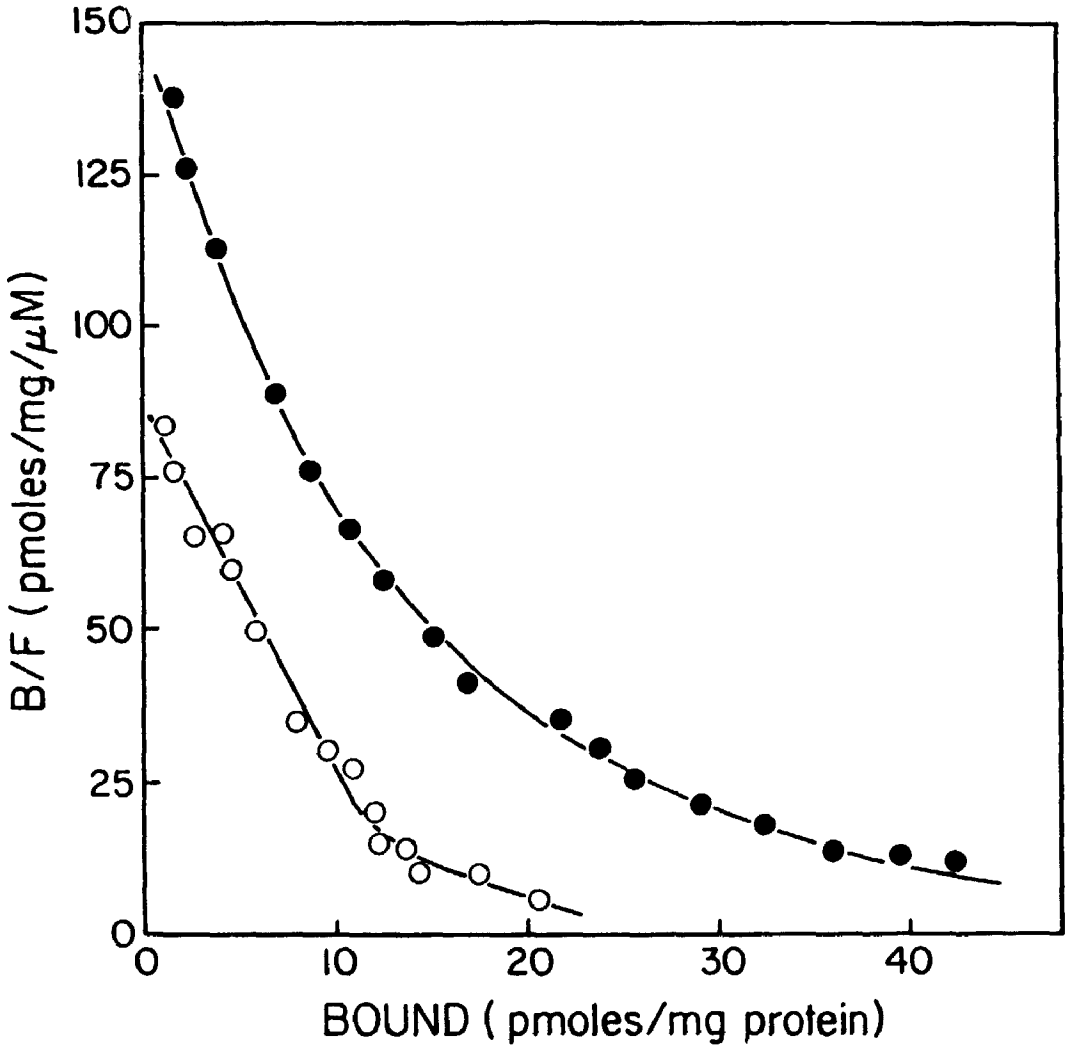
150
125
100
75
50
25
0
B/F (pmoles/mg/μM)
0
10
20
30
40
BOUND (pmoles/mg protein)

plasma membrane. Similar to whole cell binding studies, two CB binding sites (CB_H and CB_L) can be detected on this purified plasma membrane. Since different parts of the binding curve represent varying extents of contribution by the two CB binding sites, the binding affinities and Bmax values of these two sites were determined by the vectorial analysis of a curved Scatchard plot (Munck 1976; Clark and Peck, 1979), and also by a Scafit program as described in Chapter 2. The first approach gave Kd values of 0.10 and 1.44 μM, and Bmax values of 12.1 and 43.0 pmoles/mg protein for CB_H and CB_L, respectively. Similar values were obtained by the second approach with Kd values of 0.09 and 1.64 μM, and Bmax values of 11.4 and 44.6 pmol/mg protein, respectively. This represents a 16-23 fold increase in the number of CB binding sites per mg protein when compared with whole cells (Table 3.4). The ratio of the Bmax values of CB_L to CB_H is around 3.71. Since this is a fairly pure plasma membrane preparation, it may be surmised that both CB_L and CB_H are present in the plasma membrane.

3.3.3 CB Binding to Purified Plasma Membrane From Mutant D23.

We have previously demonstrated that the rat myoblast mutant D23 is defective not only in HAHT, but also in CB_L (Table 2.2 and Fig. 2.6). If CB_L is indeed associated with HAHT, then one would expect that this alteration should also be observed in plasma membrane prepared from this mutant. Fig. 3.2 shows that this is indeed the case. Analysis of this binding curve by both vectorial analysis and by the Scafit program yielded similar data. The Kd values were calculated to be 0.13 $\pm$ 0.01 and 4.18 $\pm$ 0.29 μM, and the Bmax values were 11.4 $\pm$ 0.70 and 18.1 $\pm$ 0.91 pmol/mg protein for CB_H and CB_L, respectively. The ratio of the Bmax value of CB_L to CB_H is around 1. 59. Thus the Kd and Bmax values of CB_L in D23 plasma membrane differ significantly from those of L6 plasma membrane, whereas those for CB_H remain unaltered (Table 3.4). Again, this study using plasma membrane from mutant D23 suggests that CB_L is associated with

HAHT.

3.3.4 CB Binding to Microsomal Fractions

CB binding to microsomal fractions was assessed by the same procedure used for the plasma membrane. As for plasma membrane, a biphasic curve was also observed with HDMF (Fig. 3.3). Analysis by both vectorial analysis and by the Scafit program yielded similar results: the HDMF exhibited Kd values of 0.09 ± 0.03 and 1.49 ± 0.10 μM, and Bmax values of 6.10 ± 0.07 and 22.6 ± 1.90 pmol/mg protein for CB_H and CB_L, respectively. The ratio of the Bmax values for CB_L to CB_H was around 3.7. Both CB_H and CB_L are also found in LDMF, albeit at a much reduced level (Fig. 3.3). Analysis of the data revealed the CB binding sites of LDMF exhibited Kd values of 0.11 ± 0.01 and 1.60 ± 0.61 μM, and Bmax values of 1.75 ± 0.02 and 6.75 ± 0.61 pmol/mg protein for CB_H and CB_L, respectively. The ratio of the Bmax values of CB_L to CB_H was 3.86. This study indicates that both the high and low affinity CB binding sites can be detected in the two microsomal preparations. Both sites exhibit similar binding affinities, and are present in ratios similar to those found in the plasma membrane. However, they are present in much lower quantities in LDMF when compared with the plasma membrane (Table 3.4).

3.3.5 Effect of Glucose Analogues on CB Binding to Purified Plasma Membrane

Similar to the situation in whole cells, very high concentrations of MeGlc and dGlc were required to bring about significant inhibition of CB binding to purified plasma membrane. While 400 mM sorbitol and 400 mM L-glucose have no effect on CB binding, 400 mM dGlc or 400 mM MeGlc can bring about 50% to 60% inhibition of CB binding (Table 3.1); furthermore, about 77% inhibition can be brought about by 0.1 mM phloretin. Thus the CB binding sites in plasma membrane seem to respond to various glucose analogues and inhibitors in a manner similar to that of whole cells.

Fig. 3.3 CB Binding to HDMF and LDMF from Glucose-grown L6 Myoblasts.

Preparations of HDMF and LDMF, and CB binding studies were carried out as described in the text and in Figure 3.2. (○) and (▲) denote CB binding to HDMF and LDMF respectively.

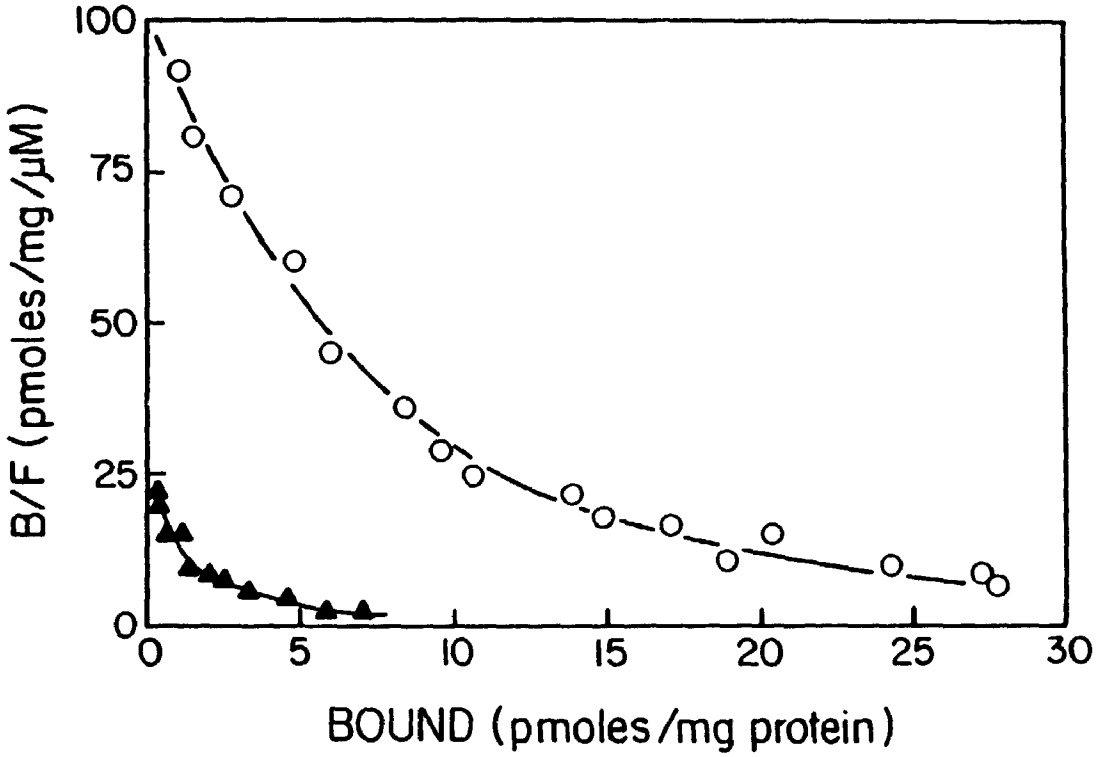
100
75
50
25
0
B/F (pmoles/mg/μM)
0
5
10
15
20
25
30
BOUND (pmoles/mg protein)

Table 3.1 Effects of Various Sugar Analogues and a Transport Inhibitor on CB Binding to Plasma Membrane.

Addition	CB bound (%)
Control	100 ± 2.6
Sorbitol (0.4 M)	99 ± 3.0
L-glucose (0.4 M)	98 ± 3.0
MeGlc (0.4 M)	49 ± 3.1
dGlc (0.4 M)	43 ± 2.0
Phloretin (0.1 mM)	23 ± 1.9

Experiments were carried out as described in the text. The concentration of CB used in this study was 0.5 μM. The control value was 16.0 ± 0.42 pmol/mg of protein, and the specific activity of the radioactive CB was 1 x 10^4 d.p.m./pmol.

Fig. 3.4 Effect of D-glucose on CB Binding to Glucose-grown L6 Myoblasts.

CB binding to whole cells was determined by the oil phase separation method as described in Chapter 2. Panel (A) is a Scatchard plot of CB binding to L6 myoblasts in the presence of 400 mM-sorbitol (●) or 400 mM-D-glucose (△). Panel (B) shows the effect of L-glucose (○) or D-glucose (●) on ^{3}H-CB (0.5 μM) binding to L6 myoblasts. The specific activity of ^{3}H-CB was 1.0 x 10^{4} d.p.m./pmol.

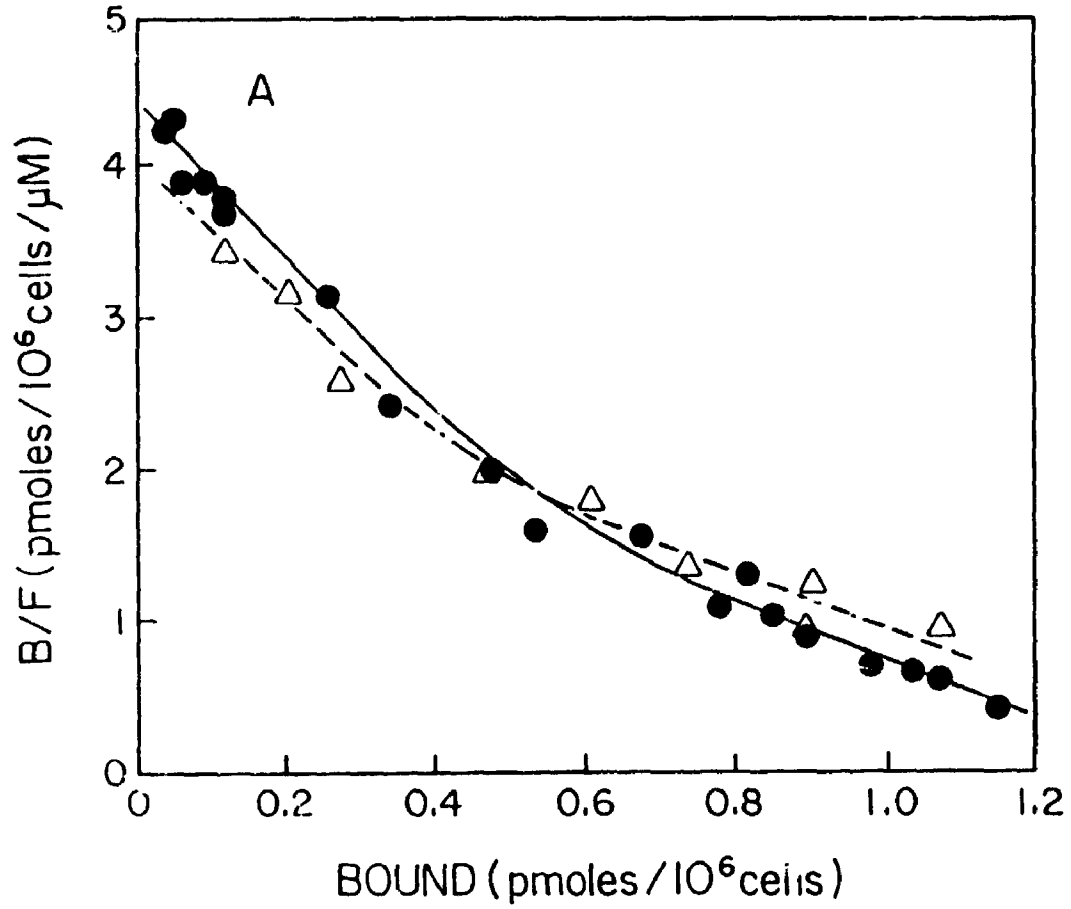
A
B/F (pmoles/10⁶cells/μM)
BOUND (pmoles/10⁶cells)
0
1
2
3
4
5
0.2
0.4
0.6
0.8
1.0
1.2

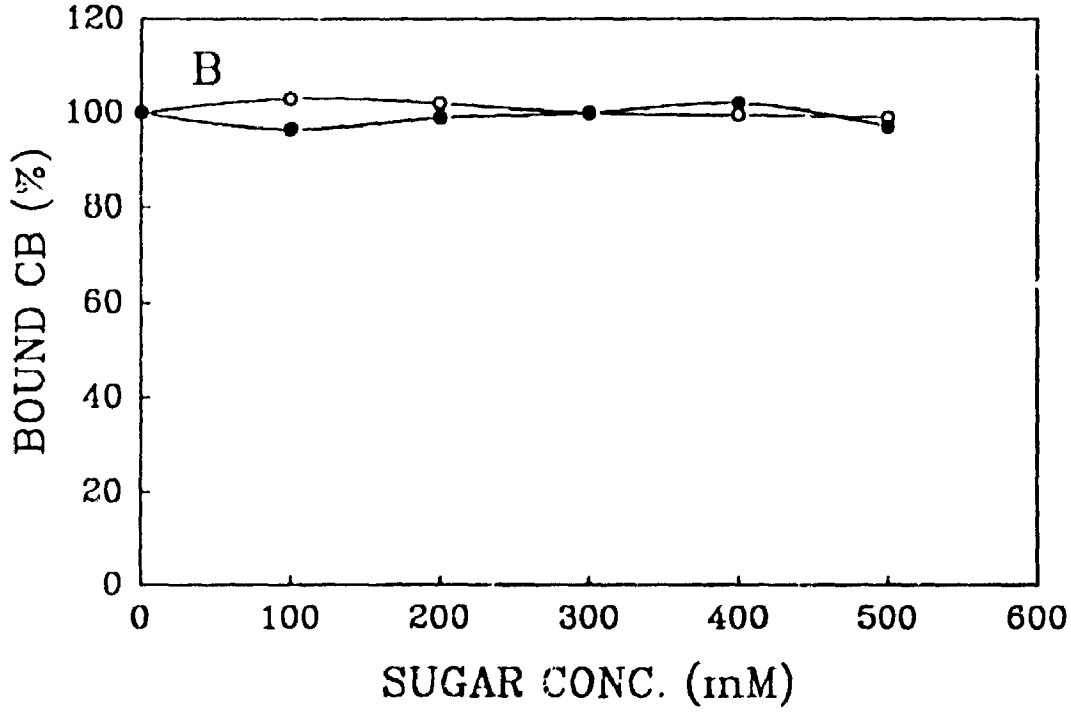
B
BOUND CB (%)
SUGAR CONC. (mM)
0
20
40
60
80
100
120
100
200
300
400
500
600

Differences between whole cells and purified plasma membrane became apparent when the effect of D-glucose on CB binding was examined. Fig. 3.4A shows that 400 mM D-glucose does not have significant effect on the binding of different concentrations of CB to glucose-grown L6 myoblasts. Similarly different concentrations of D-glucose do not have much effect on the binding of 0.5 μM of ^{3}H-CB to these cells (Fig. 3.4B). This is surprising in view of the response of these cells to the various sugar analogues (Table 3.1). The major difference between D-glucose and the sugar analogues tested is that the former is converted to different metabolites upon entrance into the cells. In order to examine the effect of D-glucose in the absence of substrate metabolism, CB binding studies were therefore carried out with purified plasma membrane, which was demonstrated to be devoid of hexokinase (Cheung and Lo, 1984). Fig. 3.5 shows that, in the presence of 400 mM D-glucose, the K_d values of CB_H and CB_L are 0.10 ± 0.01 μM and 5.00 ± 0.34 μM, and the corresponding Bmax values are 4.20 ± 0.30 and 54 ± 5.70 rmol/mg protein, respectively. The ratio of the Bmax values of CB_L to CB_H is 12.9. Thus while D-glucose does not have much effect on the binding affinity of CB_H, it reduces the latter's binding capacity by 63%; however, the reverse is true for CB_L (Table 3.4). This study shows that D-glucose can inhibit CB binding to plasma membrane.

3.3.6 Effects of Sugar Phosphates on CB Binding.

Data presented above suggest that the lack of effect of D-glucose on CB binding to whole cells may be due to the presence of glucose metabolites, such as glucose 6-P. When cells were incubated with 400 mM D-glucose under the CB binding conditions, the intracellular concentrations of free sugar and sugar phosphate were found to be around 200 mM and 30 mM, respectively. The effect of glucose 6-P was therefore tested. Table 3.2 shows that 40, 100 and 150 mM glucose 6-P can bring about 41, 77 and 103% activation of CB binding to the

Fig. 3.5 Effect of D-glucose on CB Binding to Purified Plasma Membrane from Glucose-grown L6 Myoblasts.

CB binding to plasma membrane was carried out as described in Fig. 3.2 and in the text. (●) and ( ) represent CB binding in the presence of 400 mM sorbitol and 400 mM D-glucose, respectively.

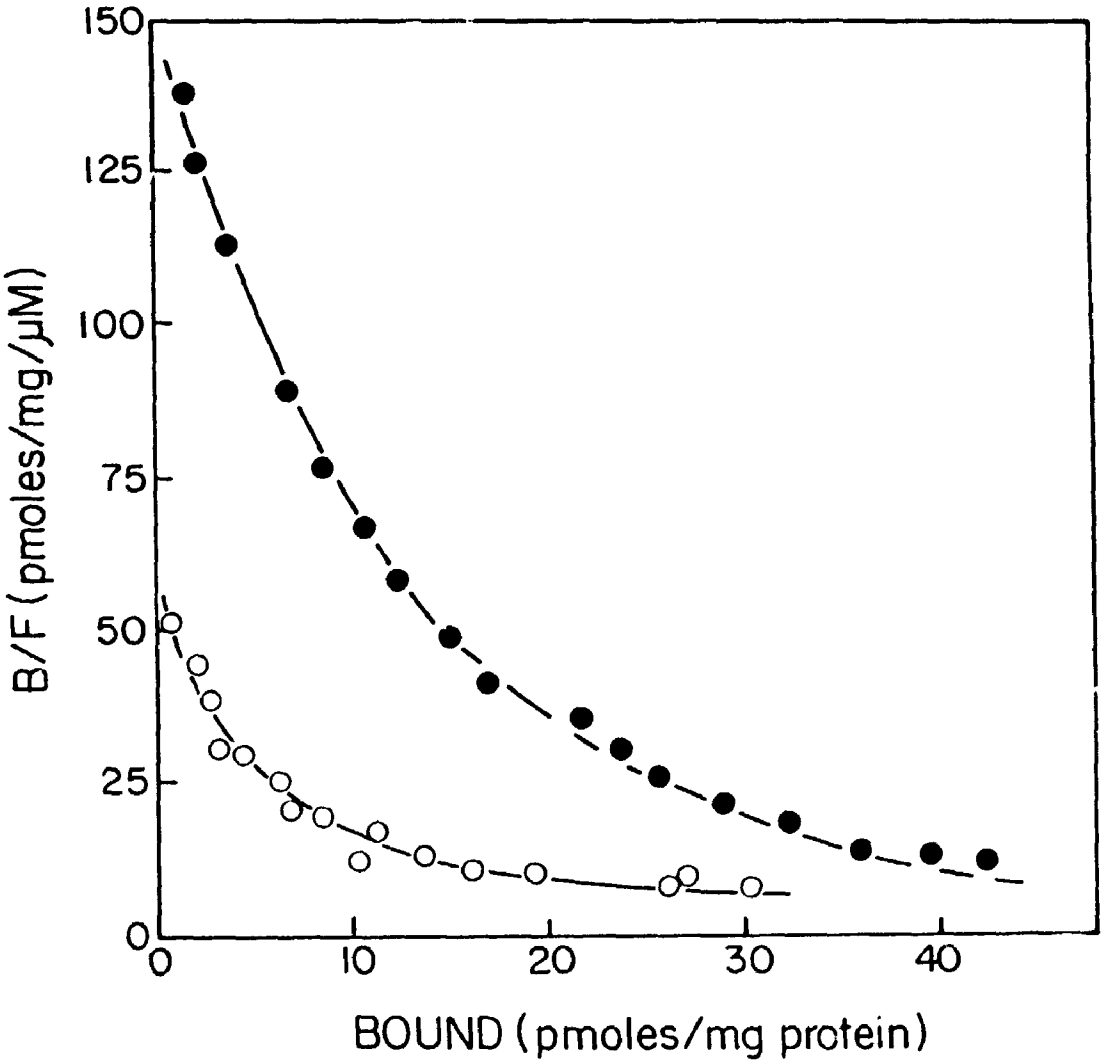
150
125
100
75
50
25
0
B/F (pmoles/mg/μM)
0
10
20
30
40
BOUND (pmoles/mg protein)

Table 3.2 Effects of Sugars and Sugar Phosphates on CB Binding to Glucose-grown L6 Myoblasts and to their Plasma Membrane.

Experiments were carried out as described in the text. The concentration of ^{3}H-CB used in this study was 0.5 μM. The control value of whole cell studies was 0.85 ± 0.01 pmol/10^6 cells, and the specific activity of the radioactive CB was 2.4 x 10^3 d.p.m./pmol. In the case of the plasma membrane studies, the control value was 16.0 ± 0.42 pmol/mg of protein, and the specific activity of the radioactive CB was 1 x 10^4 d.p.m./pmol. Abbreviations: N.D., not determined; 6-P, 6-phosphate.

Addition	CB bound (%)	
	Whole cells	Plasma membrane
Control	100 ± 1.1	100 ± 2.6
D-glucose (0.4 M)	89 ± 2.0	43 ± 2.0
Glucose 6-P		
40 mM	101 ± 2.5	141 ± 3.2
100 mM	108 ± 3.5	177 ± 1.0
150 mM	99 ± 1.5	203 ± 3.0
D-glucose (0.4 M) + glucose 6-P (40 mM)	N.D.	86 ± 2.1
dGlc (0.4 M)	59 ± 4.7	43 ± 2.0
dGlc 6-P		
40 mM	96 ± 0.5	104 ± 2.7
100 mM	101 ± 4.5	113 ± 1.0
150 mM	105 ± 2.5	120 ± 6.1
dGlc (0.4 M) + dGlc 6-P (45 mM)	N.D.	53 ± 2.1

plasma membrane, respectively. When plasma membrane CB binding studies were carried out in the presence of 400 mM D-glucose and 40 mM glucose 6-P, only 14% inhibition was observed under this condition (Table 3.2). This is similar to the effect of D-glucose on CB binding to whole cells. It is therefore conceivable that the lack of significant inhibition by D-glucose on CB binding to whole cells may be due to the activation of CB binding by D-glucose 6-P. Table 3.2 also shows that glucose 6-P has no effect on CB binding to whole cells, this indicates that the glucose 6-P binding site is not accessible to the external environment.

Table 3.2 shows that dGlc differs fro. D-glucose in its inhibition of CB binding to whole cells. This suggests that dGlc and its metabolite may be acting on the CB binding sites in a different manner. As also shown in Table 3.2, similar to D-glucose 6-P, dGlc 6-P has no effect on CB binding to whole cells. On the other hand, dGlc 6-P is not as effective as D-glucose 6-P in activating CB binding to the plasma membrane; 40, 100 and 150 mM dGlc 6-P could bring about only 4, 13 and 20% activation of specific CB binding respectively. While 400 mM dGlc inhibits CB binding to the plasma membrane by about 57%, the inclusion of 45 mM dGlc 6-P did not cause significant changes in CB binding (Table 3.2). The extent of inhibition in the presence of both dGlc and dGlc 6-P was quite similar to that of whole cells. Thus this study shows that while D-glucose and dGlc behave similarly in their ability to inhibit CB binding to plasma membranes, their phosphorylated analogues exert different effects on CB binding.

3.3.7 CB Binding Sites are not Exposed on the Cell Surface

The CB binding site of the HTer in human erythrocytes was found to reside on the inner surface of the plasma membrane (Simpson and Cushman, 1986; Deziel and Rothstein, 1984; Shanahan and D'Artel-Ellis, 1984). In order to determine their location in rat myoblasts, binding studies were carried out with trypsin treated cells. Although trypsinization resulted in detachment of cells from the plates,

Table 3.3 Effect of Trypsin Treatment on CB Binding to Glucose-grown L6 Myoblasts.

ADDITION	CONTROL (pmol/10^6 cells)	%	TRYPSIN TREATMENT (pmol/10^6 cells)	%
Sorbitol (0.4 M)	0.84 ± 0.009	100	0.84 ± 0.008	100
dGlc (0.4 M)	0.50 ± 0.040	60	0.58 ± 0.030	69
MeGlc (0.4 M)	0.53 ± 0.013	63	0.56 ± 0.020	67
L-Glucose (0.4 M)	0.81 ± 0.016	96	0.87 ± 0.026	104
D-Glucose (0.4 M)	0.75 ± 0.015	89	0.69 ± 0.007	82

Cells were trypsinized by incubating rat L6 myoblasts with 1 mg/ml trypsin for 30 min. at 37 °C. Cells were pelleted and suspended in cPBS. CB binding studies were then carried out using the oil phase separation method to remove the unbound CB as described in Chapter 2. The final concentrations of ^{3}H-CB and CE used were 0.5 μM and 10 μM, respectively. The specific activity of the radioactive CB was 2.40 x 10^3 d.p.m./pmol.

trypsinized cells still retained their viability, suggesting only cell surface components were removed by this treatment. As shown in Table 3.3, treatment of cells with 1 mg/ml trypsin did not result in a loss of CB binding activities, and the response of the CB binding sites to various sugar analogues was also not altered. This suggests that the CB binding sites are either not accessible to the external environment, or they are resistant to trypsinization. In order to distinguish between these possibilities, CB binding studies were carried out with sealed and open plasma membrane vesicles. We have previously demonstrated that rat L6 myoblast plasma membrane vesicles can be separated into fractions A (right-side-out sealed vesicles) and B (inside-out or leaky vesicles), (Cheung and Lo, 1984). These two fractions can be used to determine the effect of trypsinization on the right-side-out sealed vesicles, and on the inside-out or leaky membrane preparations. After correcting for the presence of the contaminating species, Fig. 3.6 shows that CB binding to the sealed right-side-out vesicles is relatively resistant to trypsinization; however, the reverse is true with the inside-out or leaky membrane preparations. Incubation of membrane with 50 μg/ml of trypsin for 1 hr. resulted in a 50% drop in CB binding to inside-out or leaky vesicles; whereas only a 3% drop was observed with the sealed right-side-out vesicles.

3.4 DISCUSSION

In the study of HT in human erythrocytes, fibroblasts, rat myoblasts, rat diaphragm and rat adipocytes, the evidence for the association of CB binding sites with the HTer is usually based on the inhibition of HT by CB, and the partial inhibition of CB binding to the cell membrane by high concentrations of D-glucose (Simpson and Cushman, 1986; Klip and Walker, 1983; Karnieli et al., 1981; Deziel and Rothstein, 1984; Wardzala and Jeanrenaud, 1981; Yamada et al., 1983), We have shown in this study that two specific CB binding sites can be detected in

Fig. 3.6 Effect of Trypsin on CB Binding to Sealed Right-side-out and Inside-out Plasma Membrane Preparations.

Plasma membrane fractions A and B were prepared as described in the text. Membranes were treated with trypsin (0-500 μg/ml) in 10 mM phosphate buffer, pH 7.4, containing 1 mM EDTA at 37 °C for 1 h. CB binding was initiated by adding 15 μM CE and 0.5 μM ^{3}H-CB (final concentrations). The remaining steps were carried out as described in the text. (○), shows corrected specific CB binding to right-side-out sealed vesicles; (△), represents corrected specific CB binding to inside-out vesicles or plasma membrane fragments. The specific activity of CB used was 10^4 d.p.m./pmol.

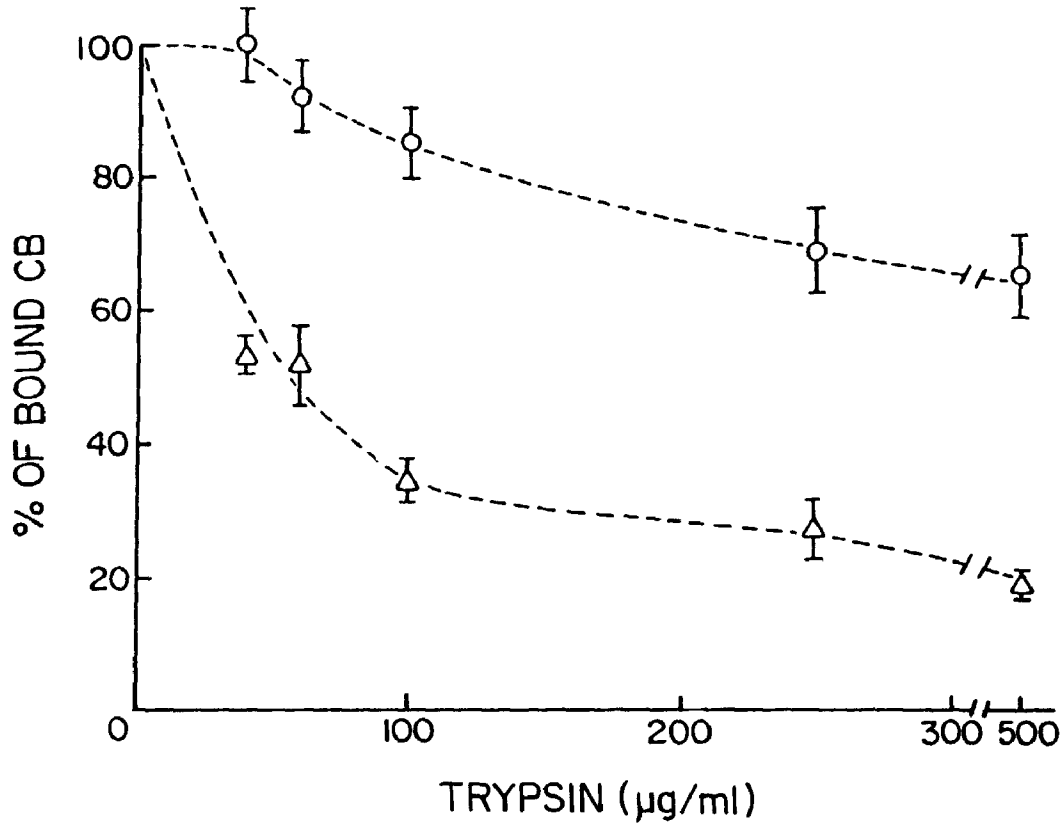
100
80
60
40
20
0
% OF BOUND CB
100
200
300
500
TRYPSIN (µg/ml)

purified rat myoblast plasma membrane preparations (Fig. 3.2). More importantly, these two sites are also sensitive to D-glucose; 400 mM D-glucose reduces the Bmax value of CB_H from 11.8 to 4.2 pmol/mg protein, and increases the Kd value of CB_L from 1.54 to 5.00 μM (Table 3.4). The observed inhibitory effect of D-glucose on these two CB binding sites can therefore be taken as an indication that these two sites are associated with the HTers in rat L6 myoblasts. More convincing proof comes from the demonstration that the mutant defective in HAHT is also altered in CB_L (Table 3.4).

Chapter 2 shows that CB binding studies with whole cells can provide valuable information on the type and level of CB binding sites present in the mutant and L6 cells grown under different conditions. Data presented in the present study also indicate similar information can be obtained using purified plasma membrane preparations. (i) Both CB_L and CB_H can be detected in purified plasma membrane and in whole cells (Table 3.4). (ii) Plasma membrane binding studies yielded K_d values of 0.10 and 1.54 μM for CB_H and CB_L, respectively; these values are quite similar to those determined by whole cell studies (Table 3.4). (iii) Both whole cell and plasma membrane studies show that CB binding can be inactivated by phloretin, dGlc and MeGlc. It should be noted in both cases very high sugar concentrations are required to bring about significant inhibition of CB binding. (iv) Both whole cell and plasma membrane binding studies indicate that CB_L is defective in mutant D23. Thus the above findings indicate that plasma membrane studies reflect fairly closely the CB binding properties of whole cells.

One of the technical problems with purified plasma membrane vesicles is the limited amount that can be isolated. For example, only around 18% of the total plasma membrane can be recovered by our purification procedure. This represents roughly 1 mg plasma membrane protein from 1.4×10^8 cells, this is equivalent to cells obtained from fifteen to twenty 140 mm diameter plastic plates. This problem

Table 3.4 CB Binding Properties of Whole Cells and Different Membrane Fractions

	CB_H		CB_L		
CONDITIONS	K_d	B_{max}	K_d	B_{max}	CB_L/CB_H
WC_{GL6}	0.11	0.40	1.01	1.06	2.65
PM_{GL6}	0.10	11.8	1.54	43.8	3.71
PM_{GD23}	0.13	11.4	4.18	18.1	1.59
$PM_{GL6+0.4\ M\ D\text{-}GLU}$	0.10	4.20	5.00	54.0	12.9
$HDMF_{GL6}$	0.09	6.10	1.49	22.6	3.70
$LDMF_{GL6}$	0.11	1.75	1.60	6.75	3.86

CB binding studies with whole cells and different membrane fractions and determinations of K_d (μM) and B_{max} (pmol/10^6 cells for whole cell binding or pmol/mg protein for membrane binding) were described in Chapter 2 & 3. Abbreviation: WC_{GL6}, glucose-grown L6 whole cells; PM_{GL6}, plasma membrane from glucose-grown L6; PM_{GD23}, plasma membrane from glucose-grown mutant D23; $PM_{GL6+0.4\ M\ D\text{-}Glu}$, plasma membrane from glucose-grown L6 in the presence of 0.4 M D-glucose; $HDMF_{GL6}$, high density microsomal fraction from glucose-grown L6; $LDMF_{GL6}$, low density microsomal fraction from glucose-grown L6.

is compounded by the observation that HT activity drops dramatically at high cell density (see Chapter 6). This essentially limits the number of experiments that can be done. Despite this limitation, studies with plasma membrane can generate some valuable information that cannot be otherwise obtained through whole cell studies.

The location of the specific CB binding sites can be determined through the use of various membrane preparations. Whole cell binding studies indicate that two specific CB binding sites are present in rat L6 myoblasts. If only one of these sites is associated with the plasma membrane, and the other with another membrane, then the ratio of the Bmax values of the two sites should vary considerably in different membrane preparations. Binding studies with various membrane preparations indicate that both CB binding sites can be detected in plasma membrane, HDMF and LDMF. The ratios of the Bmax values of CB_L to CB_H in the plasma membrane and LDMF are 3.71 and 3.86, respectively (Table 3.4). Since these two preparations are relatively free of contamination of each other, it may be surmised that both CB_H and CB_L are present in similar proportion in both plasma membrane and LDMF. It should be noted that while LDMF contains not more than 2-5% contamination by the plasma membrane (as judged by the level of Na^+, K^+-ATPase), the specific activities of both CB binding sites in LDMF are about 15% of those in the plasma membrane. This is different from rat adipocytes, in which the specific activity of the CB binding sites on the microsomes is ten times higher than that on the plasma membrane (Simpson and Cushman, 1986). On the other hand, similar levels of specific CB binding activity are found in the plasma membrane and microsomes of rat diaphragm muscle (Wardzala and Jeanrenaud, 1981). Thus there seems to be considerable variation in the distribution of specific CB binding activity in these membrane fractions of different cell types. It is of interest to note that undifferentiated rat myoblasts also differ from adipocytes in that they do not respond to insulin treatment (even though

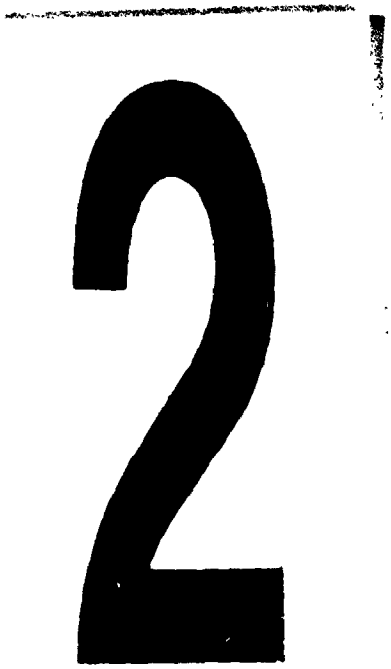

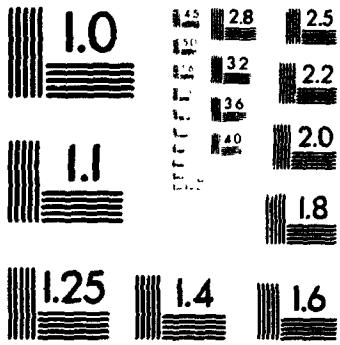
1.0
1.1
1.25
1.4
1.6
1.8
2.0
2.2
2.5
2.8
3.2
3.6
4.0

differentiated myoblasts can respond to insulin stimulation) (Klip et al., 1983a).

Plasma membrane vesicles are also useful in determining the orientation of the CB binding sites. Table 3.3 and Fig. 3.6 show that while CB binding to whole cells and sealed right-side-out vesicles is resistant to trypsinization, its binding to membrane fragments or inside-out vesicles can be abolished by trypsinization. This suggests a cytoplasmic location for the CB binding sites. A similar observation has also been made by other workers in the CB binding to human erythrocyte plasma membrane (Deziel and Rothstein, 1984; Shanahan and D'Artel-Ellis, 1984). It should be noted that the above observation can also be explained by the possibility that trypsin treatment of a component on the membrane inner surface may lead to the release of externally bound CB. If this were the case, then the present study serves to illustrate the orientation of the site of trypsin attack. Further studies on the orientation of CB binding sites or trypsin cleavage sites will be discussed in Chapter 4.

The use of plasma membrane also allows one to examine the effect of substrate metabolites on CB binding. Although D-glucose does not exert much effect on CB binding to whole cells (Fig. 3.4), it does inhibit CB binding to the plasma membrane (Fig. 3.5). This discrepancy is found to be due to the activation of CB binding by D-glucose 6-P (Table 3.2). Unlike glucose 6-P, dGlc 6-P does not have much effect on CB binding (Table 3.2). This may explain why the inhibitory effect of dGlc can be observed in whole cells (see Chapter 2), even though dGlc is accumulated and phosphorylated to a similar extent as D-glucose inside the cells. Whole cell studies reveal that this glucose 6-P binding site is not accessible on the cell surface. The above findings sugge · that a regulatory mechanism by sugar metabolites may be involved in CB binding.

Data presented in the previous and present chapters reveal some interesting findings on the regulatory mechanism of CB binding. Two models can be proposed

for the regulation of CB binding. Model A suggests that transport substrate may inhibit CB binding by competitive inhibition. Model B predicts CB binding may be regulated by an allosteric mechanism. Both whole cell and plasma membrane binding studies tend to support the second model. (i) If the ligands are competing for the same site, their K_d and K_i values should be quite similar, as seen in the case of different sugars competing for the same transporter (D'Amore and Lo, 1986a). Fig. 2.4 and 3.2 show that the K_d values of CB binding differ significantly from the K_i values of CB for both transport processes (Fig. 2.1). For example, the K_d value for CB_L in whole cells is 1.01 μM, whereas the K_i of CB for the corresponding transport system is 0.16 μM. (ii) If competitive inhibition is involved, about 50% inhibition of CB binding should be observed when the substrate:CB ratio is around that of the affinity ratios. Both whole cells and plasma membrane CB binding studies indicate that much higher concentrations of transport substrates are required to bring about 50% inhibition of CB binding. (iii) Fig. 3.5 shows that D-glucose affects the binding capacity but not the binding affinity of CB_H. This reduction in binding capacity suggests that D-glucose is not competing for the CB binding site on LAHT. (iv) Table 3.2 indicates that CB binding can be activated by D-glucose 6-P. The only evidence that may support Model A comes from the effect of D-glucose on CB_L (Fig. 3.5). However, this effect is observed at a very high concentration of D-glucose (400 mM). So this decrease in the binding affinity may not be due to competitive inhibition. The above findings suggest that a CB binding may be regulated in an allosteric manner; it is inhibited by specific HT substrates and activated by glucose 6-P. In agreement with this notion, it was also observed that high concentration of D-glucose had little effect on CB binding to various mammalian cells, such as normal and transformed mouse cells (Atlas and Lin, 1976), rat hepatoma cells (Plagemann et al., 1977) and fat cells (Czech, 1976b). It was suggested that D-glucose and CB might be binding to different sites

on the HTer (Czech, 1976b; Shanahan and Czech, 1977a,b; Greenbaum et al., 1977; Jung et al., 1986).

CHAPTER 4

PHOTOAFFINITY LABELLING OF HEXOSE TRANSPORTERS IN UNDIFFERENTIATED RAT L6 MYOBLASTS BY CYTOCHALASIN B

4.1 INTRODUCTION

The eukaryotic HTers have been identified through the use of affinity labels, reconstitution studies (Kasahara and Hinkle, 1976, 1977) and antibodies directed against human red cell HTer (Wang, 1987; Biber and Lienhard, 1986; Haspel et al., 1985; Allard and Lienhard, 1985). Photoaffinity labels such as cytochalasin B (CB) (Shanahan, 1982; Pessin et al., 1984), aryl azide derivatives of D-glucose (Shanahan et al., 1985), 6-N-(4-azido-2-hydroxyl-3,5-diiodobenzoyl)-D-glucosamine (AHDB-GlcN) (Weber and Eichholz, 1985), forskolin (Shanahan et al., 1987) and its derivative, 3-iodo-4-azidophenethylamido-7-O-succinyldeacetylforskolin (IAPS-forskolin) (Wadzinski et al., 1987) and azido adenosine (Jarvis et al., 1986) etc. have been used to identify the HTer. Of these reagents, CB was shown to be a particularly valuable natural photoaffinity label. Upon photolysis by intensive UV light, CB could be covalently linked to membrane components with apparent molecular weights ranging from 40 to 70 kDa (band 4.5) in human erythrocytes (Shanahan, 1982). The inhibition of CB photoincorporation into this region by 700 mM D-glucose but not L-glucose suggested that the components labelled by CB might be associated with the human rbc HTer (Shanahan, 1982). Proteolytic digestion of the labelled transporter suggested that the CB binding site is located near the C-terminal end of the protein, and is accessible from the cytoplasmic surface of the membrane (Walmsley, 1988; Shanahan and D'Artel-Ellis, 1984; Deziel and Rothstein, 1984). CB has also been used to identify the HTers in other cell types such as chick-embryo fibroblasts (Pessin et al., 1984), rat adipocytes (Carter-

Su and Okamoto, 1985), human placenta (Johnson and Smith, 1982), rat skeletal muscle (Klip and Walker, 1983) and erythrocytes from neonatal pig (Craik et al., 1988). It is interesting to note that more than one D-glucose inhibitable CB photolabelled component has been identified in chick embryo fibroblasts (Pessin et al., 1984) and rat adipocytes (Horuk et al., 1986). Most of the D-glucose-inhibitable CB photolabelled components in various mammalian cells are found to have molecular weights ranging from 40 to 70 kDa.

The previous Chapters have demonstrated that two CB binding sites (CB_H and CB_L) are present in undifferentiated rat L6 myoblasts, and that CB_H and CB_L are associated with LAHT and HAHT, respectively. Furthermore, about 15% of CB binding sites in the plasma membrane were found in the low density microsomal fraction (LDMF). However, not much is known about the structure of the CB binding components.

There is increasing evidence that more than one type of HTer may be present in mammalian cells, and that the HTer is tissue specific. It will be interesting and necessary to further characterize and understand the structure and function of the two HT systems in rat L6 myoblasts. Thus in this chapter, we reported detailed studies of CB photoaffinity labelling of intact L6 cells and various types of membrane fractions. The correlation between CB photolabelled components and the two HT systems were discussed.

4.2 MATERIALS AND METHODS

4.2.1 Materials

[4-^{3}H(n)] CB (22 Ci/mmol) was purchased from Amersham Canada Ltd. Ready Protein Liquid Scintillation Cocktail was from Beckman Instruments Inc. Cytochalasin B and E, glucose and its analogues, trypsin (type IX) and other chemicals used were from Sigma Chemical Co.

4.2.2 CB Photolabelling of Intact Rat L6 Myoblasts

Cells were grown on tissue-culture dishes (20 mm x 150 mm; seeded with 1.0 x 10^6 cells/dish) in glucose medium and harvested before reaching confluence (after 2 days). Cells in each plate were dissociated by incubation with 5 ml of citrate saline at 37°C for 20 min. After centrifugation at 1000 X g for 5 min, the cell pellet was suspended in cPBS to a concentration of around 3.3 x 10^7 cells/ml. 150 μl of this cell suspension was incubated with an equal volume of cPBS containing 2 μM ^{3}H-cytochalasin E (22 Ci/mmol) and 200 μM cytochalasin E (CE) in the dark for 40 min. at 37°C; sugar analogues were included whenever necessary. Unless otherwise indicated, the reaction mixture was irradiated in a Pyrex tube (15 mm x 60 mm) embedded in ice for 35 sec. at a distance of 16 cm from a Porta-Cure 1000F elliptically-focused ultraviolet irradiator (American Ultraviolet Company). In order to avoid the uneven distribution of UV light along the line perpendicular to the lamp caused by the reflector, samples were always arranged in parallel to the UV lamp during photolysis. To minimize the difference in UV exposure resulting from slight differences in timing and other factors in various irradiations, photolabelling studies shown in each set of figures were carried out in the same experiment with the same number of cells, and under the same single UV exposure. The irradiated cell suspension was diluted with 40 volumes of ice-cold cPBS, centrifuged at 40,000 X g for 10 min. at 4 °C, and washed once with 12 ml of ice-cold cPBS. Cell pellets were solubilized in Laemmli SDS sample buffer by passing through a 27-gauge ½-inch needle 5-7 times at room temperature. Unless otherwise indicated, SDS-PAGE was carried out on 1.5 mm thick, 11.25% slab gels (Laemmli, 1970), and the SDS-solubilized samples were not usually heated. After electrophoresis, the gels were stained with Coomassie blue, destained and sliced into 2 mm fractions The gel slices were digested with 250 μl of 30% H_2O_2 at 80 °C for 4 hours in Beckman Mini Poly-Q vials, cooled and the amount of

radioactivity in each vial was determined by scintillation counting in 4.5 ml scintillation fluid supplemented with 0.7% acetic acid. The data presented were results of representative experiments which were repeated at least twice and usually three or more times. Results were found to be very consistent in all cases.

4.2.3 Isolation of Plasma Membrane from Human Erythrocytes

Out-dated human red blood cells were obtained from the University Hospital (London, Ontario). Membranes were prepared by the method of Steck and Kant (1974). Briefly, red cells were washed 3-4 times with phosphate-buffered saline (PBS), and hemolyzed in 5 mM phosphate buffer (pH 8.0). Plasma membranes were pelleted by centrifugation at 27,000 X g for 10 min., washed 3-4 times with 5 mM phosphate buffer (pH 8.0) and stored at -86 °C.

4.2.4 Preparation of Plasma Membrane and Microsomal Fractions from Rat Myoblasts

Rat myoblast plasma membrane and microsomal fractions were prepared as previously described (Cheung and Lo, 1984).

4.2.5 CB Photolabelling of Plasma Membranes

Photolabelling of plasma membranes was performed as described previously (Shanahan, 1982) with some modifications. Plasma membrane (250-500 μg) in 150 μl sodium phosphate buffer (10 mM, pH 7.4) was equilibrated with an equal volume of phosphate buffer containing 2 μM CB (22 Ci/mmol) and 200 μM CE in the dark for 90 min. at 0°C. Sugar analogues were included in this buffer whenever necessary. The membrane solutions were photolyzed for 15-20 sec in 15 mm x 60 mm Pyrex test tubes embedded in ice with a Porta-Cure 1000F elliptically focused ultraviolet irradiator at a distance of 17 cm from the lamp. The same measures as described for the whole cell photolabelling were taken to minimize any differences in UV exposure. The irradiated membrane preparations were diluted with 40 volumes of phosphate buffe centrifuged at 40,000 X g for 25 min. at 4°C, and

washed once with the same buffer. The final pellets were then solubilized in SDS sample buffer at room temperature, unless otherwise indicated. The amount of ^{3}H-CB bound to various proteins was determined by the method described for whole cells.

4.2.6 CB Photolabelling of Microsomal Fractions

Photolabelling of the low density microsomal fraction (LDMF) was carried out as described for the plasma membrane, except that after photolysis, LDMF was transferred to TLA-100.2 centrifuge tubes (Beckman), diluted 4 times with phosphate buffer, and centrifuged at 436,000 X g for 45 min. at 4 °C. Membrane pellets were then solubilized in SDS sample buffer at room temperature. The amount of ^{3}H-CB bound to various proteins was determined as described for whole cells.

4.2.7 Trypsinization of Intact Whole Cells and Membrane Fractions

Intact L6 myoblasts (5 x 10^6 cells) were treated with trypsin (20 μg/ml) in 5 ml of cPBS at 23 °C for 30 min. Trypsinized cells were diluted with cPBS and centrifuged at 1,000 X g for 5 min. Cell pellets were suspended in cPBS and photolyzed in the presence of ^{3}H-CB as described earlier. In some experiments, ^{3}H-CB labelled L6 cells were incubated with 20 μg/ml of trypsin in 600 μl of cPBS at 23 °C for 30 min. The reaction was terminated by adding cPBS containing 1 mM PMSF and centrifuged at 40,000 X g for 10 min at 4 °C. The pellets were solubilized and analyzed by SDS-PAGE as described earlier.

Trypsinization of plasma and microsomal membranes was carried out after photolysis. ^{3}H-CB labelled plasma membranes or microsomal fractions were incubated with 20 or 100 μg/ml of trypsin in 600 μl of phosphate buffer (10 mM, pH 7.4) at 23 °C for 30 min; this was then followed by the addition of phosphate buffer (pH 7.4) containing 1 mM PMSF. Centrifugation, solubilization and analysis by SDS-PAGE were carried out as described for plasma membrane and LDMF,

respectively.

4.2.8 Other Procedures

For other methods and materials, see previous chapters.

4.3 RESULTS

4.3.1 Photoaffinity Labelling of Glucose-grown L6 Myoblasts

Before initiating CB photoaffinity labelling studies, we first determined the optimal exposure time required for photo-incorporation. Intact glucose-grown rat L6 myoblasts were incubated with 1 μM ^{3}H-CB and 100 μM CE; the latter was used to block CB binding to actin (Shanahan, 1982). Cells were then irradiated with a 1000 watt UV lamp for 15, 30, 60 and 90 sec, respectively, after which the total cell extracts were analyzed by SDS-PAGE. As shown in Fig. 4.1, ^{3}H-CB was found to be associated mainly with two major peaks (43 and 51 kDa), and two minor ones (35 and 18 kDa). Besides raising the background level of radioactivity, longer photolysis time also increased the amount of CB incorporated into these peaks, and also into the very high molecular weight region (Fig. 4.1). The latter was probably due to increased protein cross-linking upon prolonged photolysis. It should also be noted that while the labelling of the 43 kDa peak (which coincided with that of actin) was much lower than that of the 51 kDa peak after a short exposure time (15 sec.), the labelling of the 43 kDa peak was similar to or higher than that of the 51 kDa peak after prolonged photolysis (90 sec.). This indicates that an incomplete inhibition of CB photolabelling into actin in whole cells may occur under longer time of exposure. In other words, the labelled 43 kDa peak may contain actin upon prolonged photolysis.

Previous studies with human erythrocyte, human placenta and other mammalian cells revealed that a 17 - 18 kDa fragment was generated from the HTer upon trypsinization of the cell membranes (Haspel et al., 1985; Shanahan et

Fig. 4.1 Effect of Exposure Time on ^{3}H-CB Photolabelling of Intact Glucose-grown Rat L6 Myoblasts.

Photolabelling of intact L6 cells was carried out as described in the text. Intact cells were photolyzed for 15 (▲), 30 (◇), 60 (●) and 90 (○) sec. The photolyzed cells were solubilized in SDS sample buffer without heating. Electrophoresis was performed on a 11.25% gel as described under "Methods and Materials". The molecular weights (M_r x 10^{-3}) of marker proteins are indicated on the top of the panel.

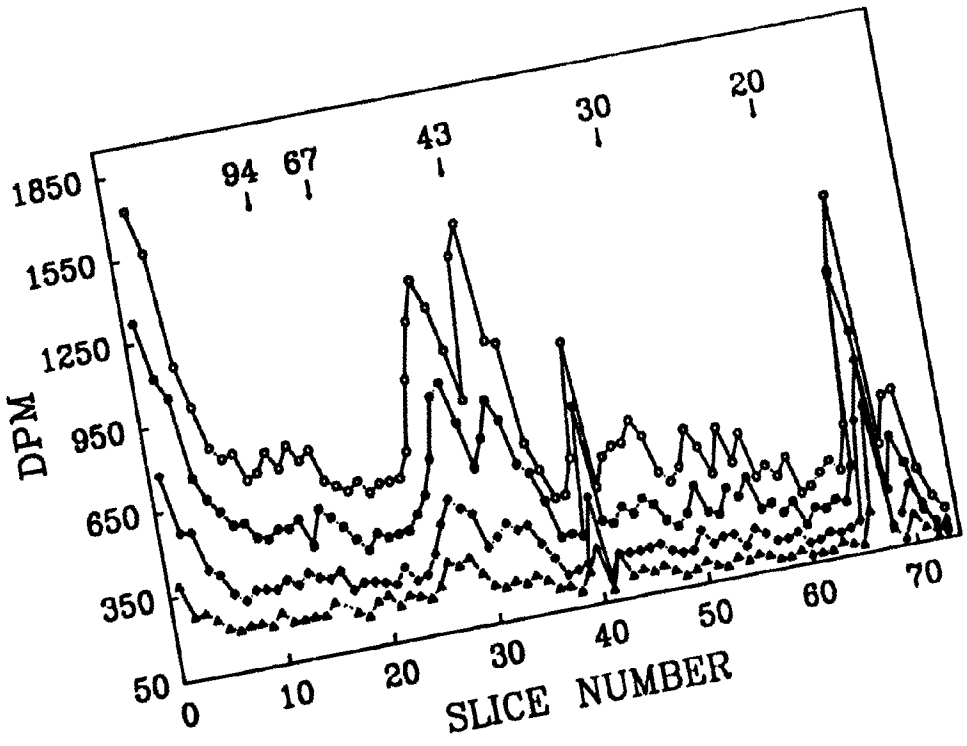
94
67
43
30
20
1850
1550
1250
950
650
350
50
DPM
0
10
20
30
40
50
60
70
SLICE NUMBER

al., 1987; Shanahan and D'Artel-Ellis, 1984; Deziel and Rothstein, 1984; Wadzinski et al., 1988; Haspel et al., 1988). Thus the 18 kDa CB-labelled peak observed in Fig. 4.1 might be the degradation product of the HTer. If this were the case, the observed increase in 18 kDa protein could be taken as an indication that prolonged photolysis might result in increased degradation of the HTer. Thus in order to minimize protein cross-linking, non-specific photo-incorporation and possible degradation, an exposure time of 30-40 sec. was chosen for CB photolabelling with intact L6 myoblasts in subsequent experiments.

Two pieces of circumstantial evidence suggest that CB photolabelled components with molecular weights ranging from 40 to 60 kDa (or referred to as CB_{50}) may contain the HTer. First, their molecular weights are similar to those of HTers found in other eukaryotic cells (Klip et al., 1983b; Pessin et al., 1984; Shanahan, 1982; Shanahan et al., 1985; Weber and Eichholz, 1985; Shanahan et al., 1987; Dick et al., 1984; Wadzinski et al., 1988). Second, photo-incorporation into this region could be inhibited by substrates of the rat myoblast HT systems; about 35%, 27%, and 18% inhibition of CB incorporation into this region could be brought about by 0.4 M dGlc, MeGlc, and D-glucose, respectively (Table 4.1).

Recent CB binding studies with whole cells, and sealed right-side-out and leaky inside-out vesicles (see Chapter 3), suggest that the majority of the CB binding sites are not accessible to the external environment. However, the location of the trypsin cleavage site has not been clearly established. It is possible that cleavage of the HTer on the cell surface may not affect the amount of CB bound on the cytoplasmic side. In order to clarify the situation, the effect of trypsinization on the sizes of the labelled proteins was tested. Trypsinization of whole cells before photolysis was found to have no effect on the amount of CB incorporated into CB_{50} (Fig. 4.2a), thus suggesting the lack of a cell surface-accessible trypsin cleavage site on the HTer. On the other hand, trypsinization of

Table 4.1 Effects of Glucose and Glucose Analogues on ^{3}H-CB Photolabelling into the 40-60 kDa Region under Different Conditions

Photolabelling of intact cells and membranes was performed as described in the text. The percentage inhibition of ^{3}H-CB photolabelling in the 40-60 kDa region in each condition was calculated relative to the photolabelling in the presence of the same concentration of L-glucose. The concentrations of glucose and glucose analogues used were indicated inside the parentheses. Abbreviations: WC_{GL6}, glucose-grown L6 whole cells; PM_{GL6}, plasma membrane from glucose-grown L6; PM_{FL6}, plasma membrane from fructose-grown L6; $LDMF_{GL6}$, low density microsomal fraction from glucose-grown L6; PM_{GD23}, plasma membrane from glucose-grown mutant D23; PM_{GF72}, plasma membrane from glucose grown mutant F72; N.D., not determined.

Condition	[CB] (μM)	Inhibition (%)			
		D-glucose	dGlc	MeGlc	dGlc+MeGlc
WC_{GL6}	1.0	18.0±3.3 (0.4 M)	35.0±2.7 (0.4 M)	27.0±3.6 (0.4 M)	N.D.
PM_{GL6}	0.2	N.D.	51.5±2.5 (0.4 M)	57.5±4.5 (0.4 M)	N.D.
	1.0	57.0±1.3 (0.6 M)	58.6±2.7 (0.4 M)	47.4±2.1 (0.4 M)	70.0±2.5 (0.4 M)
			58.0±6.0 (0.8 M)	49.0±2.3 (0.8 M)	76.0±3.0 (0.8 M)
PM_{FL6}	1.0	65.3±2.5 (0.4 M)	65.5±1.0 (0.4 M)	45.2± .9 (0.4 M)	N.D.
$LDMF_{GL6}$	1.0	8.0±2.1 (0.4 M)	N.D.	N.D.	N.D
PM_{GD23}	1.0	42.4±3.3 (0.6 M)	40.7±1.0 (0.5 M)	37.3±1.0 (0.5 M)	N.D.
PM_{GF72}	1.0	52.9±2.9 (0.5 M)	55.6±2.4 (0.5 M)	41.0±2.0 (0.5 M)	N.D.

Fig. 4.2 Effect of Trypsinization on ^{3}H-CB Photolabelling of Intact Glucose-grown Rat L6 Myoblasts.

Intact L6 cells (5 x 10^{6}) were treated with (●) or without (○) 20 μg/ml of trypsin. Panel (a) indicates trypsinization before photolysis; whereas panel (b) indicates trypsinization after photolysis. Electrophoresis was carried out on a 5-15% polyacrylamide gradient gel.

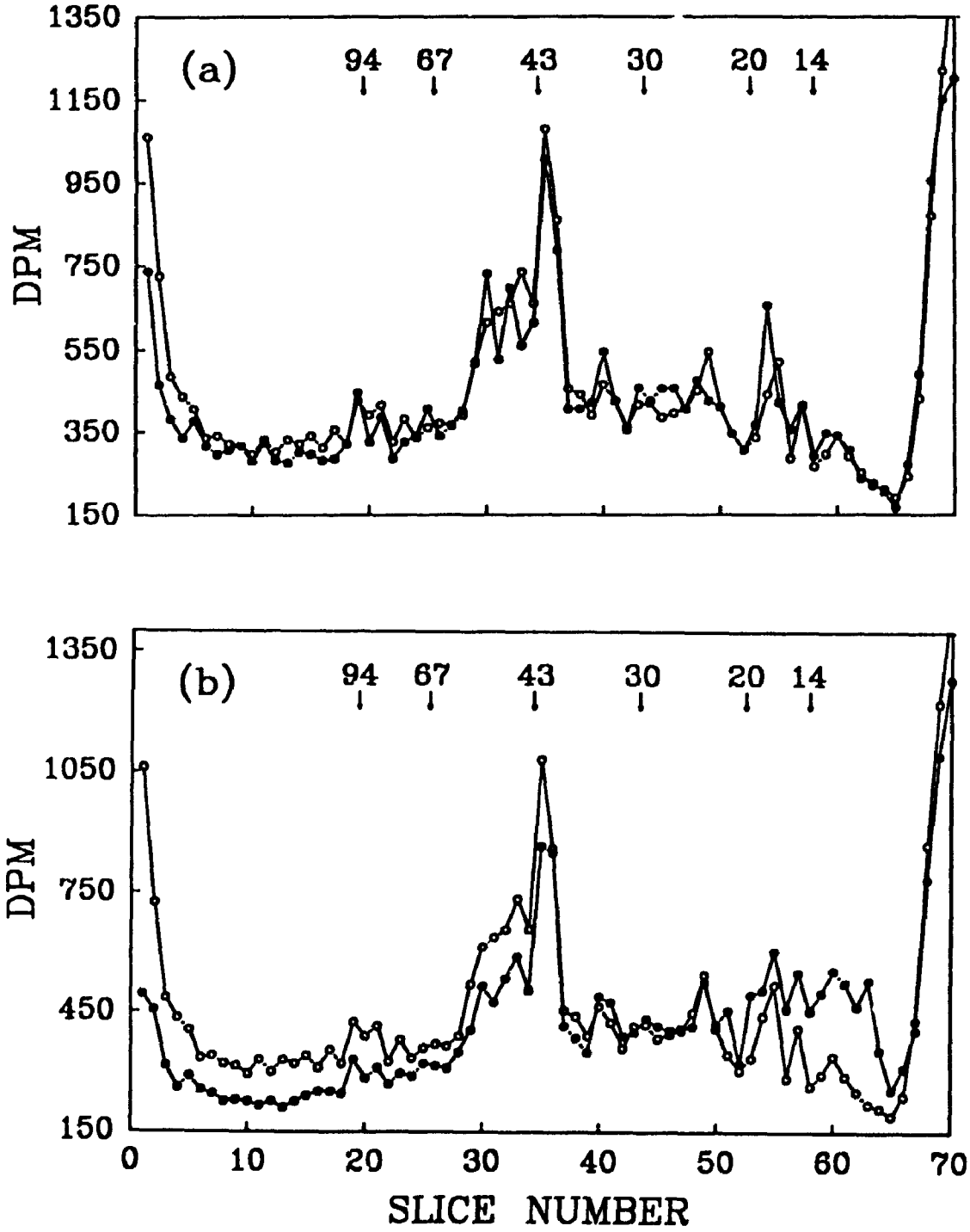
(a)
94
67
43
30
20
14
1350
1150
950
750
550
350
150
DPM
(b)
94
67
43
30
20
14
1350
1050
750
450
150
DPM
0
10
20
30
40
50
60
70
SLICE NUMBER

photolyzed cells resulted in a slight decrease of the amount of CB incorporated into CB_{50} (Fig. 4.2b), with a concomitant increase in the 12-20 kDa CB-labelled peptides. This suggests that photolysis may result in cell damage or leakage, thus allowing trypsin to gain access to the inner surface of the plasma membrane.

4.3.2 Photoaffinity Labelling of Purified Plasma Membrane from Human RBC

HTers have been found in the plasma membrane and in the low density microsomal fraction (LDMF) (Carter-Su and Okamoto, 1985; Horuk et al., 1986; Haspel et al., 1988); the distribution of these transporters is affected by various physiological and metabolic events (Carter-Su and Okamoto, 1985; Horuk et al., 1986; Haspel et al., 1988; Calderhead and Lienhard, 1988; Walker et al., 1989; Horner et al., 1987; Wheeler, 1988). Thus in order to characterize the plasma membrane HTer in the absence of various metabolic events, photolabelling studies were carried out with purified plasma membrane preparations. In view of the limited amount of plasma membrane that can be isolated from rat L6 myoblasts, we first carried out our pilot studies with purified human rbc plasma membrane. The HT system in human rbc is one of the best studied transport systems. The advantage of using human rbc is the large amount of highly purified plasma membrane that can readily be prepared.

Although not indicated here, the maximum amount of CB-labelling of human rbc plasma membrane was achieved in about 25-30 sec. In order to minimize non-specific photo-incorporation and degradation, subsequent experiments with membrane preparations were carried out with a exposure time of 15-20 sec. Fig. 4.3a shows a typical CB-labelling profile of rbc plasma membrane after photolysis with ^{3}H-CB in the presence of L-glucose or D-glucose. Similar to findings by other workers (Shanahan, 1982), the majority of radioactivity was found in the 40-70 kDa region (band 4.5). Two major peaks could be easily resolved in this region; however, it was not certain whether these two peaks were related to the HTer. The finding

Fig. 4.3 Effects of Glucose and Heating on ^{3}H-CB Photolabelling of Plasma Membrane Prepared from Human RBC.

Photolabelling of plasma membrane was performed as described in the text. Panel (a) shows photolabelling in the presence of 0.65 M D-glucose (●) or 0.65 M L-glucose (○). Membranes were solubilized at 23 °C and subjected to a 8.5% polyacrylamide gel. Panel (b) indicates the effect of heating. Photolyzed membranes were solubilized at 23 °C (○) or at 100 °C for 4 min. (●) and analyzed on a 11.25% SDS-PAGE.

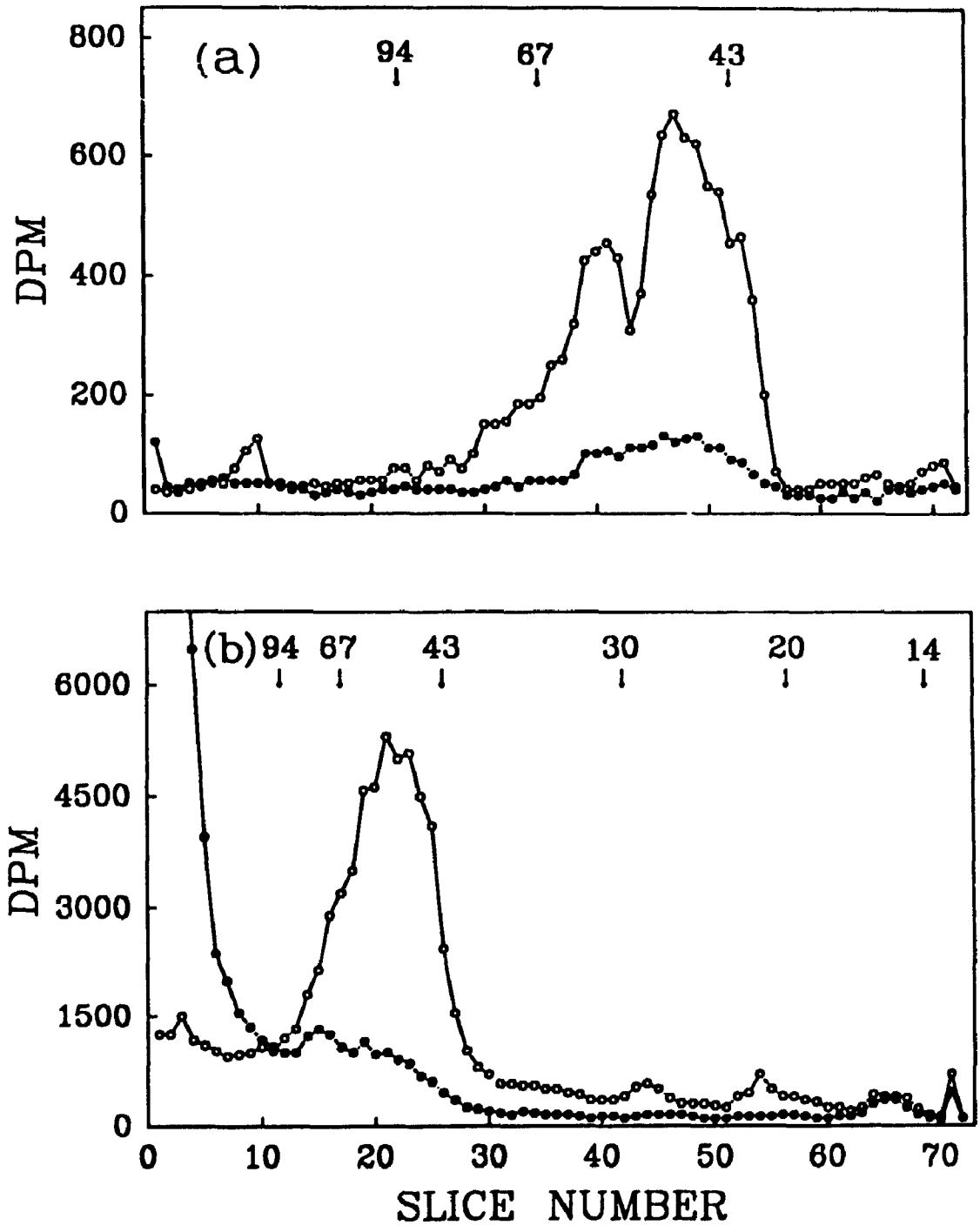
(a)
94
67
43
800
600
400
200
0
DPM
(b)
94
67
43
30
20
14
6000
4500
3000
1500
0
DPM
0
10
20
30
40
50
60
70
SLICE NUMBER

that about 85% of the photolabelling into this region can be blocked by 0.6 M D-glucose suggested that these two peaks might be related to the HTer. It is interesting to note that CB-labelling of a 220 kDa protein also displays glucose sensitivity. Similar results have been reported by other workers (Shanahan et al., 1985, 1987).

The methods of sample preparation for SDS-PAGE have been shown to affect the electrophoretic mobility of the HTer (as detected by Coomassie blue staining and immunoblotting) (Allard and Lienhard, 1985; Klip et al., 1983b) and the ^{3}H-6-[(4-nitrobenzyl)thiol]-9-ß-D-ribofuranosylpurine (NBMPR) photolabelling profile of the nucleoside transporter (Wu et al., 1983). The effects of heating on the SDS-electrophoretic mobility of the CB photolabelled proteins were therefore examined. Fig 4.3b shows when samples were heated at 100 °C for 4 min., most of the CB-labelled proteins had very high molecular weights, hardly any CB-labelled proteins could be detected in the 40-70 kDa region. It should be mentioned that a higher percentage gel was used in this experiment to separate labelled products with lower molecular weights. The two labelled peaks seen in the lower percentage gel (upper panel) appeared as a small shoulder in the higher percentage gel (lower panel) in the presence of L-glucose. Thus this observation suggested that aggregation or cross-linking of CB photolabelled components might have occurred during sample heating.

4.3.3 Photoaffinity Labelling of Purified Plasma Membrane from Glucose-grown Rat L6 Myoblasts.

Having determined the properties of CB photolabelling using human rbc plasma membranes, similar approaches were then used for purified plasma membranes from glucose-grown L6 myoblasts (PM_{GL6}). CE has been used to block CB binding to proteins other than the HTer (Shanahan, 1982). When CB photolabelling of plasma membrane was carried out in the absence of CE, with UV

exposure time of 20 sec, a very large 43 kDa peak was labelled by ^{3}H-CB (Fig. 4.4a). This peak has a molecular weight similar to actin. The addition of 100 μM CE completely block the CB labelling of this 43 kDa peak, without significantly affecting labelling of other proteins. Subsequent experiments with membrane preparations were therefore performed in the presence of 100 μM CE. It should be mentioned that in most of the CB photolabelling experiments with membrane preparations, the labelling of the 43 kDa region was hardly detectable. In some experiments, only a small shoulder or a small peak (<3% of the total labelling in CB_{50}) in the 43 kDa region was observed.

The effect of heating on the electrophoretic mobility of the CB photolabelled proteins was also examined. Fig. 4.4b shows the photolabelling profile of $PM_{GL\Phi}$ with and without heat treatment. In the absence of heat treatment, CB_{50} and some minor proteins were labelled by ^{3}H-CB. However, after heating at 100 °C for 4 min., most of the CB-labelled proteins had very high molecular weights, hardly any CB_{50} could be detected. This result is similar to that observed in human rbc plasma membrane. Interestingly, this treatment had little effect on the incorporation of CB into the 35 and 18 kDa peaks (Fig. 4.4b). It may be mentioned in passing that heat treatment seemed to have no effect on CB labelling in both plasma membrane and LDMF of rat adipocytes (Horuk et al., 1986; Matthaei et al., 1988).

Unlike intact cells, treatment of CB-photolyzed plasma membrane with 20 μg/ml trypsin reduced the amount of CB labelling in CB_{50}, with a concomitant increase of some lower molecular weight (12, 15, and 18 kDa) labelled proteins (Fig. 4.5a). Since the higher molecular weight labelled proteins were also reduced, the observed increase in 12, 15, and 18 kDa labelled proteins might be generated from both CB_{50} and the higher molecular weight labelled proteins. The use of a higher concentration of trypsin (100 μg/ml) resulted in a further reduction in CB_{50}

Fig. 4.4 Effects of CE and Heating on ^{3}H-CB Photolabelling of Plasma Membrane Prepared from Glucose-grown L6 Myoblasts.

Photolabelling of plasma membrane was carried out as described in the text. Panel (a) indicates photolabelling in the presence (○) or absence (●) of 100 μM CE. The inserted figure (1973 DPM) represents the highest value of the 43 kDa peak when the experiment was carried out in the absence of CE. Panel (b) shows the effect of temperature. Photolyzed membranes were solubilized at 23 °C (○) or at 100 °C (●) for 4 min. and subjected to a 11.25% SDS-PAGE.

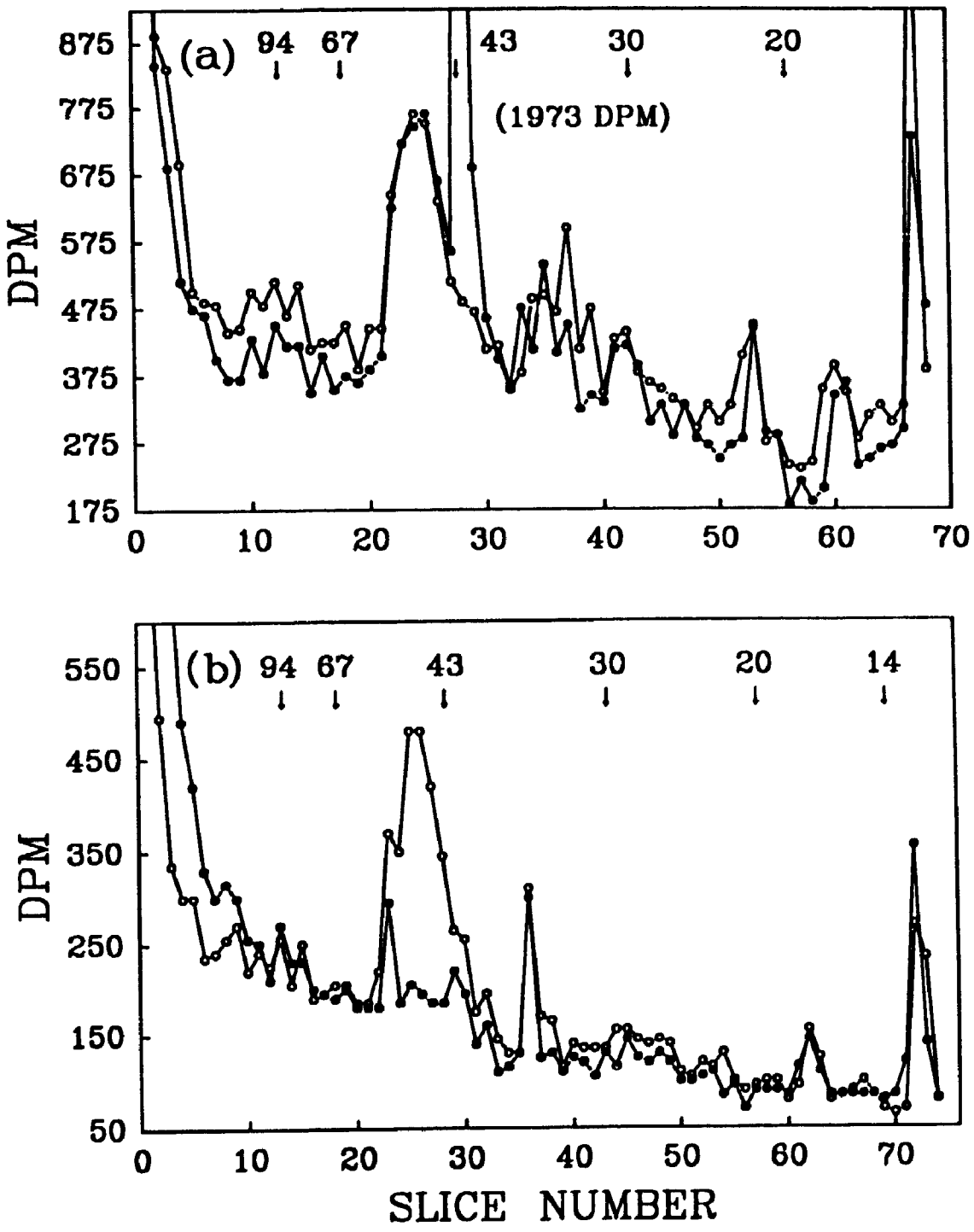
(a)
94
67
43
30
20
(1973 DPM)
DPM
875
775
675
575
475
375
275
175
0
10
20
30
40
50
60
70
(b)
94
67
43
30
20
14
DPM
550
450
350
250
150
50
0
10
20
30
40
50
60
70
SLICE NUMBER

Fig. 4.5 Effect of Trypsinization on ^{3}H-CB Photolabelling of Plasma Membrane from Glucose-grown L6 Myoblasts.

Photolabelling of plasma membrane was carried out as described in the text. Panel (a) shows the ^{3}H-CB photolabelling profiles of plasma membrane (300 μg) treated with (●) or without (○) 20 μg/ml of trypsin after CB photolabelling, and subjected to 5-15% SDS-polyacrylamide gradient gel. Panel (b) shows the profiles of plasma membrane (340 μg) treated with (●) or without (○) 100 μg/ml of trypsin after CB photolabelling, and subjected to 5-20% SDS-polyacrylamide gradient gel.

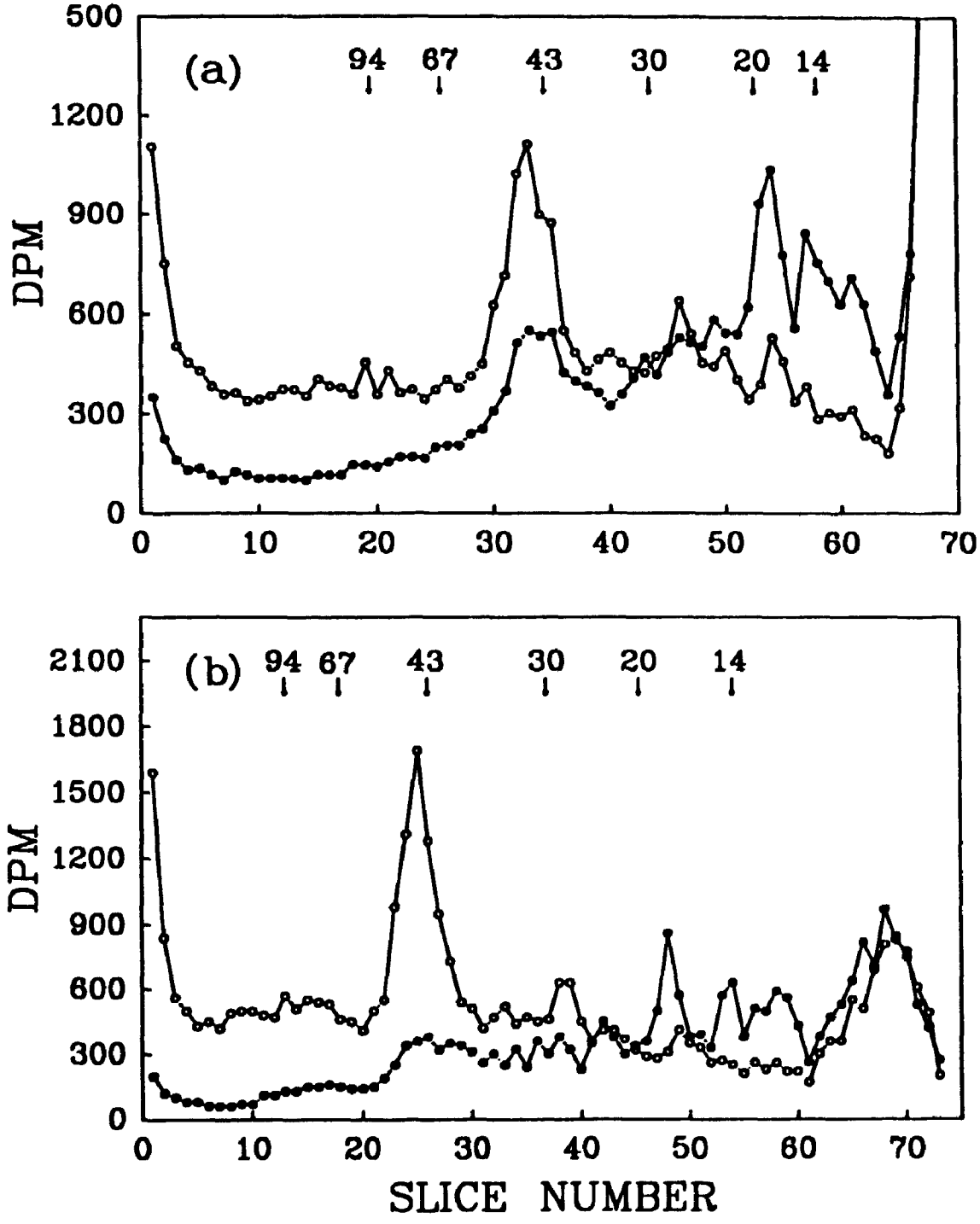
(a)
94
67
43
30
20
14
DPM
500
1200
900
600
300
0
0
10
20
30
40
50
60
70
(b)
94
67
43
30
20
14
DPM
2100
1800
1500
1200
900
600
300
0
0
10
20
30
40
50
60
70
SLICE NUMBER

(Fig. 4.5b). The above studies suggest that the trypsin cleavage site on CB_{50} is exposed to the inner plasma membrane surface.

4.3.4 Specificity of CB-Labelling of Plasma Membrane Proteins.

We have previously demonstrated that CB binding to the HTer could be specifically inhibited by D-glucose and its analogues, but not by L-glucose. The relationship between CB_{50} and the HTer was therefore explored (Table 4.1 and Fig. 4.6a). While CB-labelling of CB_{50} was not affected by 0.6 M L-glucose, about 57% inhibition of labelling could be brought about by the same concentration of D-glucose (Fig. 4.6a). As mentioned earlier, two CB binding sites (CB_H and CB_L) have been detected in rat L6 myoblasts. It is therefore necessary to ascertain whether CB_L and/or CB_H are present in CB_{50}. Since CB_L and CB_H can be preferentially inhibited by dGlc and MeGlc, respectively, an examination of the inhibitory effects of sugar analogues may shed some light on this question. Since the binding affinities and the Bmax values of CB_H and CB_L are 0.10 and 1.54 μM, and 11.8 and 43.8 pmol/mg protein, respectively, 0.2 and 1 μM CB were therefore used in these studies. When the CB concentration used was 0.2 μM, MeGlc seemed to be slightly more effective or just as effective as dGlc in inhibiting the CB photo-incorporation into CB_{50} (Table 4.1). This was probably because the majority of CB was bound to CB_H. On the other hand, when 1 μM CB was used, dGlc was more effective than MeGlc in inhibiting the photolabelling of CB to PM_{GL6} (Table 4.1).

If both CB_H and CB_L were indeed present in CB_{50}, then CB incorporation into this region should be inhibited to a greater extent by both dGlc and MeGlc than by each analogue alone. 45-60% inhibition of CB incorporation was observed with 0.4 M dGlc or 0.4 M MeGlc (Table 4.1). Doubling the sugar analogue concentrations resulted in similar or slightly higher reduction of CB-incorporation (Table 4.1). However, 70% inhibition was observed with both 0.4 M dGlc and 0.4 M MeGlc. Further inhibition, up to 75-80%, could be achieved by both 0.8 M

Fig. 4.6 Effect of Glucose on ^{3}H-CB Photolabelling of Plasma Membrane from Glucose-grown L6 Myoblasts.

Plasma membrane from glucose-grown L6 cells were photolyzed in the presence of 0.6 M L-glucose (○) or 0.6 M D-glucose (●) as described in the text. Photolyzed membranes were solubilized at 23 °C and subjected to a 11.25% [Panel (a)] or a 8.5% [Panel (b)] SDS-PAGE.

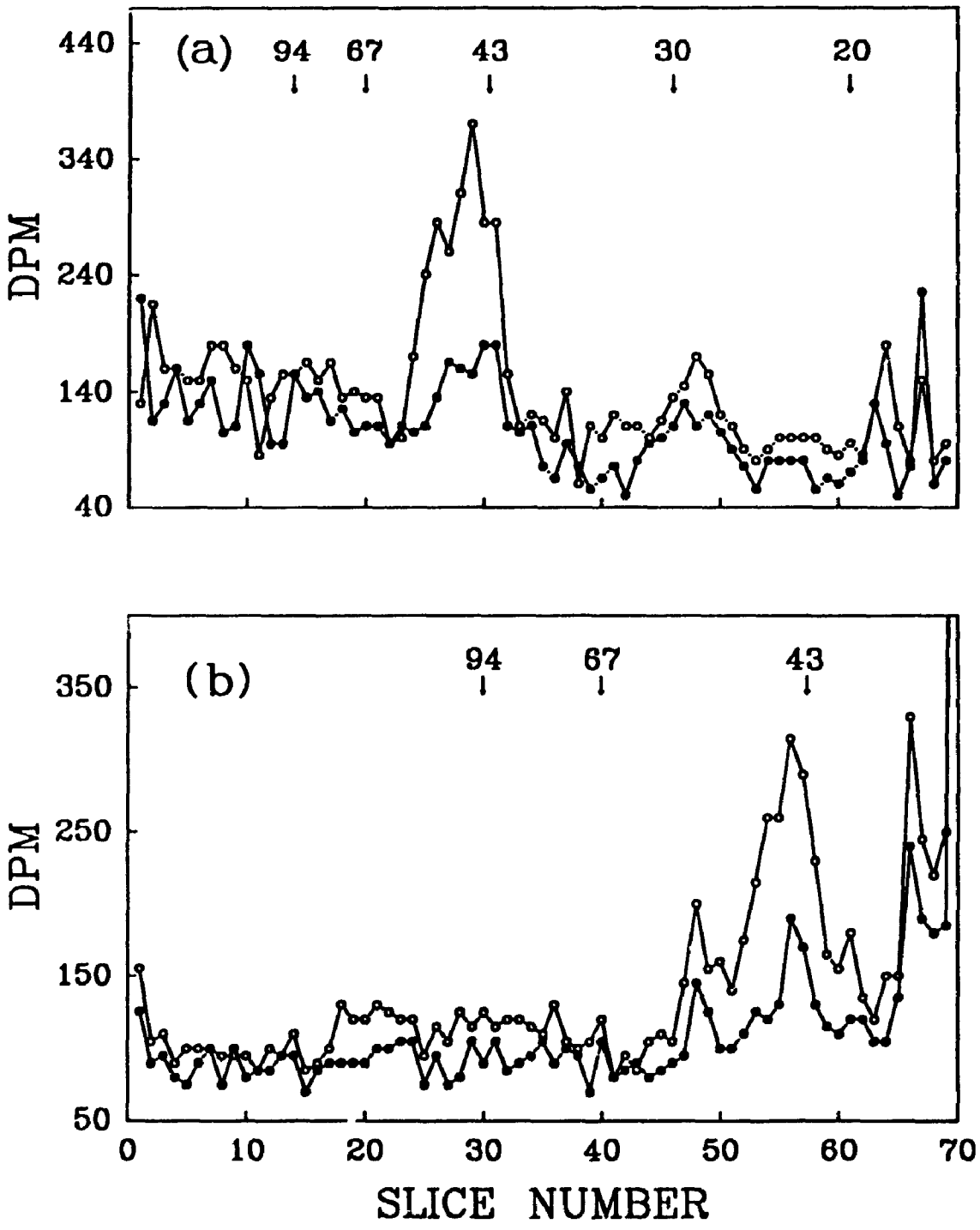
(a)
94
67
43
30
20
440
340
240
140
40
DPM
(b)
94
67
43
350
250
150
50
DPM
0
10
20
30
40
50
60
70
SLICE NUMBER

dGlc and 0.8 M MeGlc. The above observations were consistent with the notion that both CB_H and CB_L were present in CB_{50}.

Two CB labelled peaks were also observed in plasma membranes in other cell types (Pessin et al., 1984; Horuk et al., 1986; Haspel et al., 1986). In the case of rat L6 myoblasts, separation of these two peaks (46 and 51 kDa) could be better improved by using lower percentage SDS-PAGE; both CB-labelled peaks were also found to be sensitive to D-glucose (Fig. 4.6b). In view of the incomplete separation of these two peaks, the total photoincorporation into this region will be analyzed in the present study.

4.3.5 Photoaffinity Labelling of Plasma Membranes from Hexose Transport Mutants

While the above studies suggested that both CB_H and CB_L might be present in CB_{50}, more definitive evidence of their presence was revealed by analysis of the HT mutants. Several mutants have been isolated and characterized in our laboratory (D'Amore and Lo, 1986c; D'Amore et al., 1986b). Of these, two are of particular interest. Mutant D23 exhibited much reduced levels of HAHT and CB_L , while maintaining the same levels of LAHT and CB_H as compared to those of L6 cells (Chapter 3). On the other hand, while mutant F72 shows similar CB binding properties as wild type L6 cells, it is defective in HAHT (Table 4.2; D'Amore and Lo, 1986a). This mutant F72 is, therefore, thought to be a regulatory mutant (D'Amore and Lo, 1988). When compared with PM_{GL6}, plasma membrane from glucose-grown mutant D23 (PM_{GD23}) exhibited a 45-50% decrease in CB photo-incorporation into CB_{50} (Fig. 4.7a), whereas plasma membrane from glucose-grown mutant F72 (PM_{GF72}) showed a similar level of CB labelling into this region (Fig. 4.7b). This is in agreement with the notion that while both CB_H and CB_L are present in PM_{GF72} and PM_{GL6}, only residual amounts of CB_L could be detected in PM_{GD23} (see Chapter 2 and 3; Table 4.2). CB_{50} in both mutants, D23 and F72, was also sensitive to D-glucose (Table 4.1 and Fig. 4.7b). Although D-glucose could still

Table 4.2 Binding Properties of the Two CB Binding Sites in Plasma Membranes from Glucose-grown Mutant F72 and its Parental L6 Cells.

	CB_H		CB_L	
CELL TYPE	K_d (μM)	B_{max}	K_d (μM)	B_{max}
PM_{GL6}	0.10	11.8	1.54	43.8
PM_{GF72}	0.09	11.0	1.80	38.1

CB binding studies with plasma membrane and determination of K_d and B_{max} values were described in Chapter 3. B_{max} values are expressed in pmol/mg protein. Abbreviation: PM_{GL6}, plasma membrane from glucose-grown L6 myoblasts; PM_{GF72}, plasma membrane from glucose-grown mutant F72.

Fig. 4.7 ^{3}H-CB Photolabelling of Plasma Membranes Prepared from Glucose-grown Hexose Transport Mutant D23, F72 and their Parental L6 Myoblasts.

Photolabelling of plasma membranes was carried out as described in the text. In panel (a), the same amount of plasma membrane protein from glucose-grown wild type L6 (○) and mutant D23 (●) was photolabelled with ^{3}H-CB and analyzed on a 11.25% SDS-PAGE. Panel (b) shows the photolabelling of plasma membranes prepared from (i) glucose-grown wild type L6 in the presence of 0.5 M L-glucose (○), (ii) glucose-grown mutant F72 in the presence of 0.5 M L-glucose (●) or 0.5 M D-glucose (△). The same amount of membrane protein was photolyzed and subjected to 11.25% SDS-PAGE.

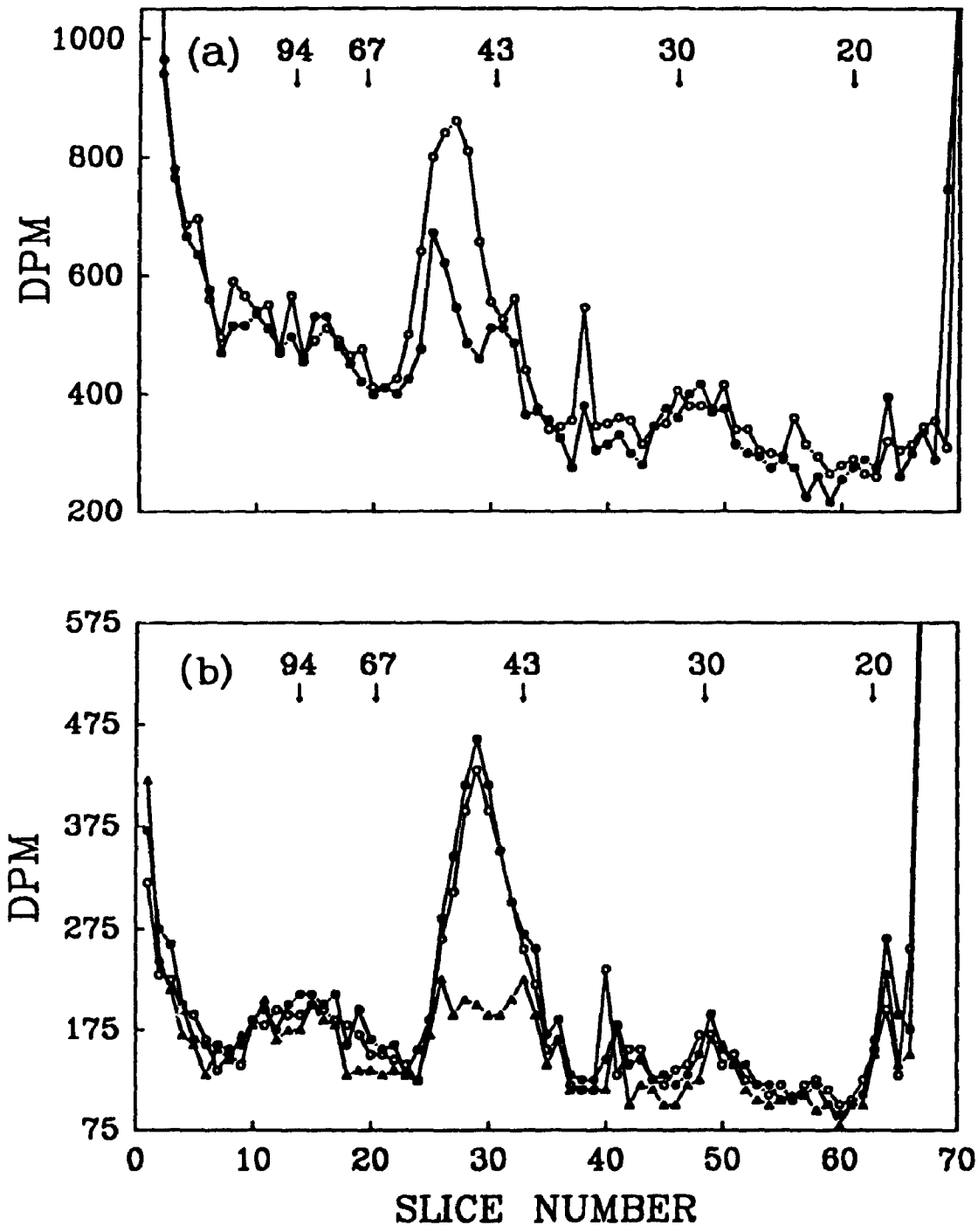
(a)
94
67
43
30
20
1000
800
600
400
200
DPM
(b)
94
67
43
30
20
575
475
375
275
175
75
DPM
0
10
20
30
40
50
60
70
SLICE NUMBER

inhibit CB photo-incorporation into PM_{GD23}, its inhibitory effect was not as high as that observed with PM_{GL6} (Table 4.1). This could be explained by the fact that CB was binding mainly to CB_H, as only residual amounts of CB_L were present in PM_{GD23}. It should be mentioned that there were no significant differences in other regions between wild type L6 and mutant D23 or F72.

4.3.6 Photoaffinity Labelling of Plasma Membrane from Glucose-starved Myoblasts.

We have recently demonstrated that the levels of CB_L and HAHT were elevated by glucose-starvation (D'Amore and Lo, 1986a; D'Amore et al., 1986a). If the CB_L is indeed present in CB_{50}, one should be able to see a corresponding increase in CB photolabelling of CB_{50} in plasma membrane prepared from glucose-starved L6 cells (PM_{FL6}). Fig. 4.8a shows that this is indeed the case. When compared with PM_{GL6}, PM_{FL6} was found to incorporate 45-50% more CB into CB_{50} even though photo-incorporation into other regions remained unchanged. Moreover, photo-incorporation into this region of PM_{FL6} could be inhibited by D-glucose, dGlc, and MeGlc (Fig. 4.8b and Table 4.1); about 65% inhibition of CB incorporation could be brought about by dGlc or D-glucose; whereas only about 45% inhibition was observed with MeGlc. This indicates that the level of CB_L is elevated in glucose-starved cells.

Additional evidence on the effect of glucose starvation on photolabelling comes from studies with transport mutants. We have previously shown that mutants D23 and F72 respond differently to glucose starvation (D'Amore et al., 1986b). The residual amounts of HAHT in mutant D23 could still be stimulated by glucose starvation, whereas HAHT in mutant F72 remained unaltered. As shown in Fig. 4.9, while glucose starvation increased the residual levels of CB_{50} in plasma membrane from glucose-starved mutant D23 (PM_{FD23}) about 40% (Fig. 4.9a), it did not have a significant effect on the level of CB_{50} in plasma membrane from glucose-starved mutant F72 (PM_{FF72}) (Fig. 4.9b). This is in agreement with the notion that CB_L was

Fig. 4.8 ^{3}H-CB Photolabelling of Plasma Membranes from Glucose-grown or Glucose-starved L6 Myoblasts and Effects of Glucose Analogues on ^{3}H-CB Photolabelling of Plasma Membrane from Glucose-starved L6 Cells.

Photolabelling of plasma membrane was carried out as described in the text. Panel (a) shows ^{3}H-CB photolabelling of plasma membranes from glucose- (●) and fructose- (○) grown L6 cells, whereas panel (b) indicates ^{3}H-CB photolabelling of plasma membrane prepared from fructose-grown L6 cells in the presence of 0.4 M L-glucose (○), 0.4 M dGlc (△) or 0.4 M MeGlc (●).

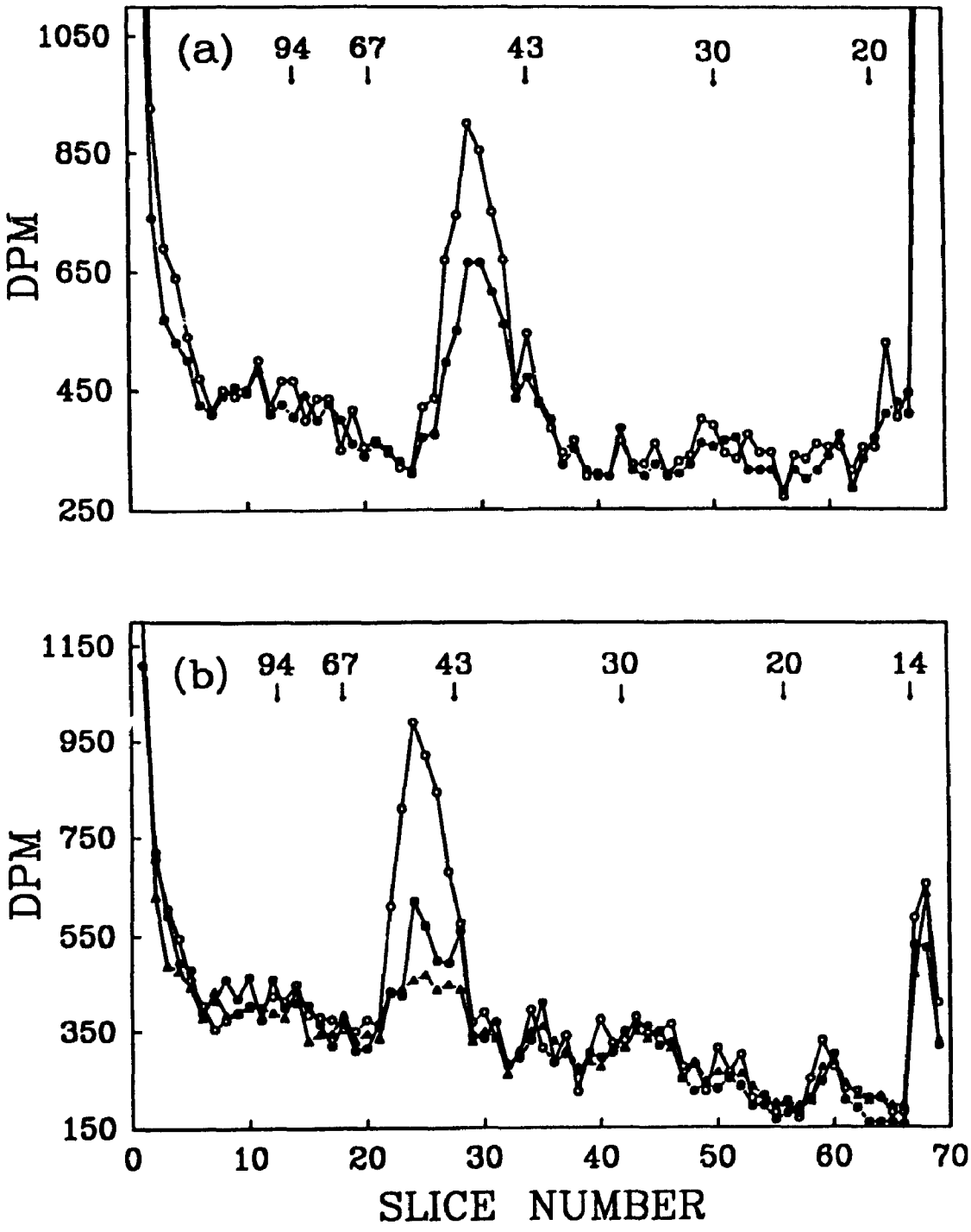
(a)
94
67
43
30
20
1050
850
650
450
250
DPM
(b)
94
67
43
30
20
14
1150
950
750
550
350
150
DPM
0
10
20
30
40
50
60
70
SLICE NUMBER

Fig. 4.9 ^{3}H-CB Photolabelling of Plasma Membranes Prepared from Glucose-grown or Glucose-starved Mutant D23 or Mutant F72.

Photolabelling of plasma membrane was carried out as described in the text. Panel (a) indicates photolabelling of plasma membrane from glucose- (●) or fructose- (○) grown mutant D23. Panel (b) indicates photolabelling of plasma membrane from glucose- (●) or fructose- (○) grown mutant F72.

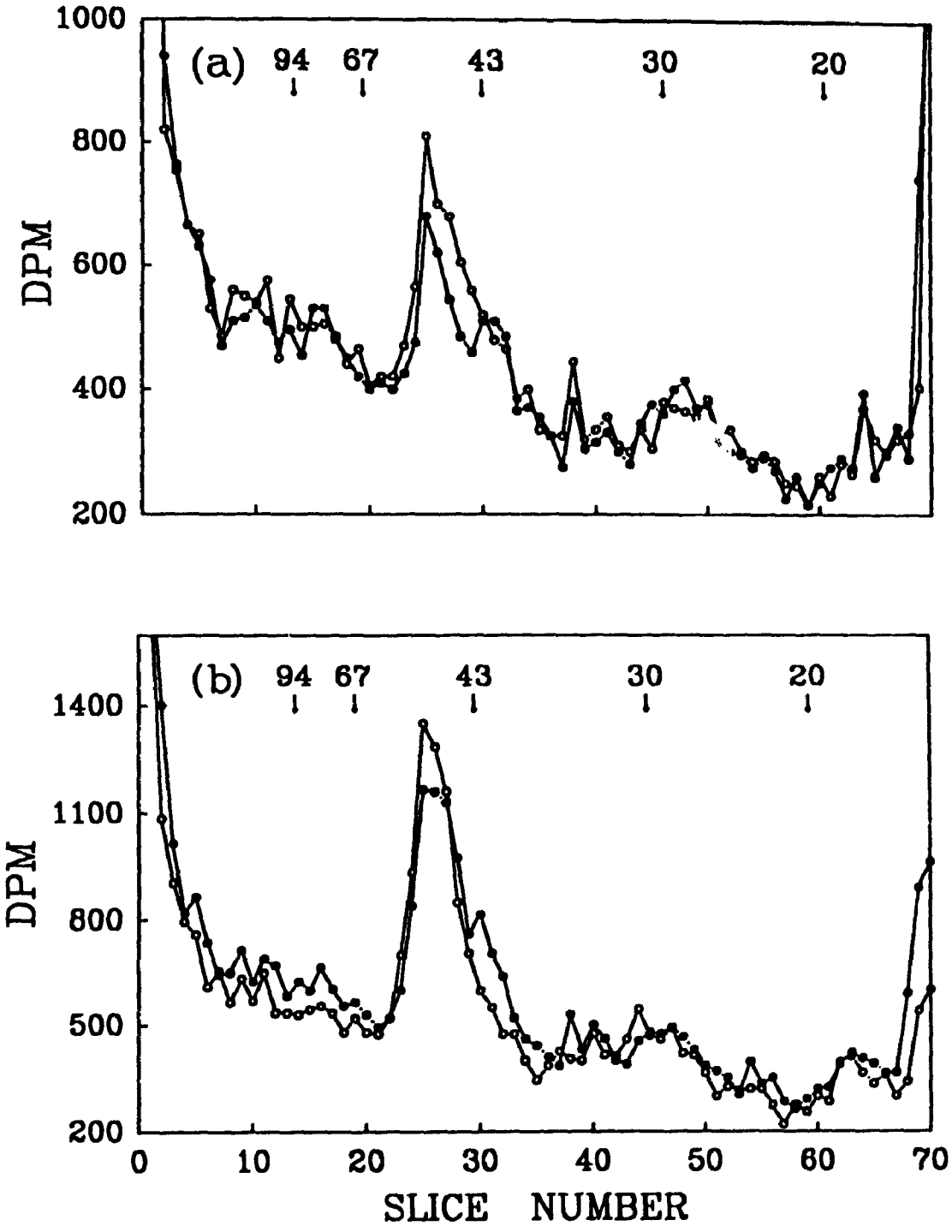
(a)
94
67
43
30
20
1000
800
600
400
200
DPM
(b)
94
67
43
30
20
1400
1100
800
500
200
DPM
0
10
20
30
40
50
60
70
SLICE NUMBER

also present, albeit at a much reduced level, in CB_{50} of mutant D23.

4.3.7 Photoaffinity Labelling of Low Density Microsomal Fraction (LDMF) from Glucose-grown Rat Myoblasts

In contrast to adipocytes, the number of CB binding sites in LDMF of glucose-grown rat L6 myoblasts was significantly lower than that in the plasma membrane. Photolabelling studies indicated that LDMF contained only about 20% of the CB incorporated into the plasma membrane CB_{50} (Fig. 4.10a). The overall pattern of CB photolabelling in LDMF and plasma membrane was quite similar, except for the low background labelling in LDMF; the difference in background labelling could be explained by the dissimilarity in protein composition (insert in Fig. 4.10a). It should be noted that the major CB-labelled peak in LDMF has a similar electrophoretic mobility as the major Coomassie blue stained band.

An examination of the CB photo-incorporation into LDMF revealed significant differences between CB_{50} found in LDMF and that in the plasma membrane. First, CB photolabelling of CB_{50} in LDMF was not sensitive to D-glucose; only about 8% inhibition was observed with 0.4 M D-glucose (Table 4.1). Second, similar levels of CB_{50} were present in LDMF prepared from both D23 and L6 cells (Fig. 4.10b). Third, the labelling patterns of plasma membrane and LDMF after trypsinization were also quite different (Fig. 4.11a). As shown in Fig. 4.5b, treatment of plasma membrane with 100 μg/ml trypsin abolished CB_{50} with the concomitant increase of several pep[illegible] (12, 15, 18 kDa). However, treatment of the same amount of LDMF (340 μg protein) with the same concentration of trypsin abolished labelling of proteins with molecular weights greater than 10 kDa. In other words, trypsinization abolished CB labelling of CB_{50}, and the 12-20 kDa proteins in LDMF; this differed significantly from that of plasma membrane. Fourth, heating at 100°C for 4 min. was found to have no effect on the labelling of CB_{50} in LDMF (Fig. 4.11b).

Fig. 4.10 ^{3}H-CB Photolabelling of Plasma Membranes and LDMF Prepared from Glucose-grown Mutant D23 and its Parental L6 Cells.

Panel (a) shows photolabelling of plasma membrane (○) and LDMF (●) from glucose-grown L6 cells. The same amount of plasma and microsomal membrane proteins was photolabelled with ^{3}H-CB, solubilized in Laemmli SDS sample buffer without heating and subjected to a 11.25% SDS-PAGE as described for the photolabelling of microsomal membranes. The insert shows the protein profiles of LDMF (top lane), and plasma membrane (bottom lane). Panel (b) shows the CB-photolabelling profiles of LDMF from glucose-grown L6 (○) and mutant D23 (●).

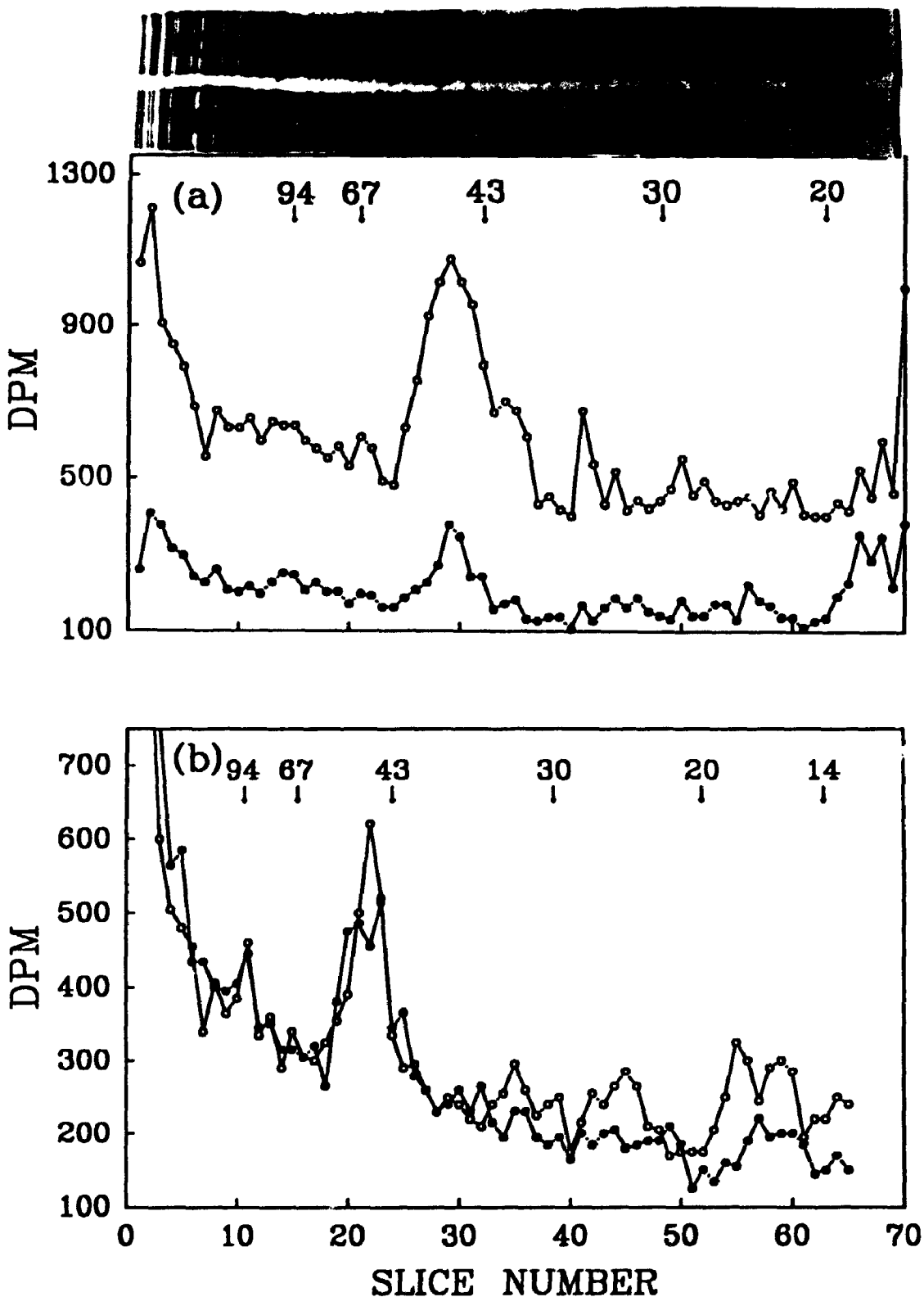
(a)
94
67
43
30
20
1300
900
500
100
DPM
(b)
94
67
43
30
20
14
700
600
500
400
300
200
100
DPM
0
10
20
30
40
50
60
70
SLICE NUMBER

Fig. 4.11 Effects of Trypsinization and Heating on the ^{3}H-CB Photolabelling Pattern of LDMF Prepared from Glucose-grown L6 Cells.

In panel (a), LDMF (340 μg) was treated with (●) and without (○) 100 μg/ml of trypsin after ^{3}H-CB photolabelling; after which samples were analyzed by electrophoresis on a 5-20% SDS-polyacrylamide gradient gel as described in the text. Panel (b) shows the effect of temperature on photolabelling of LDMF. Photolabelling of LDMF was carried out as described in the text. Solubilized LDMF was heated at 100 °C for 4 min. (●) or kept at 23 °C (○) before SDS-PAGE.

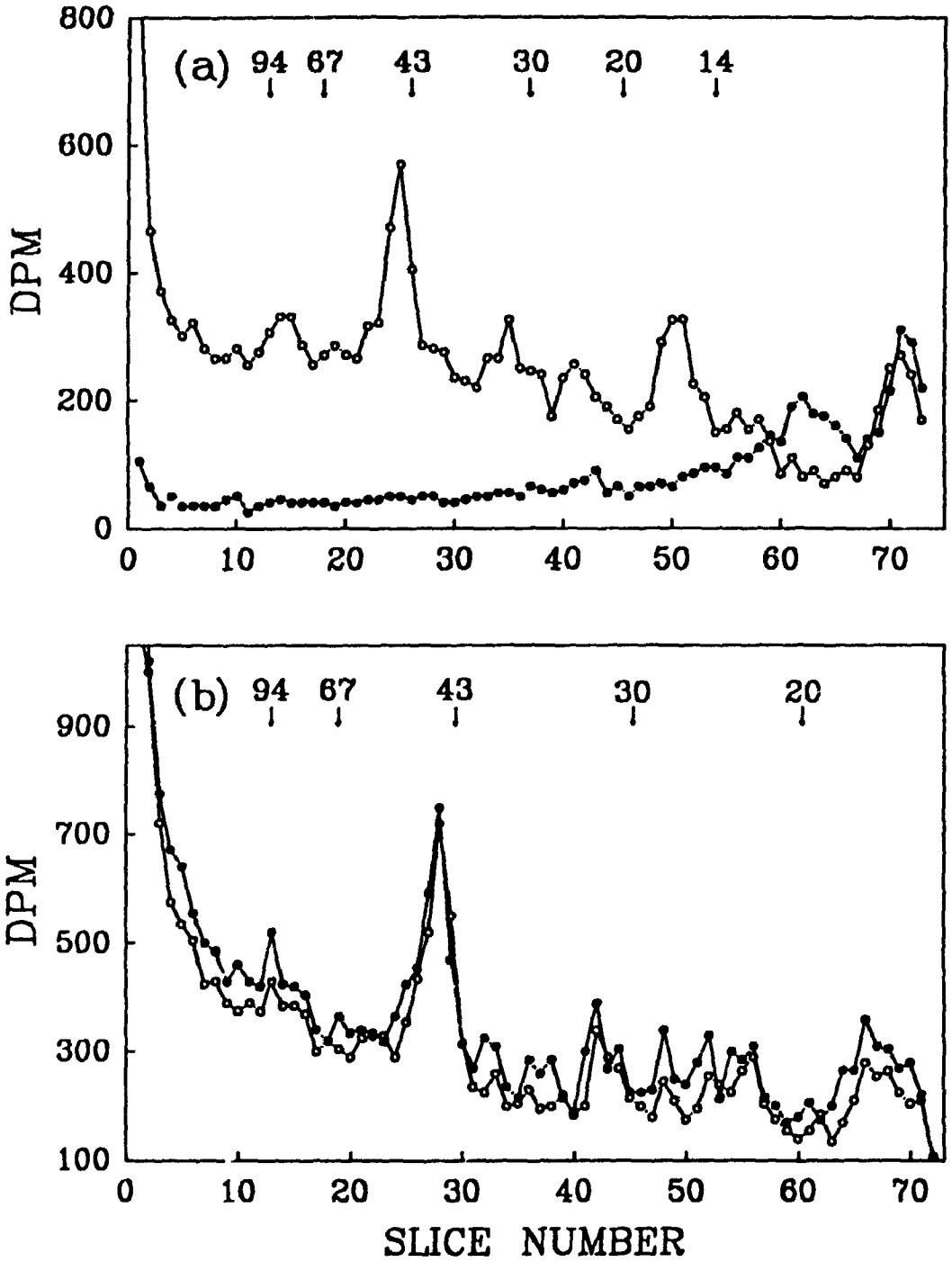
(a)
94
67
43
30
20
14
800
600
400
200
0
DPM
0
10
20
30
40
50
60
70
(b)
94
67
43
30
20
900
700
500
300
100
DPM
SLICE NUMBER

4.4 DISCUSSION

Photoaffinity labelling with CB has been widely used in the identification of eukaryotic HTers (Pessin et al., 1984; Shanahan, 1982; Craik et al., 1988; Horuk et al., 1986; Oka et al., 1988). Their identification is usually based on the inhibition of CB-photolabelling by D-glucose, but not by L-glucose (Shanahan, 1982; Johnson and Smith, 1982; Klip and Walker, 1983; Dick et al., 1984). However, there is presently no unequivocal evidence indicating that the CB-labelled components are indeed the glucose transporters. Since CB inhibits hexose transport, it is not possible to demonstrate by reconstitution studies that the CB-incorporated proteins are indeed the hexose transporter. We have recently demonstrated the presence of two HT systems (LAHT and HAHT) in undifferentiated rat L6 myoblasts (D'Amore and Lo, 1986a), and that both HTers possessed their own CB binding sites (CB_H and CB_L) (see Chapter 2 and 3). The objective of this study is to identify the rat myoblast HTers by CB photoaffinity labelling, and through the use of appropriate HT mutants. Studies with HT mutants provide a unique and definitive means of identifying and characterizing the HTers. It should be mentioned that this is the first genetic evidence indicating that the hexose transporter can indeed be photolabelled by CB.

Photolabelling studies with intact whole cells revealed that at least four components could be labelled by ^{3}H-CB (Fig. 4.1). Of the labelled components, labelling of the 40-60 kDa region (CB_{50}) was found to be inhibited by D-glucose or its analogues (Table 4.1). Judging from the levels of very high and low molecular weight CB-labelled components, it seemed likely that prolonged photolysis resulted in extensive cross-linking, non-specific photo-incorporation and degradation of the labelled components. These problems were overcome by reducing the time of photolysis, and by using purified plasma membrane instead of intact whole cells. Several lines of evidence suggest that the rat myoblast HTers may be present in

CB_{50}. (1) 50-60% of the amount of CB photo-incorporated into CB_{50} could be reduced by very high concentrations of D-glucose, dGlc, and MeGlc, but not by L-glucose (Table 4.1 and Fig. 4.6). (2) The molecular weights of the D-glucose-sensitive CB labelled proteins were similar to those of other eukaryotic HTers (Pessin et al., 1984; Birnbaum et al., 1986). (3) CB labelling of CB_{50} was not sensitive to CE (Fig. 4.4a). (4) The levels of both HT activity and CB_{50} were elevated in glucose-starved L6 and mutant D23 (Figs. 4.8a and 4.9a), whereas neither the level of transport activity nor that of CB_{50} was affected by glucose starvation in regulatory mutant F72 cells (D'Amore and Lo, 1986c; Fig. 4.9b). (5) HT mutant D23 contained not only residual levels of HAHT and CB_L (D'Amore and Lo, 1986c), but also a substantially reduced level of CB_{50} (Fig. 4.7a). In other words, the level of CB incorporated into CB_{50} and the HT activity are affected similarly by physiological, biochemical and genetic alterations. This close correlation suggests that the CB-labelled HTers may indeed be the major components present in CB_{50}.

The next question that arises is whether both HTers are present in CB_{50}. While two CB-labelled peaks (46 and 51 kDa) were sometimes observed in CB_{50} in plasma membrane (Figs. 4.4b and 4.6a), they were not always as apparent. Further separation, identification and characterization of these two peaks by the Laemmli gel system are hampered by the possible artifacts generated as a result of gel slicing; for example, depending on where the gel was sliced, the gel profile may not reveal the trough and peaks of labelled proteins with slightly different molecular weights. Nevertheless, the following pieces of evidence suggest that both CB_H and CB_L may be present in CB_{50}. The presence of CB_L in CB_{50} was indicated by the findings that glucose-starvation resulted in elevated levels of CB_L and CB_{50} (Fig. 4.8a), and that the mutant containing residual levels of CB_L also exhibited much reduced level of CB_{50} (Fig. 4.7a). Furthermore, changes in the level of CB_L,

as in the cases of glucose-grown mutant D23 and glucose-starved L6 cells, also resulted in the altered relative effectiveness of inhibition by dGlc and MeGlc (Table 4.1). The presence of CB_H in CB_{50} is indicated by the finding that a substantial amount of CB was incorporated into CB_{50} in PM_{GD23}, which contained the normal level of CB_H (Fig. 4.7a), and that this CB incorporation could be inhibited by MeGlc (Table 4.1). If only one HTer or CB binding site is photolabelled by CB, one would expect that the relative effectiveness of inhibitions by dGlc and MeGlc should be quite similar at different CB concentrations. However, MeGlc was found to be more effective than dGlc in inhibiting the binding of 0.2 μM CB to PM_{GL6}, whereas the opposite was true when 1 μM CB was used (Table 4.1). Finally, CB incorporation into CB_{50} was more effectively inhibited by both dGlc and MeGlc than comparable concentrations of either sugar analogue alone (Table 4.1). This additive inhibitory effect of dGlc and MeGlc suggests the presence of more than one CB photolabelled component.

The finding that more than one hexose sensitive CB-labelled component is present in PM_{GL6} is actually not surprising. Two hexose sensitive CB photolabelled components (46 and 52 kDa) have been identified as the HTers in chick embryo fibroblasts (Pessin et al., 1984). The levels of these labelled components were increased by glucose starvation. In rat adipocytes, two CB photolabelled components with different isoelectric points have also been detected in LDMF , only one of these is present in the plasma membrane (Horuk et al., 1986). Two HTers in rat brain (46 and 55 kDa) and in murine fibroblasts (42 and 55 kDa) have also been detected by immunoblotting studies (Birnbaum et al., 1986; Haspel et al., 1986).

When compared with plasma membrane, a very low level of CB was found to be incorporated into CB_{50} of LDMF (Fig. 4.10a). Several lines of evidence suggest that the observed CB labelling in LDMF may not be due to the presence of contaminating plasma membrane. First, CB photolabelling of CB_{50} in LDMF was

not sensitive to D-glucose (Table 4.1). Second, the difference in the levels of CB_{50} in PM_{GL6} and PM_{GD23} was not observed in LDMF prepared from mutant D23 and L6 cells (Fig. 4.10b). Third, unlike its effect on plasma membranes, trypsinization abolished CB labelling of CB_{50} and the 12-20 kDa proteins in LDMF (Fig. 4.11a). Fourth, heating was found to have no effect on the labelling of CB_{50} in LDMF (Fig. 4.11b), whereas it resulted in dramatic changes in the plasma membrane (Fig. 4.5b). The above findings point to the differences between CB_{50} found in the plasma membrane and in LDMF. The significance of this glucose-insensitive CB photolabelling in LDMF is not clear. The low inhibitory effects of glucose and its analogues on CB photolabelling in CB_{50} in whole cells may be, in part, contributed by these non-glucose-inhibitable CB photolabelling sites in LDMF.

CHAPTER 5

USE OF SPECIFIC ANTISERA IN THE IDENTIFICATION OF HEXOSE TRANSPORTERS IN UNDIFFERENTIATED RAT L6 MYOBLASTS

5.1 INTRODUCTION

D-glucose is transported across the plasma membranes of virtually all mammalian cells via a carrier-mediated stereospecific mechanism (Elbrink and Bihler, 1975). The best characterized HT systems are those present in human erythrocytes and rat adipocytes (Wheeler and Hinkle, 1985; Simpson and Cushman, 1986). HT in other mammalian cells has also been extensively examined (Colby and Romano, 1975; Olefsky, 1978; Johnson and Smith, 1982; Klip et al., 1983b; D'Amore and Lo, 1986a; Horner et al., 1987). Regardless of the cell type, most HTers were characterized by their ability to bind with the fungal metabolite, CB (Shanahan, 1982; Pessin et al., 1984), with anti-(human erythrocyte HTer) IgG (Wang, 1987), or with antibodies directed against synthetic peptides deduced from the HTer DNA sequences (Haspel et al., 1988; Oka et al., 1988). Consequently, HTers have been identified by the presence of D-glucose-sensitive CB binding site (Shanahan, 1982; Pessin et al., 1984), and by their interaction with specific antibodies (Allard and Lienhard, 1985; Haspel et al., 1985; Biber and Lienhard, 1986; Horner et al., 1987; Wang, 1987; Oka et al., 1988).

Another immunological approach used in the identification of HTers is the use of antibodies that can specifically recognize the glucose binding site. Anti-idiotypic antibodies have been used to identify specific binding sites (Farid and Lo, 1985). These are antibodies raised against the idiotype (or antigen combining site) of another antibody (Bona and Kohler, 1984). Membrane receptors, such as insulin (Sege and Peterson, 1978), acetylcholine (Wasserman et al., 1982), ß-adrenergic

(Schreiber et al., 1980) and thyrotropin receptors (Islam et al., 1983) have been identified with anti-idiotypic antibodies. An anti-idiotypic antibody raised against rabbit anti-glucosamine IgG has also been used to identify and to characterize the human erythrocyte HTer (Kay, 1985).

The previous chapters have shown our attempts to identify and characterize the two HT systems in rat L6 myoblasts using CB, an affinity ligand and a photoaffinity label of the HTer. HT mutants were used throughout these studies and found to be indispensable in the identification of specific HT systems, or transport components. It is conceivable that these mutants will also be useful in identifying the components recognized by specific antibodies. In the present study, we employed antisera directed against the purified human erythrocyte HTer (α-GT) and against rabbit anti-glucosamine IgG (α-IDIO) to further identify and characterize HTers in these cells. Two plasma membrane proteins were recognized by α-IDIO. One of the proteins was found to be missing in a mutant defective only in HAHT. This provides the first genetic evidence that the antibodies are indeed binding to a HT component.

5.2 MATERIALS AND METHODS

5.2.1 Materials

Anti-(human rbc HTer) antiserum (α-GT) and anti-[rabbit anti-(glucosamine IgG)] antiserum (α-IDIO) were raised and purified as described earlier (Kay, 1985). Brush-border membranes from rat small intestine were generous gifts from Dr. A. Berteloot (University of Montreal, Montreal, Quebec, Canada). [4-^{3}H(n)] CB (22 Ci/mmol) and sodium ^{125}I-iodide, carrier free (14.6 mCi/μg, 100 mCi/ml) were purchased from Amersham Canada Ltd. Ready Protein Liquid Scintillation Cocktail was from Beckman Instruments Inc. Electrophoresis reagents were purchased from BDH Chemicals. Nitrocellulose membranes (0.45 μm) and Bio-gel P-6DG desalting

columns were purchased from Bio-Rad Laboratories. Endoglycosidase H, N-glycanase and protein A were purchased from Genezyme Corporation. Alkaline phosphatase conjugated affinity pure goat anti-rabbit IgG (H+L) was obtained from Jackson Immunoresearch Laboratories. IODO-GEN was purchased from Pierce Chemical Company. 5-Bromo-4-chloro-3-indolyl phosphate, nitro blue tetrazolium, cytochalasin B, cytochalasin E and other chemicals were purchased from Sigma Chemical Co.

5.2.2 Preparation of Membrane Fractions from Rat Myoblasts and Human RBC

Membrane fractions were prepared from glucose-grown mutant D23 and its parental L6 cells, and human rbc according to the previously described procedures (see Chapter 3 and 4).

5.2.3 Immunoblotting Studies

Whole cell extracts were prepared by washing glucose-grown rat myoblast monolayers, grown on 20 x 150 mm tissue culture dishes, twice with PBS and by scraping into 1% hot SDS (80-90 °C). Membrane preparations from glucose-grown rat myoblasts (100-200 μg) or total cell extracts (150-200 μg) were dissolved in SDS-sample buffer at room temperature, and subjected to SDS-polyacrylamide gel electrophoresis (SDS-PAGE) using the discontinuous buffer system of Laemmli (1970). After SDS-PAGE, proteins were electrophoretically transferred from the gel onto nitrocellulose membranes (0.45 μM) using a transfer buffer [25 mM Tris, 192 mM glycine (pH 8.3), 20% methanol and 0.1% SDS] at 55 volt for 2 h (Towbin et al., 1979). In order to block nonspecific protein binding, the paper was incubated with 20% fetal calf serum in Tris buffer containing 150 mM NaCl, 10 mM Tris-HCl (pH 8.0), and 0.05% Tween 20 for at least 5 h at 23 °C. After washing once with the same Tris buffer, the paper was incubated with 1:250 dilutions of α-GT, α-IDIO or preimmune serum for 14 h at 23 °C. Subsequent to washing with the same Tris buffer 3 times (5-10 min. for each washing), the paper was incubated with ^{125}I labelled-protein A to detect the immune complexes.

Following removal of the unbound ^{125}I-protein A by washing three times with the Tris buffer, blots were dried and autoradiographed at -86 °C on Kodak X-Omat film with intensifying screen. Instead of using ^{125}I-protein A, the antigen-antibody reactions could also be detected by alkaline phosphatase-conjugated affinity pure goat anti-rabbit IgG (Huynh et al., 1985). Briefly, after electroblotting, the nitrocellulose membrane was incubated with 20% fetal calf serum in the Tris buffer for 30 min.; this was then incubated with 1:250 dilutions of α-GT, α-IDIO or preimmune serum for 1 h. After washing with the Tris buffer three times (5-10 min. for each washing), the nitrocellulose paper was then incubated with 1:7500 dilutions of alkaline phosphatase-conjugated goat anti-rabbit IgG for 30 min. Subsequent to washing with Tris-buffer three times, the paper was dried and transferred to a colour development substrate solution [100 mM Tris-HCl (pH 9.5), 100 mM NaCl, 5 mM $MgCl_2$, 0.38 mM BCIP and 0.40 mM NBT]; this was then incubated for 10-30 min in the dark. The reaction was terminated by replacing the substrate solution with the stop solution [20 mM Tris-HCl (pH 8.0) and 5 mM EDTA]. The data presented were results of representative experiments which were repeated at least twice and usually three or more times. Results were found to be very consistent in all cases.

5.2.4 CB Photoaffinity Labelling

Photoaffinity labelling in the presence or absence of unlabelled or ^{3}H-CB was performed as described previously (see Chapter 4). In studying the effect of CB on the interaction of proteins with antibodies, photolabelled membrane proteins were first separated by SDS-PAGE, and then electrophoretically transferred to a nitrocellulose membrane. The interaction of specific antibodies with the immobilized proteins was then determined as described earlier.

5.2.5 Treatment with Endoglycosidase H and N-glycanase

Plasma membrane from glucose-grown L6 myoblasts (100-150 μg) or

ovalbumin (50 μg) was solubilized in 160 μl of 100 mM sodium phosphate buffer (pH 8.6 for N-glycanase treatment, or pH 6.1 for endoglycosidase H treatment) containing 0.17% SDS, 1% Triton X-100, 1% ß-ME (v/v), 5 mM EDTA and 1 mM PMSF at 100 °C for 3 min. The mixture was then incubated with or without endoglycosidase H (5 mIU/ml), or N-glycanase (5 units/ml) at 37 °C for 22 h. The solution was mixed with 40 μl of 5 X electrophoresis sample buffer and subjected to SDS-PAGE and immunoblotting analysis as described earlier.

5.2.6 Iodination of Protein A

Iodination of protein A was performed as described previously (Markwell and Fox, 1978) with some modifications. Protein A (120 μg) was iodinated in 50 μl of 50 mM potassium phosphate (pH 7.4) with 1.0 mCi of sodium ^{125}I-iodide in an IODO-GEN (5 μg) coated glass tube for 10 min. The reaction mixture was then applied to a pre-spun 5 ml Bio-gel P-6DG desalting column (which has been washed with 5 mg/ml of BSA in PBS and equilibrated with PBS). After centrifugation at 2,000 X g for 2 min., the eluate was diluted with 1.5 ml of 50 mM potassium phosphate buffer (pH 7.4) containing 100 mM NaCl, 0.1% sodium azide and 5 mg/ml BSA, and stored at 4 °C in a lead container.

5.2.7 Other Procedures.

For other methods and materials, see previous chapters.

5.3 RESULTS

5.3.1 Anti-(Human RBC HTer) and Anti-(Anti-Glucosamine IgG) Antisera can also Recognize other Types of HTer

Antisera directed against purified human rbc HTer (α-GT) and against anti-glucosamine IgG (α-IDIO) have previously been shown to recognize the human erythrocyte HTer (Kay, 1985). In order to determine whether these antisera could also be used to identify other HTers, their ability to interact with the Na^+-

dependent intestinal brush-border HTer (BBM-HTer) was therefore tested (Fig. 5.1). While the preimmune serum could not recognize any BBM proteins, α-IDIO was found to interact with one major (78 kDa) and three minor (68, 54 and 40 kDa) proteins, whereas α-GT was able to recognize a 78 and a 49 kDa protein. This indicated that the 78 kDa protein possessed not only a glucose recognition site but also antigenic determinant site(s) homologous to those in the human rbc HTer. The molecular weight of BBM-HTer has previously been determined by both photolabelling and immunoblotting studies to be around 78 kDa (Neeb et al., 1985; Semenza et al., 1985; Neeb et al., 1987; Koepsell et al., 1988). Thus it seemed likely that the 78 kDa protein labelled by α-GT and α-IDIO might indeed be the BBM-HTer. If this were the case, then these antisera could conceivably be used as probes to identify HTers in other cell types.

5.3.2 Immunoblotting Studies with Rat Myoblast Whole Cell Extracts

One of the problems in identifying HTers with antibodies or by CB photolabelling is the uncertainty that the labelled protein(s) are indeed involved in HT. One way to ascertain the identity of the labelled proteins is to use the appropriate genetic mutants or variants. Such an approach is feasible if, and only if, well characterized transport mutants are available. Through a combination of transport kinetic, CB binding and CB photolabelling studies, the rat myoblast HT mutant, D23, was found to be defective in HAHT (D'Amore and Lo, 1986c). A comparison of the immunoblots from mutant D23 and its parental L6 cells might therefore be used for the identification of the transporter for HAHT (HAHTer). The initial studies were carried out with total whole cell extracts from glucose-grown L6 and D23 cells. Using α-IDIO as a probe, three bands (60, 63 and 104 kDa) were labelled in the L6 extract, whereas only two bands (60, 104 kDa) could be detected in the D23 extract (Fig. 5.2). This study clearly showed that the 63 kDa protein was present only in residual level in the D23 extract. It should be

Fig. 5.1 Immunoblotting Studies with Rabbit Intestinal Brush-border Membrane.

Rabbit intestinal brush-border membrane (BBM), 100 μg (lane 1), 50 μg (lane 2), 25 μg (lane 3) and 150 μg (lane 4), was immunoblotted with α-GT, α-IDIO or preimmune (PRE) serum as described in the text. The immune complexes were detected with ^{125}I-protein A. The molecular weight standards used were phosphorylase b (94 kDa), bovine serum albumin (67 kDa), ovalbumin (43 kDa), and carbonic anhydrase (30 kDa).

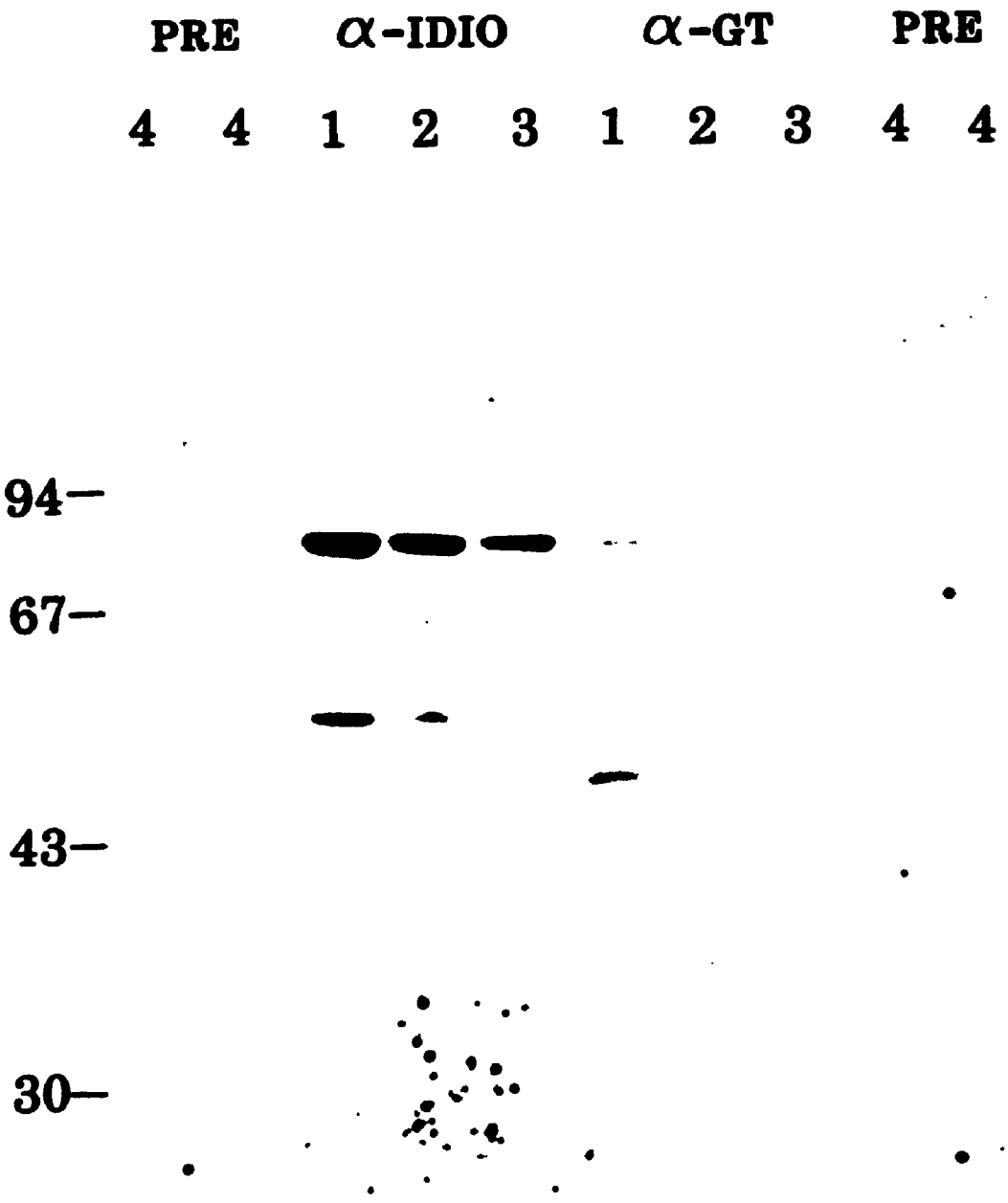
PRE
α-IDIO
α-GT
PRE
4 4 1 2 3 1 2 3 4 4
94—
67—
43—
30—

Fig. 5.2 Immunoblotting Studies with Whole Cell Extracts from Glucose-grown Mutant D23 and its Parental L6 Cells.

Immunoblotting of whole cell extracts was carried out as described in the text. Each lane was loaded with 150 μg of whole cell extracts prepared from L6 (lane 1) and mutant D23 (lane 2). After transfer to the nitrocellulose paper, lanes were then probed with α-GT and α-IDIO as indicated in the text. The immune complexes were detected with ^{125}I-protein A. The molecular weight standards used were phosphorylase b (94 kDa), bovine serum albumin (67 kDa), ovalbumin (43 kDa), and carbonic anhydrase (30 kDa).

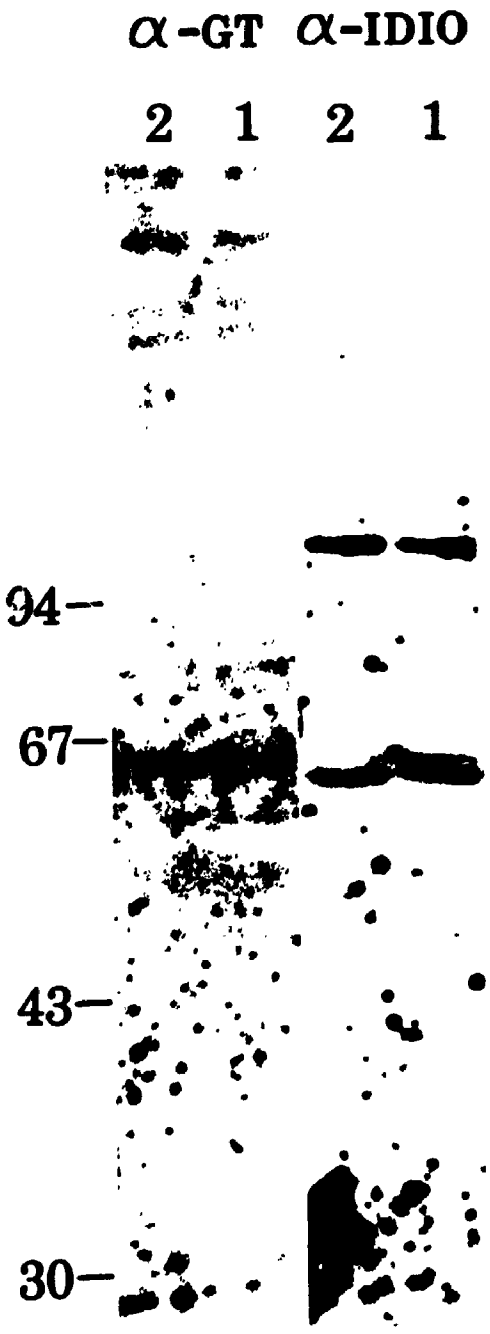
α-GT
α-IDIO
2
1
2
1
94
67
43
30

mentioned that the 104 kDa protein had the same molecular weight as hexokinase. Using α-GT as the probe, only one major protein (63 kDa) and several minor ones could be detected in the L6 extract; the 63 kDa protein was labelled to a slightly lesser extent in the D23 extract. The above studies suggested that the 63 kDa protein contained the glucose binding site, and antigenic determinant site(s) homologous to those present in the human rbc HTer; more importantly, this protein was altered in mutant D23. Thus it seemed possible that this 63 kDa protein might be the HAHTer.

5.3.3 Immunoblotting Studies with Plasma Membrane Prepared from L6 and Mutant D23.

One of the problems with whole cell extracts is that the antibodies will interact with any protein, regardless of its subcellular location, that possesses the antigenic determinant site(s). Since the HTer is present mainly in the plasma membrane, purified plasma membrane was therefore used to reduce interference by other proteins. The same amount of plasma membrane proteins from L6 and D23 was therefore probed with preimmune, α-GT, and α-IDIO sera (Fig. 5.3). While only trace amount of a 45 kDa protein could be recognized by preimmune serum, two major (60 and 63 kDa) and some minor ones were recognized by α-IDIO in the L6 plasma membrane; whereas only the 60 kDa protein was discernible in the D23 membrane. These are similar to the results obtained with whole cell extracts (above and Fig. 5.2), which suggested that the 63 kDa protein was missing or altered in the D23 plasma membrane.

The major protein recognized by α-GT in L6 membrane was the 63 kDa protein, and this was present in significantly lower amounts in the D23 membrane (Fig. 5.3). Again, this suggested that the 63 kDa protein might be the HAHTer. A 78 kDa protein was also recognized by α-GT, and its level was significantly lower in the D23 plasma membrane. It should be noted that this protein could

Fig. 5.3 Immunoblotting Studies with Plasma Membranes from Glucose-grown Rat Myoblasts.

Immunoblotting studies of plasma membranes were carried out as described in the text. Each lane was loaded with 200 μg of plasma membrane prepared from mutant D23 (lane 2) and its parental L6 (lane 1) cells. After transfer to nitrocellulose paper, each lane was probed with α-GT, α-IDIO, or preimmune (PRE) serum as indicated. The immune complexes were detected with ^{125}I-protein A. The molecular weight standards used were phosphorylase b (94 kDa), bovine serum albumin (67 kDa), ovalbumin (43 kDa), and carbonic anhydrase (30 kDa).

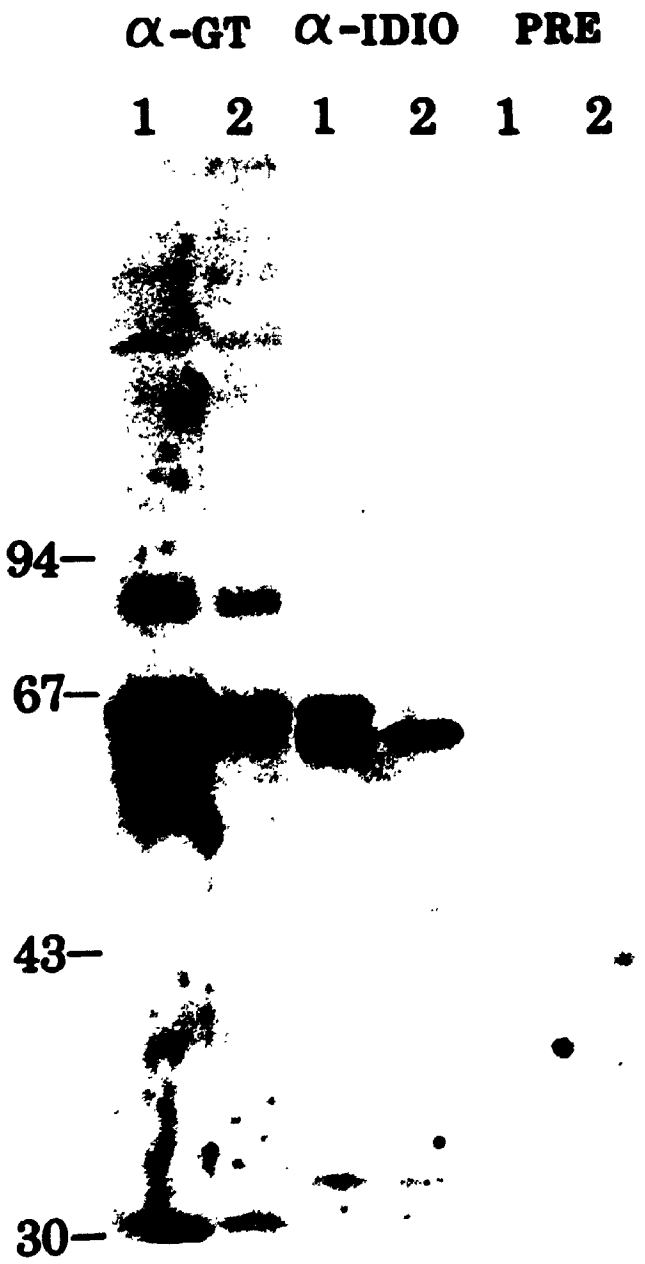
α-GT
α-IDIO
PRE
1
2
1
2
1
2
94—
67—
43—
30—

not be recognized by α-IDIO. In other words, the "normal" glucose binding site, which is recognized by α-IDIO because it is made against the active site, could not be detected on this 78 kDa protein, even though it contained homologous antigenic determinant site(s) to human rbc HTer. Another difference between the two antisera was that the 60 kDa protein detectable by α-IDIO in both L6 and D23 membranes could not be labelled by α-GT; thus indicating that this protein was antigenically quite different from the 63 kDa protein.

5.3.4 CB Photolabelling and Interaction with Specific Antibodies

Monoclonal antibodies directed against the human rbc HTer exerted a range of effects, from slight activation to strong inhibition, on CB binding to human rbc plasma membrane (Allard and Lienhard, 1985). Monoclonal antibodies directed against the renal Na^+-D-glucose cotransporter also exhibited similar effects on Na^+-dependent phlorizin binding to pig renal brush-border membranes (Wu and Lever, 1987; Koepsell et al, 1988). Thus if α-GT and α-IDIO were indeed binding to HAHTer, then this interaction might conceivably affect the interaction of CB to HAHTer. The effects of α-GT and α-IDIO on CB photolabelling were therefore examined. Purified rat myoblast plasma membrane was incubated with ^{3}H-CB, CE, and antiserum (α-GT, α-IDIO or pre-immune), photolyzed and separated by SDS-PAGE as described in "Methods and Materials". When incubated in the presence of preimmune serum, ^{3}H-CB was incorporated mainly into the 40-60 kDa region (Fig. 5.4A), which consisted of the rat myoblast HTers (see Chapter 4). CB incorporation into this region was found to be inhibited by about 35% by α-GT (Fig. 5.4A) suggesting that this antibody interacted with the myoblast CB binding component(s). In contrast, α-IDIO produced only about 5% inhibition (Fig. 5.4A). This is not surprising, as α-IDIO is thought to act in a similar manner to D-glucose, and very high concentrations of glucose are required to bring about significant inhibition of CB photolabelling. These antibodies exerted similar effects

Fig. 5.4 Effects of α-GT and α-IDIO on ^{3}H-CB Photolabelling.

Plasma membranes were incubated with 1 μM ^{3}H-CB, 100 μM cytochalasin E, and α-GT (△), α-IDIO (●) or preimmune serum (○) in 10 mM phosphate buffer (pH 7.4) at 0°C for 90 min. The mixture was then photolyzed and analyzed by SDS-PAGE as described in the text. Molecular weight (M_r x 10^{-3}) standards are shown on the top of each panel. Panel A shows the effect of antisera on ^{3}H-CB photolabelling of plasma membrane from glucose-grown rat L6 myoblasts (300 μg). Panel B shows the effect of antisera on human rbc plasma membrane (175 μg).

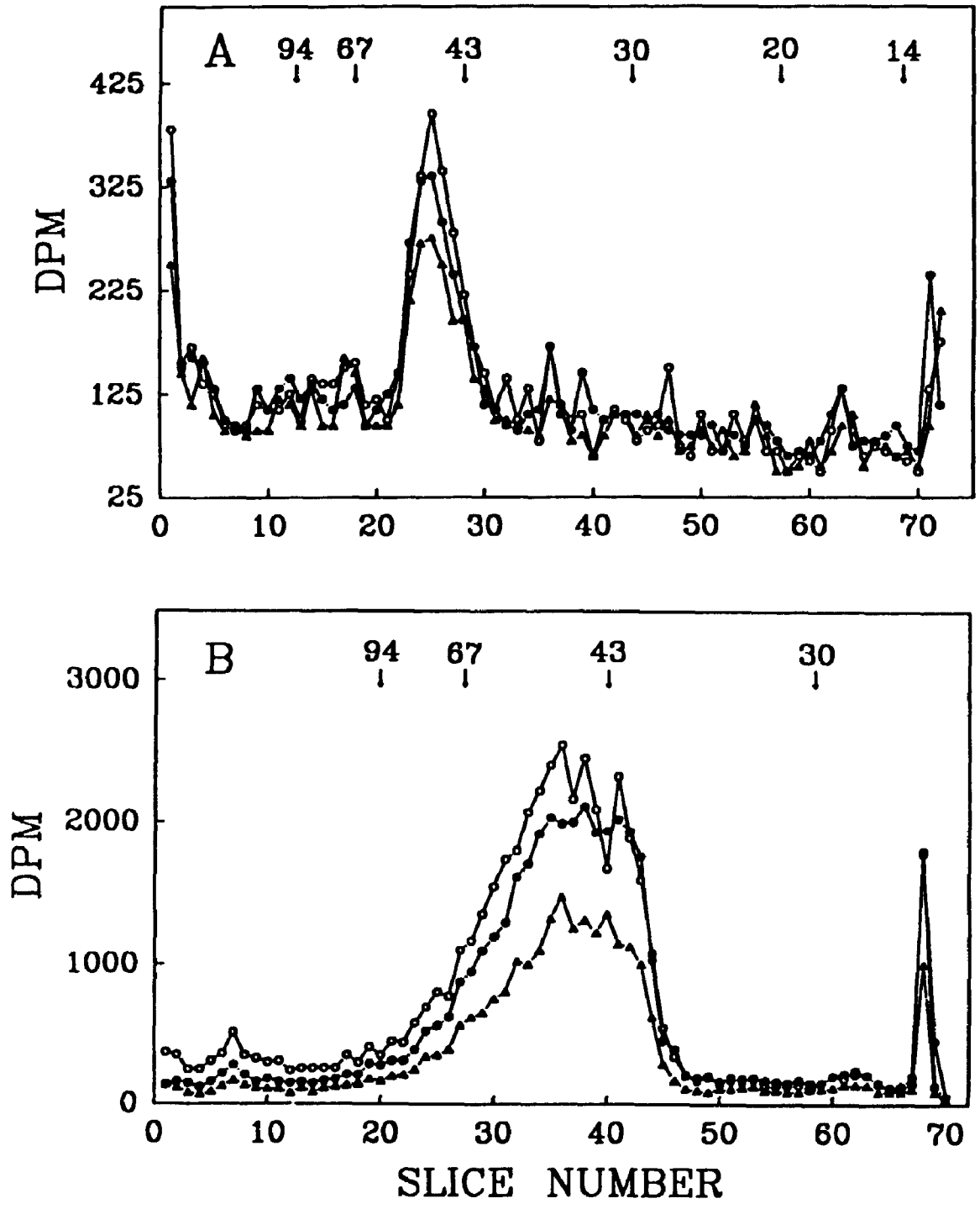
A
94
67
43
30
20
14
425
325
225
125
25
DPM
0
10
20
30
40
50
60
70
B
94
67
43
30
3000
2000
1000
0
DPM
0
10
20
30
40
50
60
70
SLICE NUMBER

on CB-photolabelling of human rbc membrane (Fig. 5.4B). CB photolabelling into the 40-70 kDa region decreased about 44% in the presence of α-GT as compared to that measured in the presence of pre-immune serum. About 11% inhibition was observed in the presence of α-IDIO.

CB binding studies suggested that CB inhibited HT activity by an allosteric mechanism (see Chapter 3). If this were the case, then CB-photolabelling of the HAHTer may affect the latter's interaction with α-GT. As indicated in Fig. 5.5a, irradiation of plasma membrane for 20 sec. with a 1000 watt ultraviolet lamp dramatically reduced the level of proteins able to penetrate the SDS-PAGE. The extent of reduction varied considerably from protein to protein. Similar alterations were also observed with human rbc membranes (Fig. 5.5b). Photolysis alone was also found to affect the labelling pattern of immunoblots by α-GT (Fig. 5.5c). The 78 kDa band observed in the control rat myoblast plasma membrane could hardly be detected in the photolyzed membrane. However, the labelling of the 63 kDa protein was not altered by photolysis. Similar observations were also made with rat adipocytes (Carter-Su and Okamoto, 1985). Photolysis in the presence of 1 μM CB was also found to increase the labelling of the 63 kDa protein, and a number of lower molecular weight components (between 50 to 63 kDa) by α-GT (Fig. 5.6a). This increase in labelled lower molecular weight components was even more apparent with human rbc membrane (Fig. 5.6b). Thus, this study showed that the interaction of the 63 kDa protein with α-GT could be affected by the specific inhibitor of HT, and that the mobility of the antibody-labelled component(s) could be affected by photolysis in the presence of CB.

5.3.5 Distribution of the Hexose Transporters in Various Subcellular Fractions

In contrast to observations made on rat adipocytes (Horuk et al., 1986), the level of HTer in low density microsomal fraction (LDMF) was less than 20% of that in the plasma membrane. Since these determinations were based on the

Fig. 5.5 Effect of Photolysis on the Protein and Immunoblotting Profiles.

Membranes were photolyzed in 10 mM phosphate buffer (pH 7.4) for 20 sec., and analyzed on SDS-PAGE as described in the text. Panels (a) and (b) show the Coomassie blue stained-gels of plasma membrane from glucose-grown rat L6 myoblasts (150 μg) and human rbc plasma membrane (400 μg), respectively. Lanes 1 and 2 indicate protein profiles before and after photolysis, respectively. Panel (c) shows an immunoblot with α-GT of plasma membrane from glucose-grown rat L6 myoblasts (150 μg) before (Lane 1) and after (Lane 2) photolysis. Membranes were photolyzed and immunoblotted as described in the text.

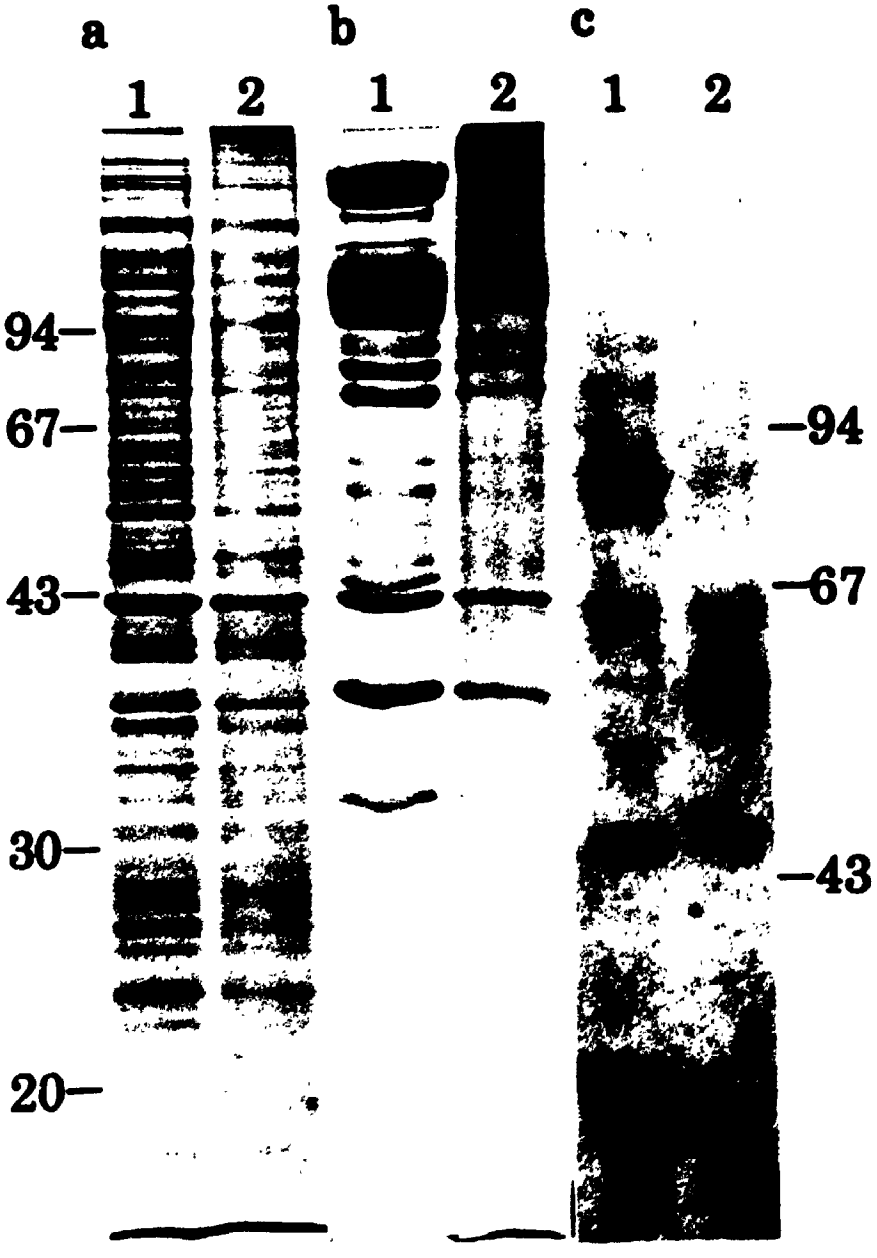
a
b
c
1
2
1
2
1
2
94
67
43
30
20
94
67
43

Fig. 5.6 Effect of CB on the Immunoblotting Profiles with α-GT.

Membranes were photolyzed and immunoblotted with α-GT as described in the text. Panels (a) and (b) show the immunoblotting profiles of the plasma membrane from glucose-grown rat L6 myoblasts (200 μg) and the human rbc plasma membrane (250 μg), respectively. Membranes were photolyzed in the absence (Lane 1) or in the presence (Lane 2) of 1 μM CB. The immune complexes were detected with ^{125}I-protein A. The molecular weight standards used were phosphorylase b (94 kDa), bovine serum albumin (67 kDa), ovalbumin (43 kDa), and carbonic anhydrase (30 kDa).

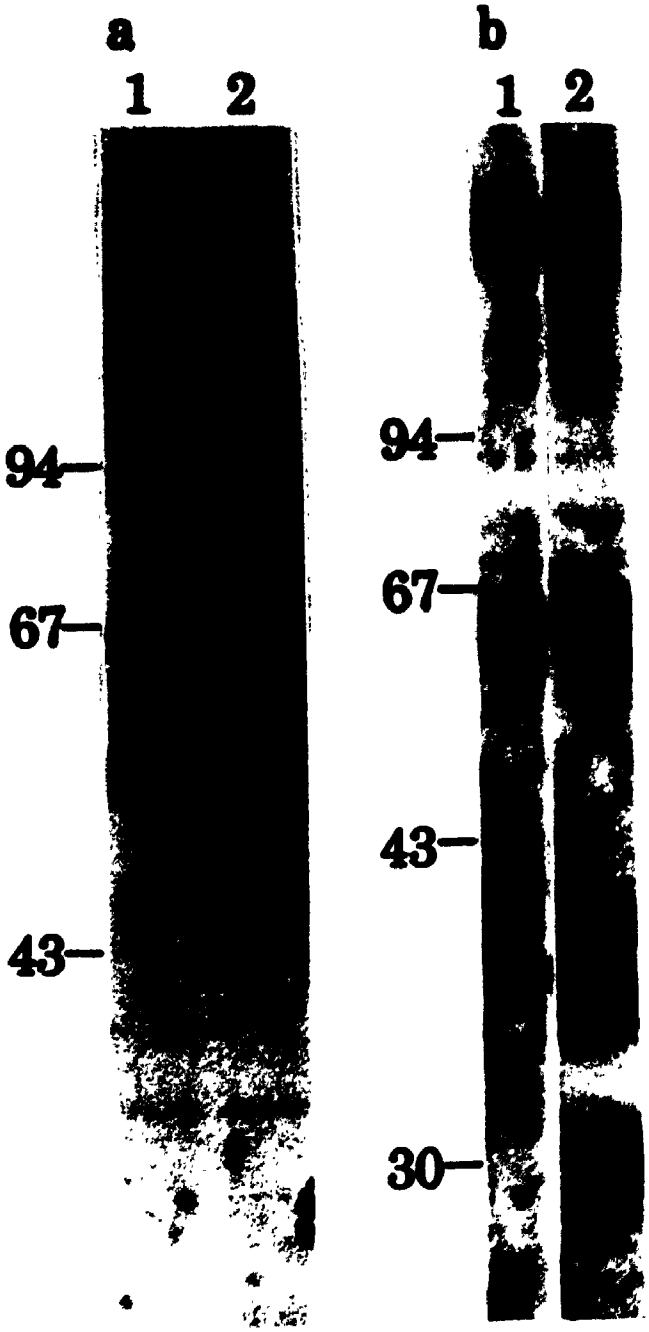
a
1
2
94
67
43
b
1
2
94
67
43
30

interaction of CB with the HTer, they might not reflect the distribution of both inactive and active transporters. Immunoblotting studies were therefore carried out with various membrane preparations (Figs. 5.7 and 5.8). Fraction C contained a mixture of various membranes including the mitochondria; whereas the plasma membrane fraction and LDMF were relatively free of contamination from each other. In agreement with CB binding and photolabelling studies, the α-GT labelled HAHTer (i.e. the 63 kDa protein) was detected mainly in the plasma membranes, only a residual level was present in the LDMF (Fig. 5.7). More importantly, the level of this 63 kDa protein was significantly reduced in various membrane fractions prepared from mutant D23. The α-GT labelled 78 kDa protein was detectable mainly in the L6 plasma membrane; only residual levels could be detected in the D23 plasma membrane. Thus it seems possible that the 78 kDa protein may be related to the 63 kDa protein. While not much was known about their nature, significantly different levels of the 97, 82, and 33 kDa proteins were found in the D23 HDMF and LDMF (Fig. 5.7).

A slightly different picture was observed when similar studies were carried out with α-IDIO (Fig. 5.8). The levels of 63 and 60 kDa proteins in the L6 plasma membrane were significantly higher than those in the L6 LDMF. This suggested that the "normal" glucose binding site could not be detected in LDMF, even though residual level of this protein could still be detected by α-GT (Fig. 5.7). The 63 kDa protein could hardly be detected by α-IDIO in all D23 membrane fractions. On the other hand, the 60 kDa protein was present in similar amounts in both L6 and D23 plasma membrane and HDMF; however it could not be detected in LDMF.

5.3.6 Effect of Glycosidases on the Hexose Transporters in L6 Myoblasts

It has been shown that various eukaryotic HTers are heterogeneously glycosylated (Wang, 1987). In order to determine whether the 63 and 78 kDa proteins in L6 myoblasts are also glycosylated, we examined the effects of

Fig. 5.7 Distribution of Proteins Recognizable by α-GT in Different Membrane Fractions Prepared from Glucose-grown Mutant D23 and its Parental L6 Cells.

Plasma membrane, fraction C, HDMF and LDMF (300 μg) prepared from glucose-grown mutant D23 (Lane 2) or its parental L6 cells (Lane 1) were immunoblotted with α-GT as described in the text.

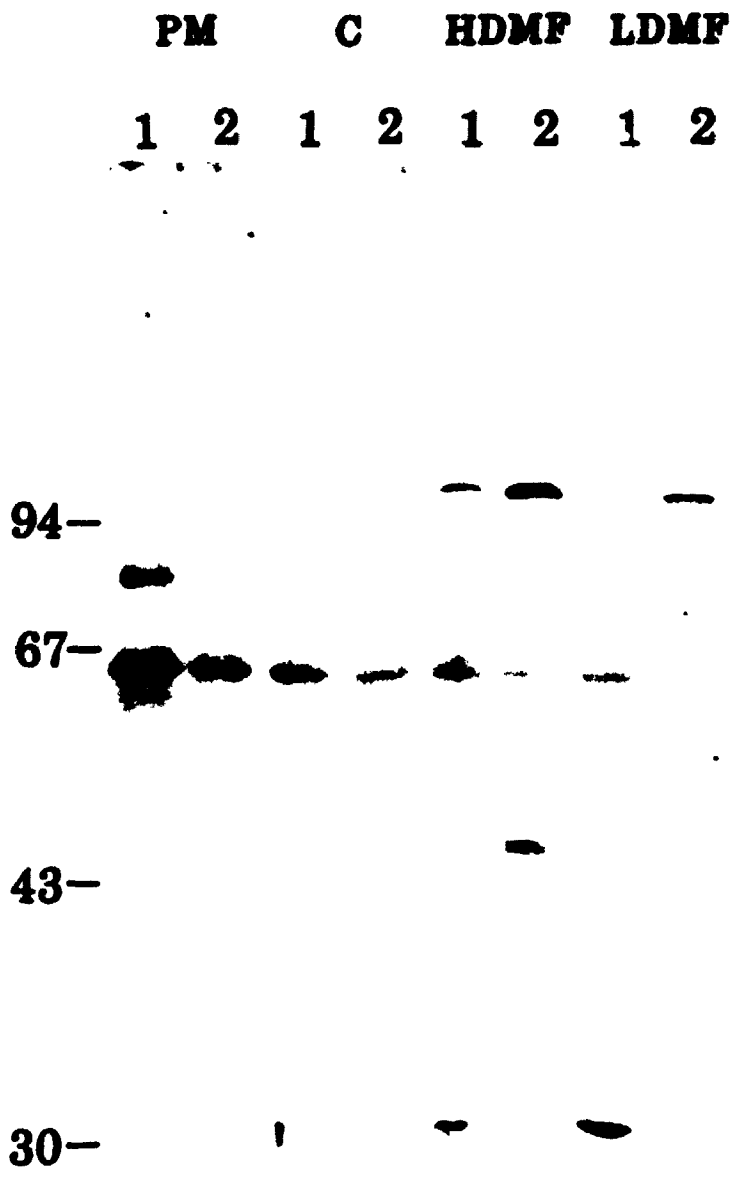
PM
C
HDMF
LDMF
1 2 1 2 1 2 1 2
94–
67–
43–
30–

Fig. 5.8 Distribution of Proteins Recognizable by α-IDIO in Different Membrane Fractions Prepared from Glucose-grown Mutant D23 and its Parental L6 Cells.

Plasma membrane, HDMF and LDMF (200 μg) prepared from glucose-grown mutant D23 (Lane 2) or its parental L6 cells (Lane 1) were immunoblotted with α-IDIO as described in the text.

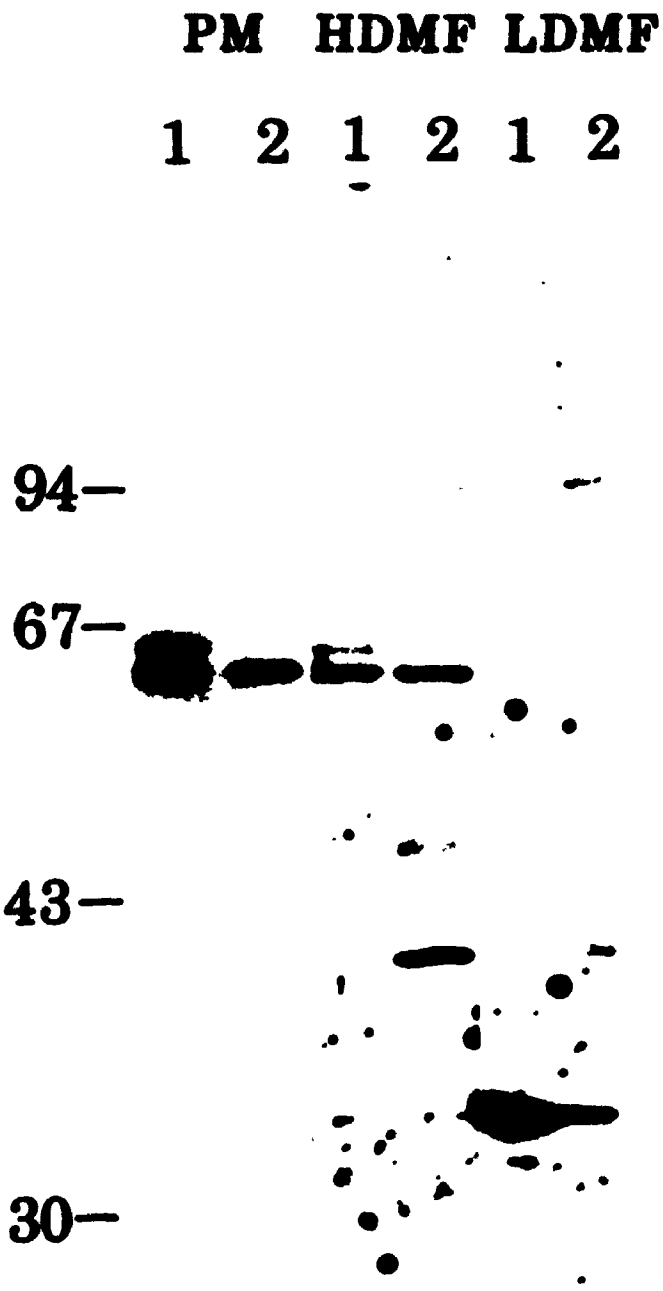
PM HDMF LDMF
1 2 1 2 1 2
94—
67—
43—
30—

endoglycosidase H (Endo H) and N-glycanase on the labelling of these proteins (Fig. 5.9). Treatment with Endo H was found to have no effect on the mobility of various α-GT labelled bands (Fig. 5.9a), while this treatment altered the mobility of ovalbumin from 43 to 40 kDa (Fig. 5.9b). Treatment with N-glycanase caused a shift of the mobility of the 63 kDa protein to some lower molecular weight proteins (55-63 kDa) (Fig. 5.9c). The above studies using N-glycanase suggests that the 63 kDa protein might indeed be a glycoprotein.

5.4 DISCUSSION

Various approaches have been used in the identification of eukaryotic HTers. Some of these approaches are based on affinity binding with specific ligands such as cytochalasin B, forskolin, and anti-(human rbc HTer) (Shanahan, 1982; Shanahan et al., 1987; Allard and Lienhard, 1985). Since these assays do not reflect the functional state of the labelled proteins, it is difficult to prove unequivocally that the labelled proteins are indeed involved in HT. To this end, we have used HT mutants to verify the identity of the cytochalasin B labelled components (see Chapter 4). The present investigation uses two antisera, anti-(human rbc HTer) (α-GT) and anti-(rabbit anti-glucosamine IgG) (α-IDIO), to identify and characterize the HTers in undifferentiated rat myoblasts. The former recognizes antigenic determinant sites also present in human rbc HTer, whereas the latter recognizes proteins with glucose-binding sites. Identification of proteins by immunoblotting studies has the distinct advantage that the proteins are freely accessible to the antibodies, and that the proteins have not been subjected to treatments such as photolysis and cross-linking reagents.

The following pieces of evidence suggest that both α-GT and α-IDIO can be used for the identification of HTer. First, both antibodies were able to recognize the Na^+-dependent brush border HTer, which has a molecular weight around 78

Fig. 5.9 Effects of Endoglycosidases on the Mobility of Proteins Recognizable by α-GT.

Treatment of plasma membrane with endoglycosidases and immunoblotting were performed as described in the text. Panel (a) shows an immunoblot with α-GT of plasma membrane from glucose-grown L6 myoblasts (150 μg) treated with (Lane 2) or without (Lane 1) endoglycosidase H using the alkaline phosphatase conjugated goat anti-rabbit IgG to visualize the bound IgG. Panel (b) shows a Coomassie blue stained gel of ovalbumin (50 μg) treated with (Lane 2) or without (Lane 1) endoglycosidase H. Panel (c) indicates immunoblots of plasma membrane from glucose-grown L6 myoblasts (100 μg) treated with (Lane 2) or without (Lane 1) N-glycanase, using ^{125}I-protein A to visualize the bound IgG, respectively.

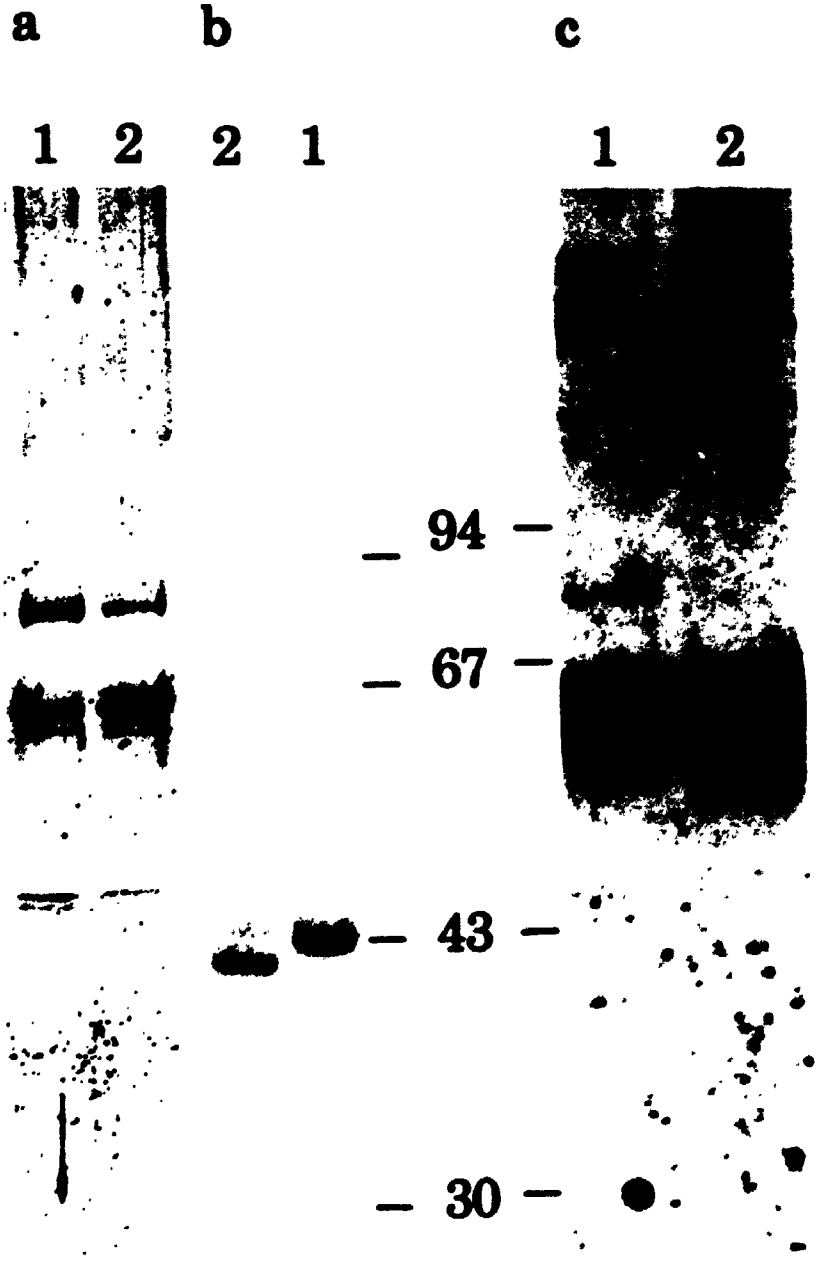
a
b
c
1
2
2
1
1
2
94
67
43
30

kDa (Fig. 5.1). These two antisera have previously been shown to bind to the human rbc HTer (Kay, 1985). Second, transport kinetics, CB binding and photolabelling studies indicated that the rat myoblast HAHT was present only in residual level in the plasma membrane of mutant D23 (D'Amore and Lo, 1986c). Immunoblotting studies with both antisera also showed that a 63 kDa labelled protein was missing or present in much reduced level in the plasma membrane from this mutant (Figs. 5.3, 5.7, and 5.8). This provides the most convincing evidence that the 63 kDa protein recognized by α-GT and α-IDIO is indeed involved in HAHT. Third, if the antibody is binding to the HTer, which possesses its own CB binding site, then the antibody may affect CB binding, and vice versa. Indeed, α-GT, a polyclonal antibody, was found to reduce CB labelling by about 35% (Fig. 5.4A). On the other hand, 1 μM CB was found to increase the antibody binding to the rat myoblast 63 kDa protein (Fig. 5.6a). Similar results were also obtained with human rbc plasma membrane (Figs. 5.4B and 5.6b). Fourth, both CB binding and photolabelling studies indicated that the rat myoblast HTers were present primarily in the plasma membrane. Immunoblotting studies with both α-GT and α-IDIO showed that the 63 kDa protein was present mainly in the plasma membrane; only a residual amount could be detected in LDMF (Figs. 5.7 and 5.8). Finally, similar to other HTers, the 63 kDa protein was found to be a glycoprotein (Fig. 5.9) (Horner et al., 1987; Wang, 1987). The above findings are in accordance with the concept that the 63 kDa protein recognized by both α-GT and α-IDIO may indeed be the HAHTer. This study suggests that the HAHTer possesses not only a glucose binding site, but also antigenic determinant site(s) homologous to those in the human rbc HTer.

Besides the 63 kDa protein, several other proteins were also recognized by either one of the two antisera used. The 104 kDa protein recognized by α-IDIO in whole cell extracts was detectable only in the plasma membrane, and was present

in similar amounts in both D23 and L6 extracts (Fig. 5.2). We have also previously shown that both D23 and L6 extracts contained similar levels of hexokinase (D'Amore et al., 1986b). Based on its molecular weight, interaction with α-IDIO, its level in both D23 and L6 whole cell extracts, and its absence in plasma membrane preparations, this 104 kDa protein may conceivably be hexokinase. Since this protein did not interact with α-GT, it might therefore be surmised that hexokinase did not have antigenic determinant sites homologous to that in the human rbc HTer. The 78 kDa protein recognized by α-GT was present primarily in the rat myoblast plasma membrane (Figs. 5.3 and 5.7). Irradiation of the plasma membrane with UV-light abolished the ability of this protein to be recognized by α-GT (Figs. 5.5 and 5.6). Similar to the 63 kDa protein, this 78 kDa protein was recognized by α-GT and was present in substantially reduced amounts in mutant D23. This correlation could be taken as an indication that this protein might be related to the 63 kDa protein. For example, it could be a precursor form of the 62 kDa protein. The lack of interaction with α-IDIO suggested that the "normal" glucose binding site was not present in this protein. If this 78 kDa protein is the precursor for the HTer, then this suggests that the antigenic determinant site recognizable by α-IDIO is likely an "assembled" (or referred to as discontinuous) epitope, which is affected by the folding of the peptide.

The only other major plasma membrane protein recognized by α-IDIO is the 60 kDa protein. We have previously demonstrated that the HAHTer and the transporter for LAHT (LAHTer) are present mainly in the plasma membrane (Cheung and Lo, 1984). The following lines of evidence suggested that this 60 kDa protein might be the LAHTer. (1) By its very nature, one would expect that the LAHTer should possess its own glucose-binding site. Since the 60 kDa protein is the only other major plasma membrane protein recognized by α-IDIO, it is therefore possible that this protein may be the putative LAHTer. (2) Both

transport kinetics and CB binding studies revealed that the level of LAHTer was not altered in the D23 plasma membrane (D'Amore and Lo, 1986c). Data presented in Fig. 5.8 showed that the level of the 60 kDa protein was quite similar in various membrane fractions prepared from L6 and D23 cells. (3) CB binding studies suggested that the level of LAHTer was hardly detectable in LDMF. Similar reduction in the 60 kDa protein was also observed in LDMF (Fig. 5.8). (4) CB photolabelling studies indicated that the molecular weight for the LAHTer should be around 40-60 kDa. The above observations suggest that the 60 kDa protein may be the LAHTer. Studies with α-GT indicated that this protein did not contain antigenic determinant sites homologous to those of the human rbc HTer. Further studies are being carried out with mutant D23 to determine the identity and properties of the 60 kDa protein.

Besides identifying the rat myoblast HTers, the present investigation unveiled several side effects of photolysis. Even though plasma membranes were irradiated with high intensity UV light for less than 30 sec., there was extensive cross-linking and aggregation of proteins (Figs. 5.5a and b). It may be apparent from the Coomassie blue stained gels that the amount of proteins able to penetrate the SDS-PAGE was considerably reduced in the photolyzed sample (Fig. 5.5a and b). Furthermore, the degree of reduction varied considerably from protein to protein. A similar observation was also made using rat adipocytes (Carter-Su and Okamoto, 1985). Aside from the poor efficiency of incorporation of CB, this observation may explain why ten times more human rbc proteins were required to produce sufficient signal for CB photolabelling than for immunoblotting studies (Oka et al., 1988). The observation that UV-irradiation abolished the ability of the 78 kDa protein to be recognized by α-GT also served to illustrate the extensive alteration of protein properties by photolysis (Fig. 5.5c). Another striking effect of photolysis was on the mobility of proteins on SDS-PAGE. Immunoblotting studies with α-GT and α-

IDIO showed that the molecular weights of HAHTer and the putative LAHTer were 63 and 60 kDa, respectively (Figs. 5.2 and 5.3). Photolysis in the presence of 1 μM CB also resulted in a noticeable increase in lower molecular weight α-GT labelled proteins (Fig. 5.6a). This effect was even more apparent with the human rbc (Fig. 5.6b). This alteration in molecular weight was also apparent in ^{3}H-CB photolabelling studies (Fig. 5.4), in which about 1-8% total HTer was labelled (Carter-Su et al., 1982; Shanahan, 1982; Klip et al., 1983b). These studies showed that the CB labelled HTers have molecular weights ranging from 40-60 kDa. It may therefore be concluded that a subpopulation of the CB-photolabelled HTers exhibits slightly different mobility on SDS-PAGE. This may explain why the CB-labelled HTer is characterized by a broad range of molecular weights (Fig. 5.4), whereas immunoblotting studies show sharp and discrete bands (Fig. 5.3). In agreement with this idea, it was previously demonstrated that the conformation of the HTer might be altered by the photoaffinity labelling with ^{3}H-CB (Kurokawa, et al., 1986). Thus, the present investigation shows that immunoblotting studies have several distinct advantages over the CB photolabelling studies. First, this procedure does not involve drastic treatments such as photolysis. Second, the molecular weight and identity of the HTer can be clearly resolved by immunoblotting studies. Finally, this procedure allows us to distinguish proteins with glucose binding sites from those with inactive glucose binding sites.

CHAPTER 6

REGULATION OF HEXOSE TRANSPORT IN RAT MYOBLASTS DURING GROWTH AND DIFFERENTIATION

6.1 INTRODUCTION

Studies on the regulation and properties of HT in eukaryotic cells revealed several mechanisms by which HT can be affected. The first type involves changes in the intrinsic properties of the transporter. This is often reflected by the alteration in the transport affinity, substrate specificity, and/or response to various inhibitors. Both biochemical and kinetic analyses suggest that the intrinsic properties of the HTer can be modulated by reagents such as cytochalasin B (Jung et al., 1986), phloretin (Krupka and Deves, 1986), ATP (Carruthers, 1986; Herbert and Carruthers, 1986), insulin (Whitesell and Abumrad, 1985; Baly and Horuk, 1987; Kahn and Cushman, 1987; Toyoda et al., 1987; Joost et al., 1988), adenosine and catecholamine (Smith et al., 1984; Joost et al., 1986). Positive regulator(s) have been postulated to be involved in the activation of HT (Yamada et al., 1983; Haspel et al., 1986; D'Amore and Lo, 1988). Activation of HT can also be brought about by covalent changes, such as limited proteolytic cleavage, and treatment with specific antibodies (Lo and Duronio, 1984a,b; D'Amore et al., 1986a; D'Amore and Lo, 1988). It should be noted that the phosphorylation of the HTer is not involved in the regulation of HT (Witters et al., 1985; Gibbs et al., 1986; Frost et al., 1987; Joost et al., 1987).

HT can also be regulated by altering the number of functional transporters in the plasma membrane. This effect is often revealed by changes in transport capacity, with no change in transport affinity and substrate specificity. The number of transporters present is dependent on the rates of synthesis and degradation,

and/or translocation of the transporter from the intracellular storage site to the plasma membrane. Glucose-starvation (Christopher et al., 1976a; Franchi et al., 1978; Kalckar and Ullrey, 1984; Van Putten and Krans, 1985; D'Amore et al., 1986a; Haspel et al., 1986; D'Amore and Lo, 1988), cell density (Gay and Hilf, 1980), insulin (Simpson and Cushman, 1986; Garvey et al., 1987), nicotinamide (Amos et al., 1984), and glucocorticoids (Carter-Su and Okamoto, 1985; Horner et al., 1987) have been shown to alter the number of HTers in the plasma membrane via one or more of the above mechanisms.

The presence of two HT systems in undifferentiated rat L6 myoblasts has been established through the kinetic, CB binding, CB photolabelling studies and the use of specific antibodies against human erythrocyte HTer (see previous chapters). However, only one HT system has been demonstrated by other laboratories (Klip et al., 1982; Beguinot et al., 1986; Lee et al., 1987). An examination of the growth conditions revealed that these studies were carried out with myoblasts grown to different densities, and in different sera. More importantly, multinucleated myotubes were used in the transport studies. It is therefore possible that the observed discrepancies might actually reflect differences in HT properties in undifferentiated myoblasts and myotubes. Cellular differentiation has been demonstrated to alter the properties of the sodium, and potassium transport systems in different types of cells (Gargus et al., 1983; Rosoff and Cantley, 1983).

Rat myoblast L6 is able to undergo myogenic differentiation (Yaffe, 1968; Sanwal, 1979; Pearson, 1981; Wakelam, 1985). After subculturing, mononucleated myoblasts will proliferate, align and fuse to form multinucleated myotubes. Since myogenesis involves cessation of DNA synthesis and irreversible withdrawal from the cell cycle, the rate of fusion is therefore dependent on the concentration of growth promoting constituents, or mitogens in the serum; high serum concentrations will prevent an early cessation of DNA synthesis, and therefore myogenesis will not

occur. Morphological differentiation is accompanied by biochemical differentiation. Both increases and decreases of specific proteins have been observed during biochemical differentiation. For example, while the syntheses of creatine phosphokinase, myosin, actin, the type I cAMP-dependent protein kinase, acetylcholine receptor, and mannosylated glycoproteins are increased during differentiation (Sanwal, 1979; Pearson, 1981; Cates et al., 1984; Rogers et al., 1985; Lorimer et al., 1987), the binding sites for the transforming growth factor-ß are found to decrease dramatically as myoblasts fuse to form the myotubes (Ewton et al., 1988). It is therefore conceivable that events associated with myogenesis may also alter the properties of the HT systems in rat L6 myoblasts. In this chapter, we will turn from the identification of the HT systems in rat L6 myoblasts to the regulation of HT during myogenic differentiation.

6.2 MATERIALS AND METHODS

6.2.1 Materials

2-Deoxy-D-[1,2-^{3}H]glucose (50 Ci/mmol) and 3-0-[methyl-^{3}H]-methyl-D-glucose (50 Ci/mmol) were purchased from ICN Biochemicals, Canada Ltd. N-ethylmaleimide (NEM), p-chloromercuribenzenesulfonic acid (pCMBS), and 5-bromo-2'-deoxy-uridine (BrdUrd) were purchased from Sigma Chemical Co. All other chemicals were obtained from commercial sources and were of the highest available purity.

6.2.2 Cell Lines and Culture Media

The maintenance of Yaffe's L6 cell line (Yaffe, 1968) and the preparation of glucose starvation medium (or referred to as 'fructose medium') were described in Chapter 2. Unless indicated otherwise, cells were routinely plated at a density of 1.5 x 10^6 cells/well in six-well (35 x 15 mm) Costar plates. Mutant D1 was a generous gift from Dr. B.D. Sanwal, Department of Biochemistry, University of Western Ontario, London, Ontario, Canada (Cates et al., 1984). This mutant was

derived from L6 by mutagenesis with ethylmethanesulfonate and subsequent exposure to 150 μg/ml concanavalin A. For fusion experiments, this mutant was first allowed to attach to the plates for 48 hrs. in 10% horse serum, after which the medium was replaced with fresh medium containing 1% horse serum (Clarke et al., 1988).

6.2.3 Whole Cell Transport Studies.

Transport studies were carried out with 6-well Costar plates on different days after subculturing as described in Chapter 2. The properties of HAHT were examined by using the low concentration range (0.05 mM - 1 mM) of dGlc; whereas that of LAHT was examined using MeGlc (0.05 mM - 1 mM) as the transport substrate.

6.2.4 Transport Studies With Plasma Membrane Vesicles.

Plasma membrane vesicles were isolated and purified from glucose-grown rat L6 myoblasts by a previously described method (Cheung and Lo, 1984; Mesmer et al., 1986), which separated sealed right-side out plasma membrane vesicles (fraction A) from leaky membrane sheets or inside-out plasma membranes (fraction B). Transport assays were determined by the flow dialysis method, transport rates were indicated by the difference between hexose associated with fraction A and with fraction B.

6.2.5 Determination of Fusion Index

Cells were fixed and stained with 6% Giemsa stain. Cell fusion was quantitated by determining the proportion of nuclei within myotubes (Morris and Cole, 1972). Only structures containing three or more nuclei were counted as myotubes.

6.2.6 Protein Determination.

Cells in two wells on each 6-well Costar plate were detached with 1 mM EDTA in PBS, and the amount of protein per well was determined by the method of Lowry (Lowry et al., 1951), using bovine serum albumin as a standard.

6.3 RESULTS

6.3.1 Effect of Cell Density on Hexose Transport

A review of the literature indicates that there are considerable variations in the rat myoblast HT kinetics (Klip et al., 1982; Beguinot et al., 1986; D'Amore and Lo 1986a; Lee et al., 1987). One of the reasons for the observed discrepancy may be due to cell density of the cultures used. Cell density has been demonstrated to affect HT in rat mammary adenocarcinoma cells (Gay and Hilf, 1980).

Two approaches were used in this section to examine the effects of cell density and growth on HT. The first approach involved plating myoblasts at a density of 1.0×10^5 cells per 35 mm well and measuring transport activity on different days after subculturing. After an initial lag phase, the L6 myoblasts were found to have a doubling time of 22 hrs (D'Amore and Lo, 1988). Similar rates of dGlc uptake were observed when the cell densities were less than 4.4×10^4 cells per cm^2 (Fig. 6.1). However, the rate of dGlc uptake decreased dramatically when cells were grown to higher densities. The question that arises is whether the observed decrease is due to the growth stage or the density of the confluent cells. Thus the second approach involved plating cells at different densities, and determining transport rates two days after subculturing. Both dGlc and MeGlc transport activities were found to drop dramatically at cell density greater than 4.4×10^4 cells per cm^2 (Fig. 6.1). Since Day-2 cultures were used in these studies, the observed decrease was likely to be due to the cell density effect. HT studies were also carried out with plasma membrane vesicles prepared from cells grown to different densities (Fig. 6.1). In agreement with the whole cell studies, plasma membrane vesicles prepared from cells grown to a density higher than 4.4×10^4 cells/ cm^2 exhibited much reduced rates of transport than those prepared from cells grown to a lower density.

Fig. 6.1 Effect of Cell Density on Hexose Transport.

Both whole cell and plasma membrane vesicle transport studies were carried out as described in the text. In whole cell transport studies, the concentration of dGlc used was 0.06 mM, and its specific activity was 3.0 x 10^4 d.p.m./nmol. The amount taken up by cells at a density of 1.31 x 10^5 cells/35mm well was 26 pmol/10^5 cells/min; this was regarded as 100%. In the case of plasma membrane vesicle transport studies, the concentration of dGlc used was 0.5 mM with a specific activity of 16 mCi/mmol; the control value was 336 nmoles/mg protein/min. The concentration of MeGlc used was 0.1 mM, and its specific activity was 2.9 x 10^4 d.p.m./nmole. The amount of MeGlc taken up by cells at a density of 3 x 10^5 cells/35 mm well was 0.012 nmoles/10^5 cells/min. (○) denotes the rates of dGlc uptake by glucose-grown L6 cells seeded at 1 x 10^5 cells/well on Day 0, and transport activities were then determined on different days (up to Day 4) after subculturing. (●) and (△) denote the rates of dGlc and MeGlc uptake by glucose-grown L6 cells seeded at different densities, and transport activities were determined on Day 2 after subculturing, respectively. (▲) denotes uptake by plasma membrane vesicles prepared from glucose-grown L6 cells seeded at different densities.

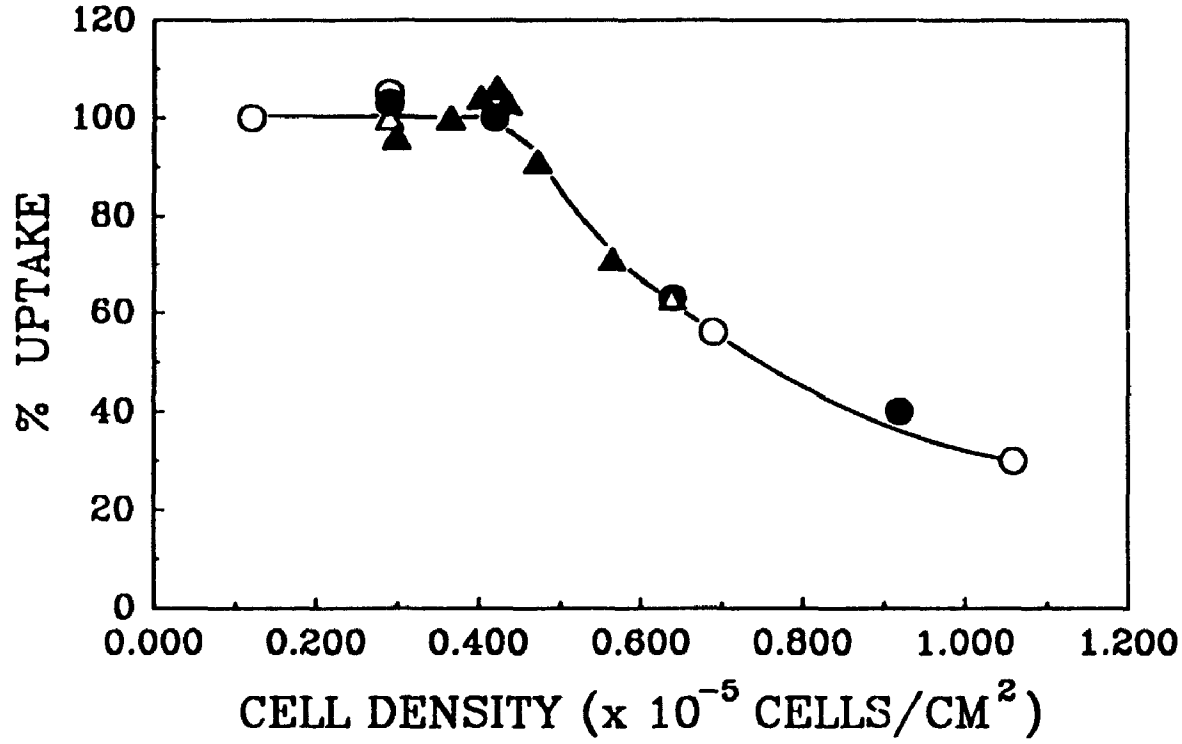
120
100
80
60
40
20
0
% UPTAKE
0.000
0.200
0.400
0.600
0.800
1.000
1.200
CELL DENSITY (x 10^{-5} CELLS/CM^{2})

6.3.2 Hexose Transport by Rat L6 Myoblasts at Different Stages of Myogenesis

Rat myoblast L6 is a permanent skeletal muscle cell line capable of undergoing myogenesis (Yaffe, 1968; Sanwal, 1979). Figs. 6.2A-6.2C show the transition of proliferating L6 myoblasts to multinucleated myotubes. These cells remained undifferentiated on Day 2 (Fig. 6.2A); cell alignment could be observed on Day 3; multinucleated myotubes could be easily detected on Day 4.5 (Fig. 6.2B); and fusion was essentially complete on Day 6. (Fig. 6.2C). The extent of differentiation was quantitated by measuring the % fusion (i.e. fusion index) on different days after subculturing (Fig. 6.3A). While no fusion was observed on days 2 and 3, the fusion indices for days 4, 4.5, 5, and 6 cultures were 28%, 65%, 95% and 100%, respectively. In other words, under our growth conditions, fusion was initiated between day 3 and day 4, and was essentially complete on day 6.

While most HT studies by other laboratories were carried out with myotubes, our previous studies were carried out with undifferentiated myoblasts (Klip et al., 1982; Beguinot et al., 1986; D'Amore and Lo, 1986a; Lee et al., 1987). Thus it is possible that the observed discrepancy in HT kinetics may also be due to the growth stage of the cultures used. In order to resolve this problem, the transport affinity and capacity of the uptake of dGlc and MeGlc were determined at different stages of myogenesis. As indicated in Fig. 6.3A, the average Km values of MeGlc uptake remained around 3.7 mM in both undifferentiated myoblasts and myotubes. On the other hand, the average Km values of dGlc transport increased from 0.6 mM to 3.6 mM upon prolonged period of growth (Fig. 6.3A). While it was not altered in undifferentiated myoblasts (Day-2 and Day-3 cultures), the dGlc transport affinity was found to decrease upon the onset of fusion (i.e. on day 4). This decrease seems to be proportional to the extent of differentiation. This observation suggests that the dGlc transport system may be degraded faster or modified during myogenesis.

Fig. 6.2 Morphology of Glucose-grown Rat L6 Myoblasts on Different Days after Subculturing.

Rat L6 myoblasts were plated at a density of 1.5 x 10^5 cells/35 mm plate. On different days after subculturing, cells were fixed and stained with 6% Giemsa stain. Panels A-C show the morphology of glucose-grown L6 cells on Day 2, Day 4.5 and Day 6 after subculturing, respectively. Panels D-F show the morphology of the Day-2, Day-5, and Day-6 L6 cells grown in the presence of 7.5 μM 5-bromo-2'-deoxy-uridine (BrdUrd), using D-glucose as the sole carbon source. These figures serve to illustrate that BrdUrd inhibits myogenesis in rat L6 myoblasts. The bar indicates 100 μm.

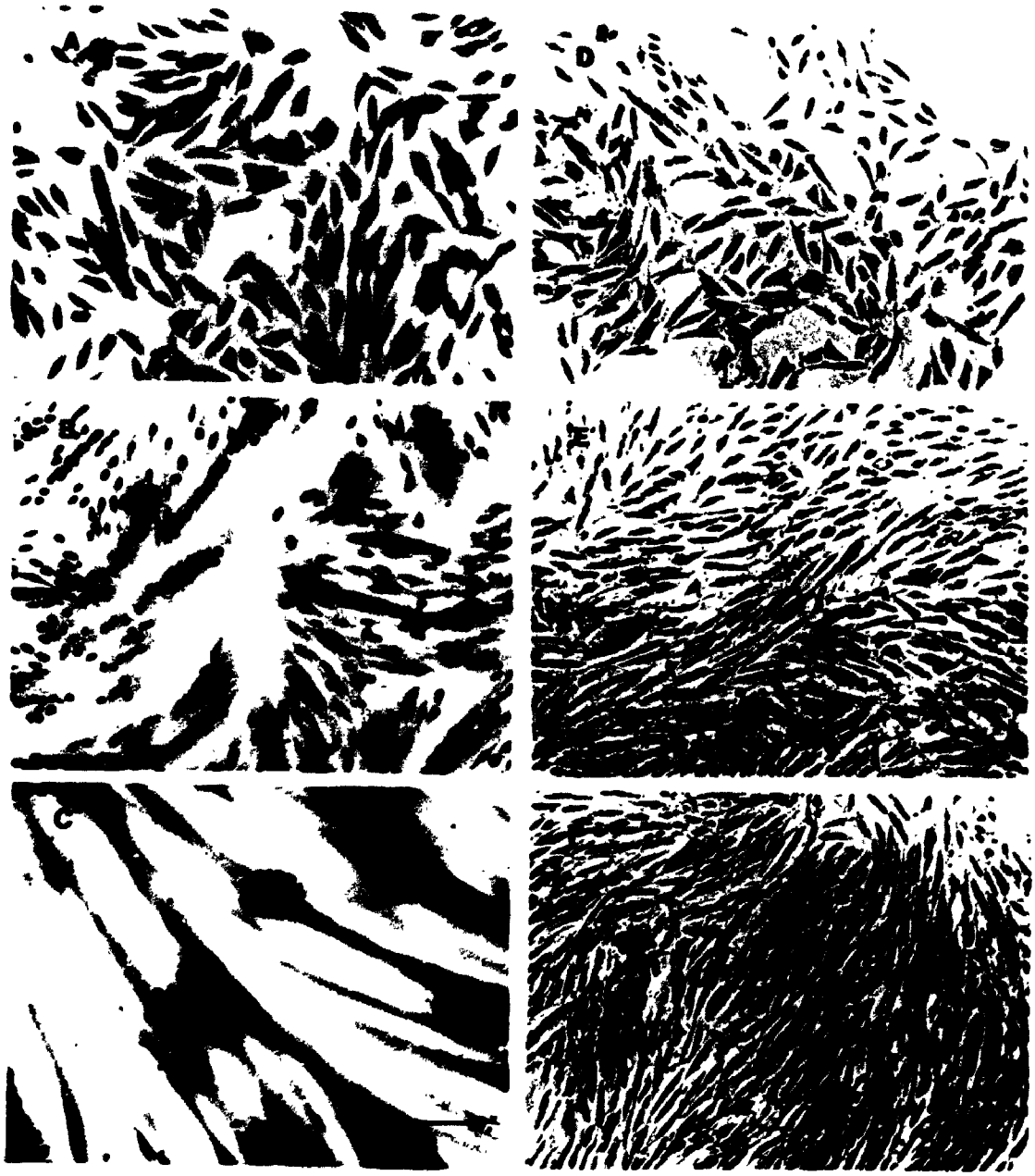

Fig. 6.3 Hexose Transport during Myogenic Differentiation of Glucose-grown Rat L6 Myoblasts.

Transport studies were carried out as described in the text. Rates of uptake were determined for dGlc and MeGlc using five concentrations ranging from 0.05 mM to 1.0 mM, over a 1-min. period (15, 30, 45 and 60 sec.). The Km and Vmax values were determined from double reciprocal plots of the initial rates versus substrate concentrations. Fusion indices were determined as described in the text. Panel A shows the Km values of dGlc and MeGlc uptake and the fusion indices on different days after subculturing. (▲), Km values for MeGlc uptake; (●), Km values for dGlc uptake; and ( ), fusion indices. Panel B shows the Vmax values on different days after subculturing. (▲), Vmax values for MeGlc uptake; (●), Vmax values for dGlc uptake.

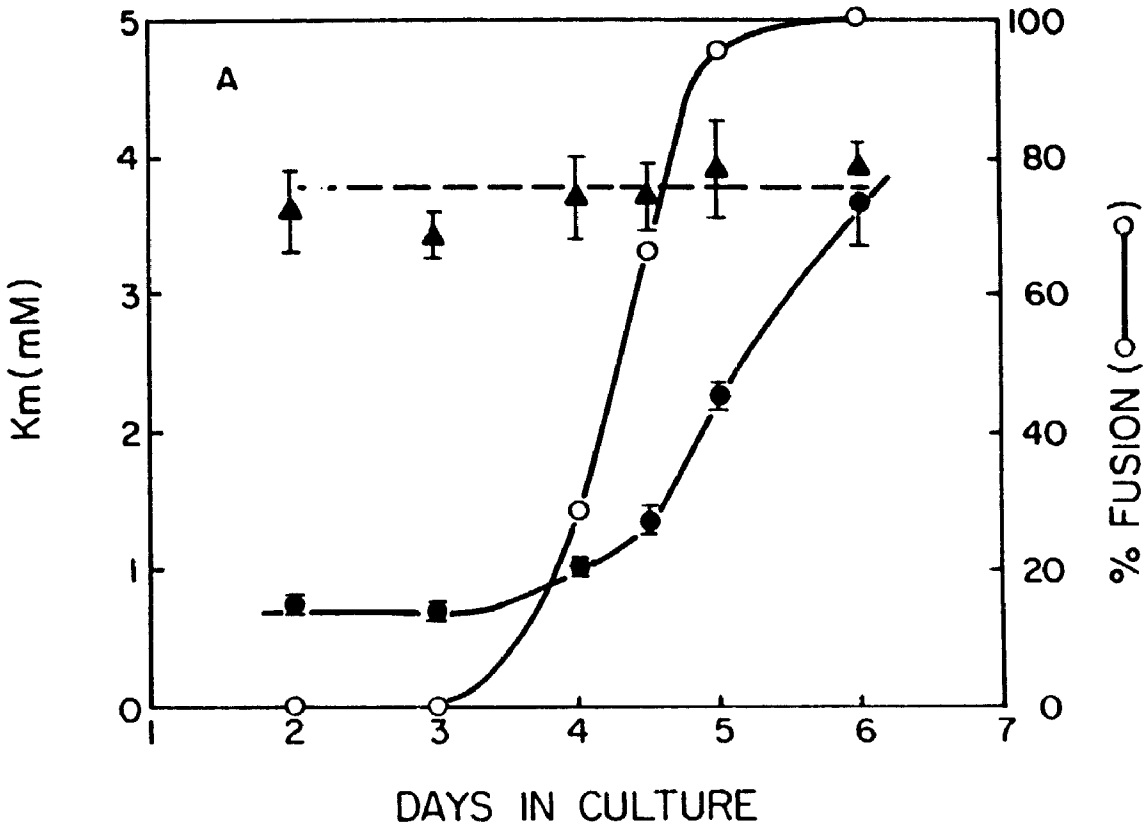
A
Km(mM)
% FUSION (○)
DAYS IN CULTURE

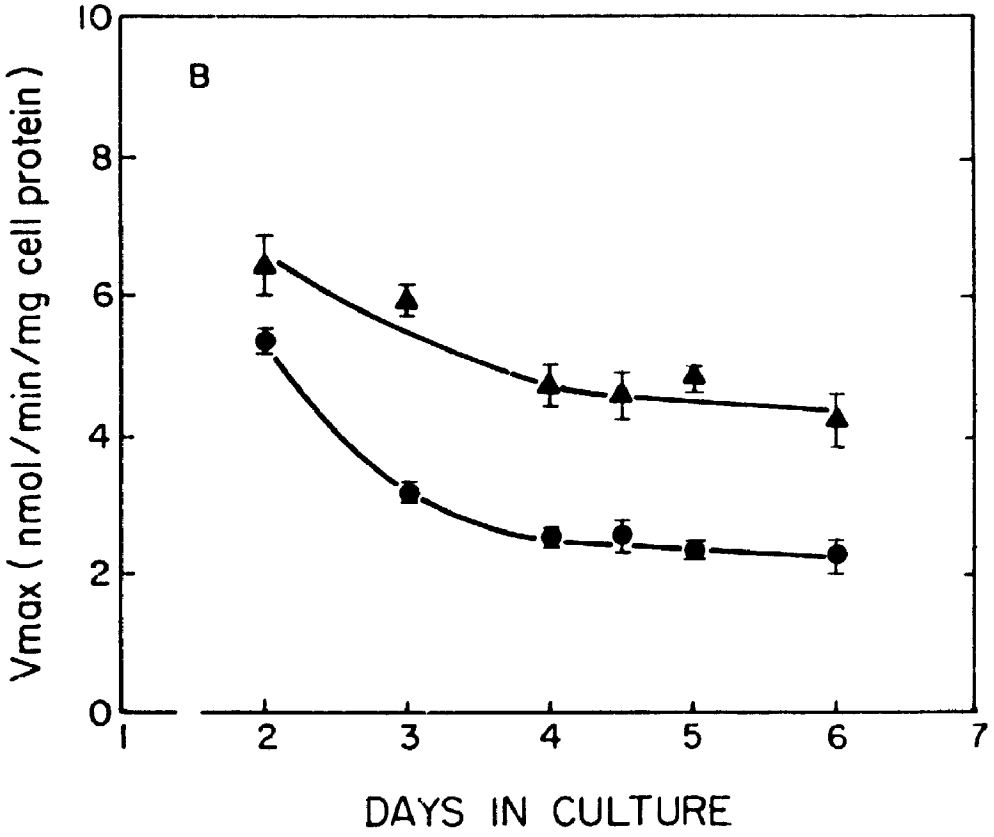
B
Vmax (nmol/min/mg cell protein)
DAYS IN CULTURE

The transport capacities of both MeGlc and dGlc uptake systems were found to decrease dramatically with growth; and this decrease was considerably slower after day 4 (Fig. 6.3B and Table 6.1). The initial decrease was probably due to the cell density effect on HT. The Vmax values of dGlc transport by Day-2 and Day-5 cultures were 5.30 and 2.30 nmoles/mg protein/min., respectively; this represented a 57% drop in the transport capacity. On the other hand, the corresponding MeGlc Vmax values were 6.36 and 4.80 nmoles/mg protein/min., respectively; this represented a 24% drop in the transport capacity. This observation also illustrates the differences between the two uptake processes.

6.3.3 Hexose Transport and Myogenesis by Glucose-starved L6 Cells

The relationship between HT and myogenesis was also examined in glucose-starved cells. Glucose-starvation has been shown to increase the HT capacities in a variety of cell types (Kalckar and Ullrey, 1984; D'Amore et al., 1986a; Haspel et al., 1985,1986; D'Amore and Lo, 1988). It can be achieved by growth in medium containing fructose as the sole carbon source. Glucose-starvation was found to have no effect on the ability of rat myoblast L6 to undergo myogenesis; about 0% and 95% fusion were observed in Day-2 and Day-6 cultures, respectively. Moreover, the dGlc Km values for glucose-starved Day-2 and Day-6 cultures were 0.6 and 3.2 mM, respectively; whereas the corresponding values for MeGlc uptake were 3.5 and 3.9 mM, respectively. Thus glucose-starvation does not have much effect on the rate and extent of myogenesis, and on the myogenesis-associated alteration in dGlc transport affinity.

The transport capacities of dGlc uptake by glucose-starved Day-2 and Day-6 cultures were about 40% higher than their glucose-grown counterparts (Table 6.1). A different picture emerged when MeGlc was used as the transport substrate; glucose-starved Day-2 culture exhibited about 70% increase in the MeGlc transport capacity, as compared with its glucose-grown counterparts. Previous studies with HT

Table 6.1 Transport Capacities of Rat Myoblasts on Different Days after Subculturing.

All cultures were grown in the presence of 10% horse serum. Transport studies were carried out as described in the text. Rates of uptake were determined for dGlc and MeGlc using five concentrations ranging from 0.05mM to 1.0 mM, over a 1-min period. The Vmax values were determined from double reciprocal plots of the initial rates versus substrate concentrations. Abbreviations: G_{L6}, glucose-grown L6 cells; F_{L6}, fructose-grown L6 cells; $G_{L6+BrdUrd}$, glucose-grown L6 cells in the presence of BrdUrd; G_{D1}, glucose-grown mutant D1.

TRANSPORT CAPACITIES

(nmol/mg protein/min)

	dGlc UPTAKE: days				MeGlc UPTAKE: days			
	2	4.5	5	6	2	4.5	5	6
G_{L6}	5.30±0.15	2.49±0.20	2.30±0.13	2.20±0.20	6.56±0.47	4.57±0.29	4.80±0.20	4.20±0.39
	(100%)	(47%)	(43%)	(42%)	(100%)	(72%)	(76%)	(66%)
F_{L6}	7.20±0.54	----	----	3.15±0.13	10.84±0.65	----	----	4.40±0.30
	(100%)			(44%)	(100%)			(41%)
$G_{L6+BrdUrd}$	3.25±0.10	----	1.01±0.05	0.83±0.06	4.17±0.30	----	1.82±0.10	1.27±0.12
	(100%)		(31%)	(26%)	(100%)		(44%)	(31%)
G_{D1}	4.31±0.12	1.64±0.05	----	1.03±0.06	6.25±0.19	2.69±0.13	----	2.04±0.20
	(100%)	(39%)		(25%)	(100%)	(46%)		(33%)

mutants indicated that this additional MeGlc transport activity might be due to the participation of HAHT in glucose-starved cells. Unlike the dGlc uptake system, MeGlc uptake by glucose-starved Day-6 culture was similar to that by its glucose-grown counterpart. In view of the possible involvement of more than one transport system in the uptake of MeGlc, the significance of this observation is not clear.

6.3.4 L6 Grown in the Presence of 5-Bromo-2'-Deoxyuridine

If the alteration in HT is caused by events associated with myogenesis, then one would expect changes in dGlc transport affinity should not be observed in myoblasts impaired in myogenesis. 5-Bromo-2'-deoxyuridine (BrdUrd) has been used by various investigators to inhibit both biochemical and morphological differentiation of myoblasts (Sanwal, 1979; Pearson, 1981). When L6 cells were grown in the presence of 7.5 μM BrdUrd, myotubes could not be detected even in Day-5 and Day-6 cultures (Figs. 6.2E-6.2F). It is interesting to note that this concentration of BrdUrd has no effect on the rate of growth of the culture. Transport studies with these cultures revealed that the Km values for both dGlc and MeGlc uptake remained relatively constant at all stages of growth (Fig. 6.4). Thus changes in the dGlc transport affinity cannot be observed in cells impaired in myogenesis.

The transport capacities for both sugar analogues were about 37% lower in the BrdUrd-treated Day-2 cells (Table 6.1). The reason for this reduction is currently not clear. The dGlc and MeGlc Vmax values of Day-6 BrdUrd-treated myoblasts were 0.82 and 1.27 nmoles/mg protein/min., respectively. Thus these Day-6 undifferentiated myoblasts exhibited only 26% and 31% of the dGlc and MeGlc transport activities found in Day-2 cells, respectively. This decrease is probably due to cell density effect. More importantly, the levels of both transport processes in the myotubes were about three times higher than those in undifferentiated Day-6 myoblasts (Table 6.1). This may reflect either faster rates of degradation in the

Fig. 6.4 Hexose Transport Affinities of Rat L6 Myoblasts Grown in the Presence of 5-Bromo-2'-Deoxyuridine.

Rat L6 myoblasts were grown in normal medium plus 7.5 μM 5-bromo-2'-deoxyuridine. Transport studies were carried out as described in Fig. 6.3. (▲), Km values of MeGlc uptake; (●), Km values of dGlc uptake.

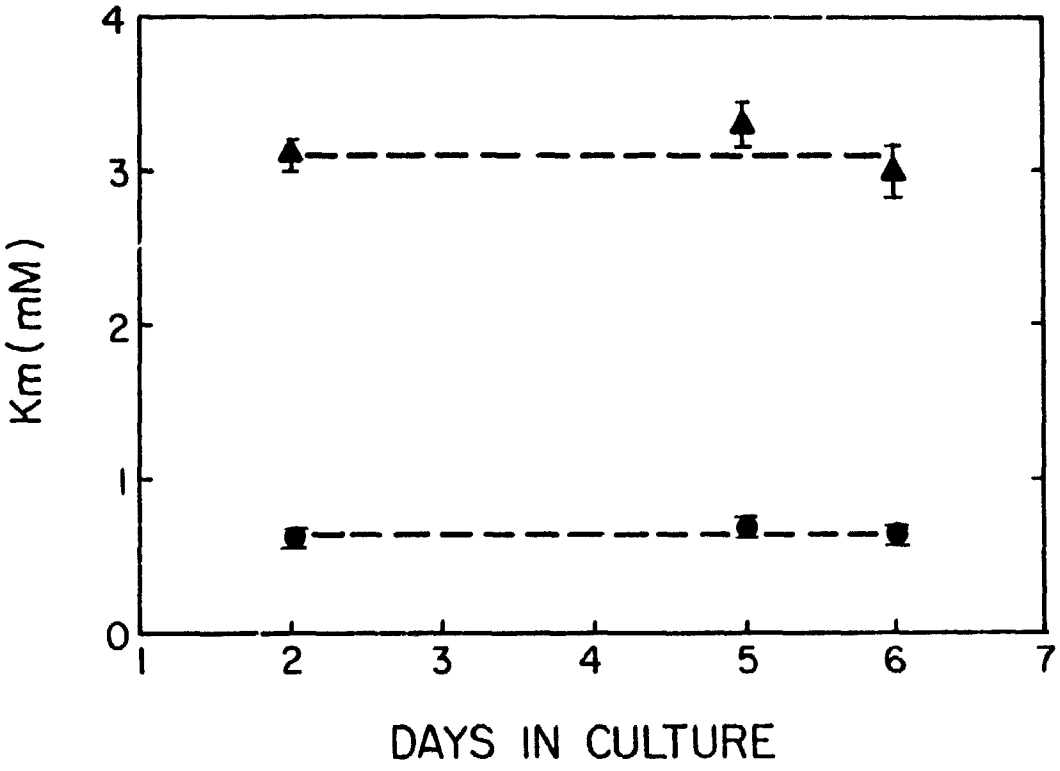
4
3
2
1
0
Km (mM)
1
2
3
4
5
6
7
DAYS IN CULTURE

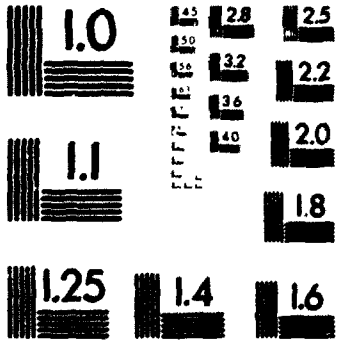

undifferentiated myoblasts, or elevated levels of HT activities in the myotubes.

6.3.5 Rat Myoblast Mutant D1

The relationship between the alteration in HT and myogenesis was further explored using a myogenesis-defective mutant. A concanavalin A-resistant mutant, D1, was used in this study (Cates et al., 1984). This mutant was impaired in both morphological and biochemical differentiation and was recently found to contain undermannosylated glycoproteins (Clarke et al., 1988). Mutant D1 was unable to form multinucleated myotubes when grown in 10% (the normal concentration used) horse serum (Fig. 6.5A-6.5C); cells failed to align even on day 6. An examination of the apparent Km values for both dGlc and MeGlc transport processes in mutant D1 revealed that these values remained unaltered even after prolonged periods of growth (Fig. 6.6A). This observation again indicates events associated with myogenesis may be responsible for the changes in the transport affinity of the dGlc transport system.

Unlike the BrdUrd-treated myoblasts, the transport capacities of both dGlc and MeGlc uptake systems in the Day-2 mutant D1 were similar to those of its parental L6 cells (Table 6.1). However, the transport capacities in the D1 Day-4.5 and Day-6 cultures were significantly lower than those of the glucose-grown L6 cultures. The Day-6 D1 mutant retained around 29% of the dGlc and MeGlc transport capacities found in its Day-2 cultures. More importantly, the levels of both HT processes in these undifferentiated myoblasts were less than half of those observed in the Day-6 L6 myotubes.

One of the interesting and unique features of mutant D1 is that it is able to form myotubes when cultured in 1% horse serum (Figs. 6.5D-6.5F); 13%, 50% and 87% fusion were observed on Day-4, Day-5.5 and Day-7 cultures, respectively (Fig. 6.6B). It was thought that the demand for serum mitogens was not as stringent in the mutants as in L6 cells; consequently the mutant cells continue to

Fig. 6.5 Morphology of Mutant D1 Grown in the Presence of 10% and 1% Horse Serum.

Panels A-C show the morphology of mutant D1 grown in the presence of 10% horse serum on Day 2, Day 4.5 and Day 6, respectively. Cells were plated at a density of 1.5 x 10^5 cells/35 mm well. These figures serve to illustrate that this mutant is unable to form multinucleated myotubes when grown in the presence of 10% horse serum. Panels D-F show the mutant D1 grown in the presence of 1% horse serum, on Day 4, Day 5.5 and Day 7, respectively. Cells were seeded at a density of 3.1 x 10^5 cells/35 mm well in the presence of 10% serum. The medium was changed to that containing 1% horse serum on Day 2. This set of figures serve to demonstrate the ability of mutant D1 to differentiate when grown in the presence of 1% horse serum. The bar indicates 100 μm.

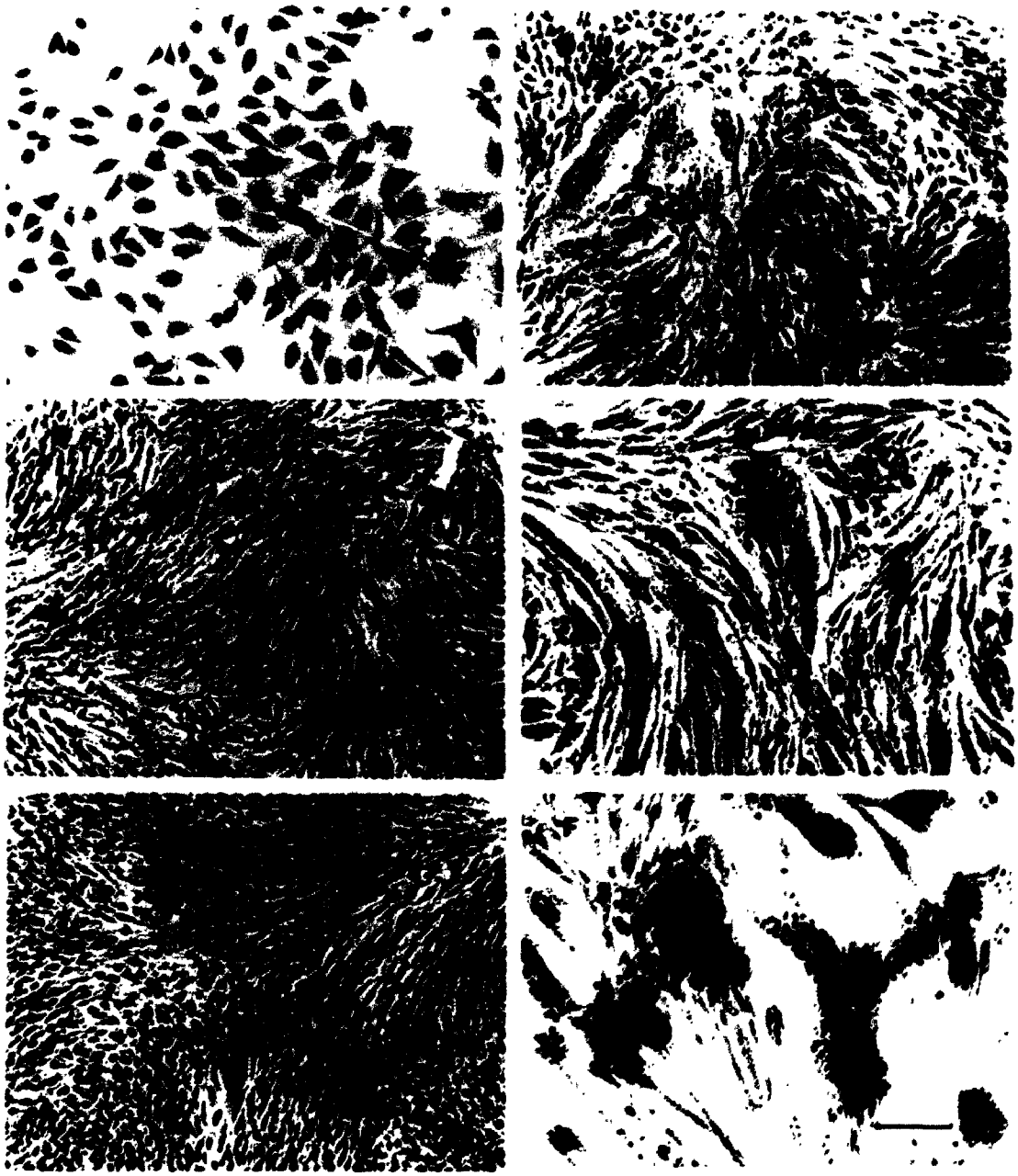

Fig. 6.6 Hexose Transport Affinities of Mutant D1 under Different Growth Conditions.

Mutant D1 was grown as described in Fig. 6.5. Transport studies were carried out and analyzed as described in Fig. 6.3. Fusion index was determined as described in the text. Panel A shows the transport affinities of this mutant when grown in the presence of 10% horse serum. (▲), Km values of MeGlc uptake; (●), Km values of dGlc uptake. Panel B shows the transport affinities and fusion indices of this mutant when grown in the presence of 1% horse serum. (▲), Km values of MeGlc uptake; (●), Km values of dGlc uptake; (○), fusion indices of this mutant grown in the presence of 1% horse serum.

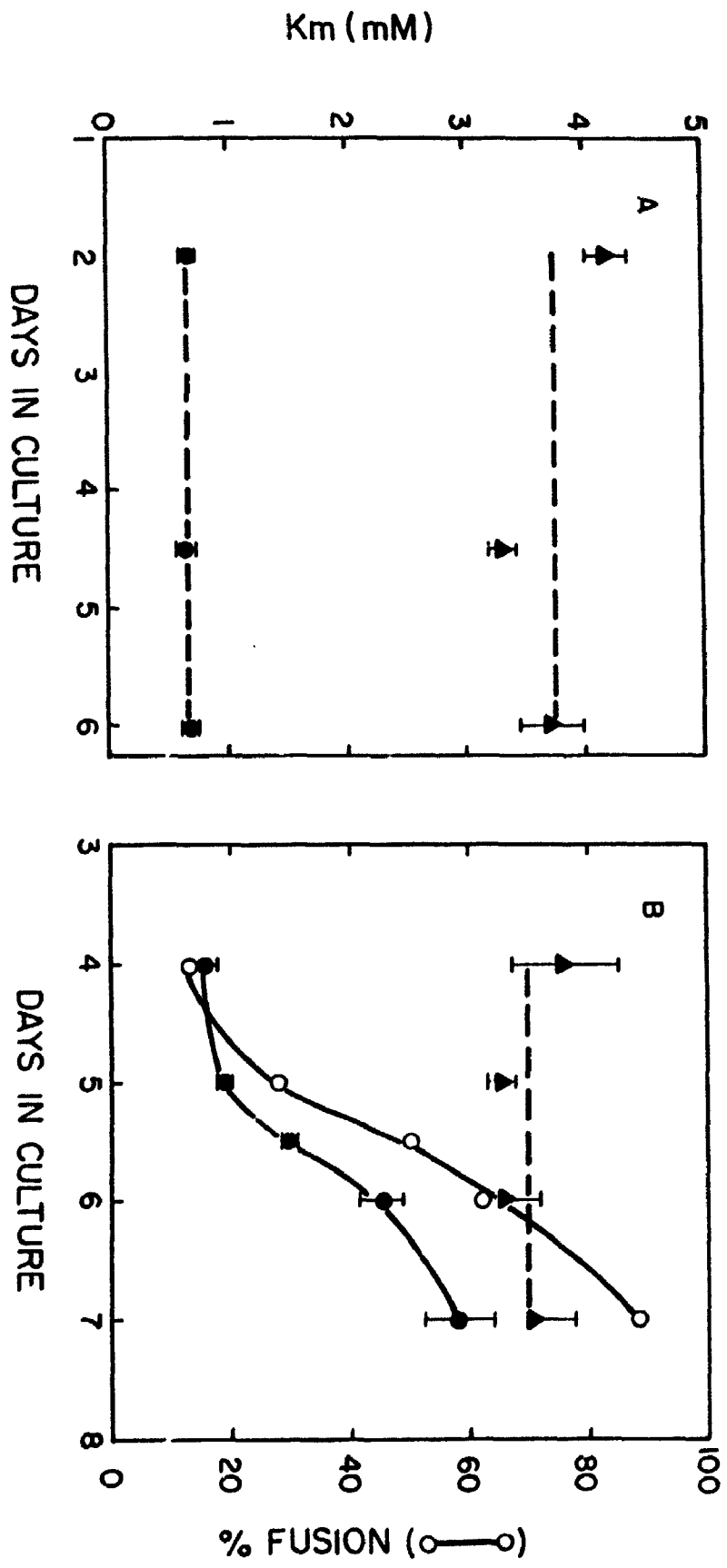
Km (mM)
0
1
2
3
4
5
A
DAYS IN CULTURE
2
3
4
5
6
B
DAYS IN CULTURE
3
4
5
6
7
8
0
20
40
60
80
100
% FUSION (o—o)

divide and could not withdraw easily from the cell cycle in 10% horse serum, but could do so in 1% serum where the mitogen concentration initially was low (Clarke et al., 1988). The observation that the average rate of fusion for the mutant (when grown in 1% horse serum) was slightly slower than that for L6 was in agreement with the notion that the serum mitogen concentration essential for preventing the mutant from withdrawing from the cell cycle was much lower than that for the L6 cells.

The ability of this mutant to undergo myogenesis provides a unique opportunity to examine the relationship between changes in transport activity and myogenesis. Similar to the L6 myoblasts, the Km values for dGlc uptake by this mutant were found to increase, concurrent with the formation of myotubes (Fig. 6.6B). The average Km value for dGlc uptake was 2.9 mM for Day-7 culture, which was 87% fused. On the other hand, the Km values of MeGlc uptake remained around 3.5 mM at all stages of growth. Thus the above mutant studies substantiate the notion that changes in the dGlc transport affinity may be brought about by events associated with myogenesis.

6.3.6 Effects of Sulfhydryl Reagents

We have previously shown that HAHT, but not LAHT, in Day-2 culture is very sensitive to sulfhydryl reagents such as pCMBS and NEM (D'Amore and Lo, 1986b). These two reagents were therefore used to determine whether the myotube dGlc transport system was also altered in its response to these reagents. Treatment of Day-2 cells with 1 mM NEM or 1 mM pCMBS was found to result in around 66 % and 55% inhibition of dGlc uptake, respectively (Fig. 6.7). On the other hand, these reagents did not have much effect on the myotube (Day-5) dGlc uptake process. This indicates that the myotube dGlc transport system differs from the myoblast dGlc transport system in its insensitivity to the sulfhydryl reagents. As expected, the MeGlc transport systems present in both undifferentiated myoblasts

Fig. 6.7 Effects of Sulfhydryl Reagents on Hexose Transport.

Rat L6 myoblasts were grown in normal medium for 2 (open symbols) or 5 (solid symbols) days. Cells were preincubated with various concentrations of sulfhydryl reagents for 5 min. The uptake of 0.05 mM dGlc or 0.05 mM MeGlc by these cells was then determined over a 1-min. period. The specific activities of dGlc and MeGlc used were 3.0×10^4 d.p.m./nmole. Panels A and B indicate the effect of sulfhydryl reagents on uptake of dGlc (○ , ●) and MeGlc (△ , ▲).

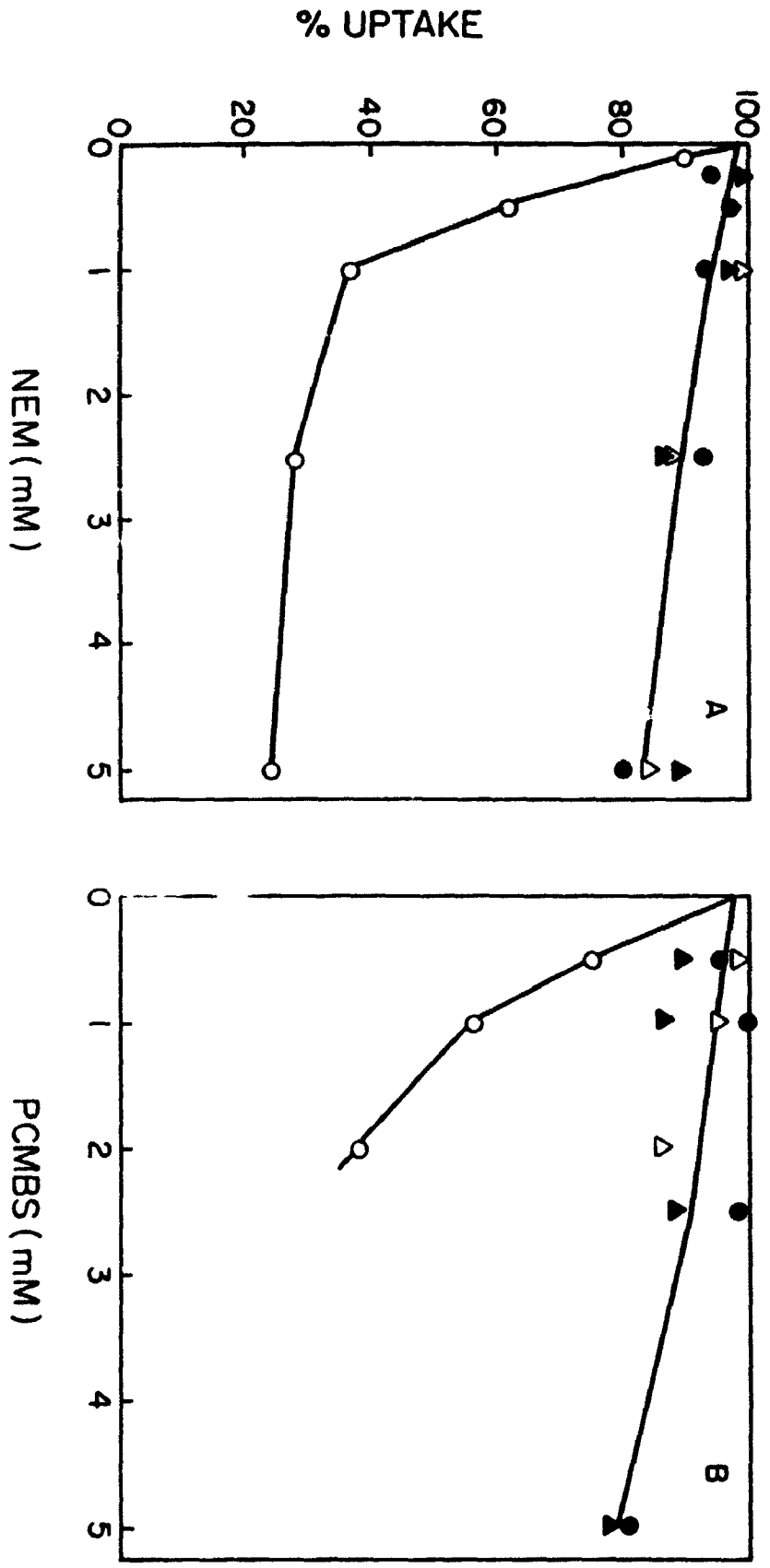
% UPTAKE
0
20
40
60
80
100
0
1
2
3
4
5
NEM (mM)
A
PCMBS (mM)
B

and myotubes were resistant to sulfhydryl reagents (Fig 6.7). In other words, the dGlc transport system in Day-5 culture (myotubes) seem to be altered not only in its transport affinity, but also in its sensitivity to sulfhydryl reagents. The above observation is in agreement with the notion that the dGlc transport system is altered in its intrinsic properties during myogenesis.

6.4 DISCUSSION

The regulation of HT has been studied quite extensively by a number of workers; substantial efforts have been spent in determining the mechanisms of the insulin-mediated activation of HT in adipocyte (Whitesell and Abumrad, 1985; Simpson and Cushman, 1986; Kahn and Cushman, 1987; Joost et al., 1988). Earlier studies indicated that insulin activated HT in adipocyte by increasing the translocation of HTers from intracellular storage sites to the plasma membrane (Simpson and Cushman, 1986). More recently, the insulin-mediated activation of HT was also found to be due to changes in the intrinsic activity of the HTers (Joost et al., 1986; Baly and Horuk, 1987; Toyoda et al., 1987; Joost et al., 1988). In other words, HT can be modulated by altering the number of functional HTers and also by changing the intrinsic activity of the transport system.

We have recently examined the properties and regulation of HT in rat myoblasts through a combination of biochemical and genetic approaches (D'Amore and Lo, 1986 a,b,c). Our studies show that activation of HT could be brought about by covalent modification of the transporter. Both whole cell and plasma membrane vesicle studies showed that the antibody-mediated dimerization of a cell surface 112K protein resulted in activation of HT (Lo and Duronio, 1984 a,b; Mesmer et al., 1986; D'Amore and Lo, 1988). The transport capacities, but not the affinities, of both HT processes were elevated by this treatment. Mutants defective in this 112K protein were not responsive to this antibody-treatment

(D'Amore and Lo, 1988). Since pretreatment of cells or plasma membrane vesicles with protease inhibitors could prevent this antibody-mediated activation, it was surmised that membrane associated protease(s) might be involved in this activation process (Lo and Duronio, 1984b; Mesmer et al., 1986). In agreement with this notion, pretreatment of whole cells or plasma membrane vesicles with very low concentrations of trypsin was also found to activate HT.

The present investigation demonstrates several mechanisms by which HT can be altered by physiological events. The first one involves changes due to increases in cell density. As indicated in Fig. 6.1, the specific activity of HT remained unchanged at subconfluent cell density (i.e. less than 4.4 x 10^4 cells/ cm^2). However, both dGlc and MeGlc transport activities decreased dramatically at higher density. Essentially the same observation was made when cells were plated at or grown to different densities. Regardless of their ability to differentiate, the transport capacities of both MeGlc and dGlc transport processes decreased dramatically from Day 2 to around Day 4 (Fig. 6.3A and Table 6.1). This initial decrease may be attributed to the cell density effect. Since undifferentiated myoblasts exhibited a loss in transport capacity without altering the transport affinity (Figs. 6.3, 6.4, 6.6A and Table 6.1), it may be surmised that the observed decrease may be due to a reduced number of functional transporters in the plasma membrane.

HT is also found to be altered by myogenic differentiation. Under our normal growth conditions, rat myoblast L6 began to fuse between days 3 and 4, and fusion was essentially complete on day 6 (Fig 6.2). Transport kinetic studies showed that while the Km values for dGlc remained constant (0.6 mM) in undifferentiated myoblasts, these values were elevated upon the onset of fusion, and this increase seemed to be directly proportional to the degree of fusion (Fig. 6.2A). It reached a value of around 3.6 mM when the fusion index was 100%.

The myotube dGlc uptake system was also altered in its sensitivity to sulfhydryl reagents (Fig. 6.7). These studies suggest that the intrinsic activity of the dGlc transporter may be altered by events associated with myogenic differentiation.

If the observed alteration in dGlc transport affinity was caused by myogenesis, then one would expect that these changes should not be observed in myoblasts impaired in myogenesis. This hypothesis was tested by both biochemical and genetic approaches. The biochemical approach involved inhibiting myogenesis by growth in the presence of 5-bromo-2'-deoxyuridine (BrdUrd) (Fig. 6.2; Sanwal, 1979; Pearson, 1981). As shown in Fig. 6.4, changes in dGlc transport affinity could not be observed in myoblasts impaired in myogenesis. The above conclusion was corroborated by studies with a mutant originally isolated from rat myoblast L6. Under the normal growth conditions (i.e. in the presence of 10% horse serum), mutant D1 was unable to form multinucleated myotubes (Fig. 6.5). Data presented in Fig. 6.6A showed that the Km values for dGlc transport remained constant at all stages of growth. However, under conditions permissible for myogenesis (i.e. by growth in 1% horse serum) (Fig. 6.5), the decrease in dGlc transport affinity could be observed upon the onset of fusion (Fig. 6.6B). Similar to the L6 cells, the extent of alteration correlated closely with the degree of fusion. Thus the above biochemical and genetic manipulations strongly suggest that the observed changes in the dGlc transport affinity are likely caused by events associated with myogenesis.

While alteration in dGlc transport affinity was observed upon the onset of fusion, changes in MeGlc transport affinity could not be observed with both myogenesis competent and impaired cultures. This again serves to demonstrate the differences between the dGlc and MeGlc transport systems in rat myoblasts. More importantly, this indicates that the increase in HT is the result of changes in a specific transport system, and is not due to changes in general membrane

permeability.

The observed changes in the dGlc transport system may be brought about by one of the following mechanisms. The first one postulates that myogenesis results in faster inactivation or degradation of HAHT. The observed lower affinity dGlc transport may be due to the participation of LAHT. This may explain why the myotube dGlc uptake process has similar transport affinity and response to sulfhydryl reagents as LAHT. Our previous studies with mutants defective in HAHT suggested that LAHT could also take up dGlc, albeit with much lower affinity (D'Amore et al., 1986b). Since the HT capacities of myotubes were much larger than those of undifferentiated myoblasts (Table 6.1), this will then predict that the level of LAHT may be elevated in the myotubes. In other words, the first mechanism predicts that myogenesis results not only in faster degradation or inactivation of HAHT, but also in elevated level of LAHT. The second mechanism postulates that myogenesis results in the alteration of the intrinsic activity of HAHT. The modified HAHT (MHAHT) is altered in its dGlc transport affinity and also in its response to sulfhydryl reagents (Figs. 6.3 and 6.7). Table 6.1 shows that MeGlc uptake by Day-6 myotubes is significantly higher than the corresponding undifferentiated myoblasts. If the level of LAHT is not altered in the myotubes, then this would suggest MHAHT may also be responsible for this elevated transport activity. The difference in the transport capacities between the undifferentiated myoblasts (Day-6 D1 culture) and myotubes (Day-6 L6 culture) may also imply different turnover rates of the MHAHT. Indeed, the decrease in MeGlc and dGlc transport capacities was considerably slower after the onset of fusion (Fig. 6.3B). We are currently exploring the above possibilities by examining the properties of mutants defective in HAHT.

The present investigation also examines the effect of glucose-starvation on HT. We have previously shown that glucose-starvation results in the activation of

HT, and this activation cannot be detected in mutants defective in a 112K cell surface protein, or in a putative positive regulatory protein (D'Amore and Lo, 1986 a,b,c; D'Amore and Lo, 1988). It is interesting to note that these two regulatory mutants are also impaired in myogenesis. Thus the possibility exists that both myogenesis and the glucose-starvation effect may be regulated by similar component(s). The present investigation shows that glucose-starvation has no effect on the rate and extent of fusion and on the myogenesis-related changes in dGlc transport activity.

Table 6.1 shows that both dGlc and MeGlc transport capacities are elevated in glucose-starved L6 cultures. Both transport and cytochalasin B binding studies with mutants defective in HAHT indicated that only the level of HAHT was elevated in glucose-starved myoblasts; the transport capacity and affinity of LAHT were not altered in these cells (D'Amore et al., 1986a,b). It follows from these findings that the observed increased MeGlc transport capacity in glucose-starved L6 cultures may be due to the participation of HAHT. This suggests that HAHT in glucose-starved cells (FHAHT) can take up MeGlc with a much higher efficiency. While a similar glucose-starvation mediated increase in transport capacity has also been observed by other workers (Gay and Hilf, 1980; Haspel et al., 1985; 1986), the above finding has not been reported.

CHAPTER 7

SUMMARY AND FUTURE PROSPECTS

The overall objective of the studies described in this thesis was to identify and characterize the HT systems in rat L6 myoblasts. HT systems have been intensively investigated in a variety of mammalian cells. It is now generally accepted that in mammalian cells there is a family of closely related HTer-like proteins which exhibit different degrees of tissue specificity. Therefore, in order to fully understand the molecular mechanisms of HT in mammalian cells, it is important and necessary to characterize individual transport systems in different cell types or tissues. An understanding of the structure and function of the HT systems in rat L6 cells would add valuable information to the area of eukaryotic HT.

CB, a potent inhibitor of HT, was used in this study as a probe for the HT systems in undifferentiated rat L6 myoblasts. Whole cell CB binding studies showed that two distinct CB binding sites (CB_H and CB_L) are present in rat L6 myoblasts. They differ not only in their binding affinity and capacity, but also in their response to the inhibitory effects of dGlc and MeGlc, the preferred substrates of HAHT and LAHT, respectively. Furthermore, these two specific CB binding sites are differentially expressed in glucose-starved cells. In addition, only the CB_L, but not the CB_H, is altered in HAHT defective mutant D23. Based on the close correlation between the two CB sites and the two HT systems, it seems likely that CB_L and CB_H are associated with HAHT and LAHT in rat L6 myoblasts, respectively.

These two CB binding sites were further characterized by CB binding studies with purified membrane fractions prepared from the HAHT defective mutant D23 and its parental L6 cells. This study showed that both CB binding sites were

present in plasma membrane and in LDMF with binding affinities similar to those of whole cells. Moreover, the specific activities of both CB binding sites in LDMF were only about 15% of those in the plasma membrane. This differs from that in rat adipocytes in which the specific activity of CB binding to LDMF is ten times higher than that in the plasma membrane. Plasma membrane CB binding studies also showed that CB_L was defective in mutant D23, in agreement with the notion that the two HT systems in rat L6 myoblasts might possess their own CB binding sites.

The observation that CB binding was inhibited by D-glucose and activated by glucose 6-P suggested that an allosteric regulatory mechanism might be involved in CB binding. Based on transport kinetic studies and the above observation, it was also suggested that CB and D-glucose may be binding to different sites on the HTer. Since the study of CB-transporter interaction involves, in part, an examination of the structure and mechanism of the transporter, much research has been directed towards the understanding of the mechanism by which CB inhibits HT. However, as indicated in Chapter 1, the molecular mechanism of CB inhibition still remains unclear. A better understanding of the molecular mechanism may have to await more structural information about the transporter.

Studies presented in Chapter 4 described our attempts in identifying and characterizing the two HT components by CB photolabelling. These studies not only confirmed the findings of the whole cell and plasma membrane CB binding studies, but also revealed some interesting observations on the structure and function of HT systems. A broad band with molecular weights ranging from 40 to 60 kDa was covalently labelled by ^{3}H-CB, upon exposure to an intense UV light. Further detailed studies on the effects of glucose and its analogues on CB photoincorporation into whole cells and membrane fractions prepared from HT mutants and their parental L6 cells, grown under different conditions, indicated that

the CB photolabelled components (40-60 kDa) might be associated with both HAHT and LAHT in rat L6 myoblasts. Furthermore, proteolytic digestion of CB photolabelled whole cells or plasma membrane revealed that trypsin only acted on the cytoplasmic side of the HTer. The exofacial side of the transporter was resistant to trypsin cleavage. This study taken together with the effect of trypsin on CB binding to whole cells and plasma membrane also suggested that the CB binding sites were probably located in the inner surface of the transporter. In addition, studies on the effects of glucose, trypsin and heating on CB photolabelling indicated some structural differences between the CB photolabelled components in LDMF and those in plasma membrane.

Considerable efforts have been spent to improve the separation of CB photolabelled components. However, we have not been able to completely separate these CB photolabelled components by the Laemmli SDS-PAGE system. It is certainly essential to separate and isolate these components for further characterization. An alterative approach to achieve this would be the use of the isoelectrofocusing technique to separate the CB photolabelled components. Two CB photolabelled components in rat adipocytes have, in fact, been identified by this technique (Horuk et al., 1986). It would also be interesting to further characterize the CB photolabelled components in LDMF. An understanding of their structure and distribution would provide clues as to the biosynthesis and regulation of HTers.

To further identify and characterize the HT components in rat L6 myoblasts, we have used two antisera, α-GT and α-IDIO. While the former can detect proteins with antigenic determinant sites homologous to the human rbc HTer, the latter can be used to detect proteins containing the glucose binding site. Immunoblotting studies with these antisera on whole cell extracts and membrane fractions prepared from a HAHT defective mutant D23 and its parental L6 cells suggested the

molecular weights of HAHTer and LAHTer to be 63 and 60 kDa, respectively. The strongest evidence for the involvement of these two proteins in HT comes from the studies with mutant D23 in which the 63 kDa protein is present only in a residual level. The only major protein recognized by these antisera in this mutant is the 60 kDa. More experiments concerning the identities of these proteins, especially the 60 kDa protein, will certainly be useful. Much work on the characterization of other proteins (e.g. 78 and 97 kDa) recognized either by α-GT or by α-IDIO, remains to be done. It would also be interesting to examine the biosynthesis of these proteins. Eventually, one could attempt to use these antisera to affinity purify the myoblast HT components.

As also discussed in Chapter 5, CB photolabelling could affect the mobility of proteins on SDS-PAGE. This observation may explain why the CB photolabelled components migrated as a broad band on SDS-PAGE; whereas immunoblotting studies showed sharper bands. The effect of CB photolabelling on the conformation of the HTer has also been reported by other workers (Kurokawa et al., 1986).

It may be apparent from the above studies that HT mutants can be extremely helpful in identifying HT systems and their transport components, and in elucidating the molecular mechanism of HT. Studies with these mutants have provided strong and definitive evidence for the identities of CB binding sites, CB photolabelled components and components recognized by specific antisera. As discussed in Chapter 1, some of the HTer-like proteins in different cell types have been identified by affinity ligands and anti-(human rbc HTer) antibodies. Since these assays do not necessarily reflect the functional aspect of the labelled proteins, it is uncertain whether these labelled proteins are indeed involved in HT. The use of transport mutants combined with the above approaches should provide an unequivocal means of identifying the labelled proteins.

Another aspect of the HT systems in rat L6 myoblasts which was examined

in this project was the regulation of these systems during growth and myogenic differentiation. It was observed that the transport capacities of HAHT and LAHT decreased dramatically when the cell density was higher than 4.4 x 10^4 cells/cm^2, suggesting that the HT, especially the number of functional transporters in the plasma membrane might be affected by cell density. Furthermore, dGlc and MeGlc transport kinetic studies with myogenic defective mutant D1 and its parental L6 cells, grown under different conditions and to different stages of myogenesis revealed that HAHT and LAHT may be regulated differentially during myogenic differentiation. While the transport affinity of dGlc was altered by events associated with myogenic differentiation, the transport affinity of MeGlc remained unchanged. Glucose starvation was also found to alter the transport properties of HAHT, without affecting LAHT. These results provide a preliminary indication that HAHT and LAHT may play different roles in the cells. Obviously, a great deal of work will be involved in understanding the mechanisms by which HT is altered by physiological events, such as cell density, glucose starvation and myogenic differentiation. Similar approaches used in identification and characterization of the HT systems in undifferentiated rat L6 myoblasts can be applied to cells grown to different densities, and to different stages of myogenesis. Furthermore, HT mutants can also be used in these studies. In fact, preliminary results from these mutant studies suggested that HT may play an important role in myogenic differentiation. Further studies on the regulation of these two systems may also provide clues as to the physiological significance of the presence of more than one HT system in various mammalian cells.

Fig 7.1 shows a tentative model for the two hexose transport systems in rat L6 myoblasts. dGlc and D-glucose are preferentially transported by HAHT. Both whole cells and plasma membrane vesicle studies indicate that HAHT is an active transport process. It is derepressed upon glucose starvation and can be inactivated

Fig 7.1 Tentative Model for the Two Hexose Transport Systems in Rat L6 Myoblasts

Two hexose transport systems are diagrammatically shown in this model. (▼ , △) The substrate recognition sites in HAHT; (▮ , ▯) the substrate recognition sites in LAHT; (◓ , ◠) CB_L and CB_H in HAHT and LAHT, respectively. SH represents the cell surface sulfhydryl groups present on HAHT. Treatment with sulfhydryl reagents results in inhibition of substrate (S) translocation by HAHT. Binding of specific substrates to the intracellular substrate recognition site results in inhibition of CB binding. Binding of CB to CB_L or CB_H results in inhibition of substrate translocation by HAHT and LAHT, respectively. (-) represents inhibitors or inhibition. A comparison of the properties of these two systems is also shown in this figure.

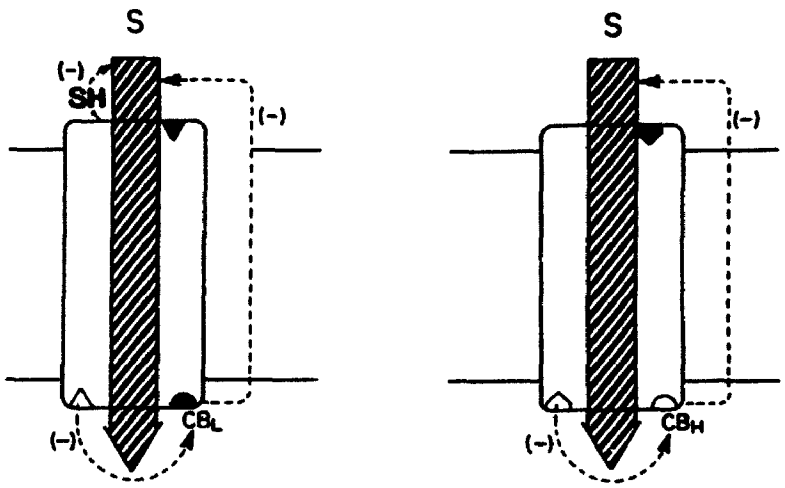

		HAHT	LAHT
(1)	K_m	0.6 mM	3.6 mM
(2)	Substrate specificity	dGlc, D-Glucose	MeGlc
(3)	Type of Transport	Active transport	Facilitated diffusion
(4)	Sulfhydryl Reagents	Sensitive	Insensitive
(5)	Glucose Starvation	Derepressed	Not affected
(6)	CB Inhibition	K_i = 0.16 μM	K_i = 0.016 μM
(7)	CB Binding	CB_L, K_d = 1.5 μM	CB_H, K_d = 0.1 μM
(8)	CB Photolabelling	40-60 kDa	40-60 kDa
(9)	Immunoblotting	63 kDa	60 kDa
(10)	Mutant D_{23}	Altered (HAHT$^-$, CB_L^-, 63 kDa$^-$)	Not altered
(11)	Myogenesis	Altered	Not altered

by low concentrations of sulfhydryl reagents. CB binding studies show that CB_L is associated with HAHT and that this site is not accessible to the external environment. CB photolabelling studies suggest that CB_L or HAHT is associated with CB photolabelled components (40-60 kDa). Immunoblotting studies reveal that the 63 kDa polypeptide might be the HAHTer. HAHT, CB_L and 63 kDa polypeptide are found to be defective in transport mutant D_{23}. Furthermore, this system is found to be altered during myogenic differentiation. On the other hand, MeGlc is transported primarily by LAHT. Studies with energy poisons and ionophores suggest that this system involves facilitated diffusion. It is sensitive to very low concentration of CB, but not to sulfhydryl reagents. CB binding studies suggest that CB_H is related to LAHT. Similar to CB_L, CB_H does not seem to be exposed to the external environment. CB photolabelled components (40-60 kDa) may also contain the CB_H. Immunoblotting studies suggest that the 60 kDa polypeptide may be related to LAHT. Moreover, this system remains unchanged during glucose starvation or myogenesis and is not altered in the transport mutants characterized.

In conclusion, we have identified and characterized the HT systems in rat L6 myoblasts through a combination of biochemical, physiological and genetic approaches. Regulation of these transport systems during growth and myogenic differentiation have also been the subject of this project. Although it is obvious that much work remains to be done, the results from this study should provide a good basis for further isolation and characterization of these HT systems. A better understanding of the structure and function of these HTers and their regulation during growth and myogenic differentiation will await the results of cloning and gene expression studies which are being carried out in our laboratory. The techniques that have been used in this study may also be helpful in the identification and characterization of HT systems in other cell types.

REFERENCES

Allard, W. J. and Lienhard, G. E. (1985) Monoclonal antibodies to the glucose transporter from human erythrocytes. J. Biol. Chem. 260, 8668-8675

Amos, H., Mandel, K. G. and Gay, R. J. (1984) Deprival of nicotinamide leads to enhanced glucose transport in chick embryo fibroblasts. Feder. Proc. 43, 2265-2268

Atlas, S. J. and Lin, S. (1976) High-affinity cytochalasin B binding to normal and transformed BALB/3T3 cells. J. Cell. Physiol. 89, 751-756

Avruch, J., Price, H. D., Martin, D. B. and Carter, J. R. (1973) Effect of low levels of trypsin on erythrocyte membranes. Biochem. Biophys. Acta. 29, 494-505

Baldwin, J. M., Gorga, J. C. and Lienhard, G. E. (1981) The monosaccharide transporter of human erythrocyte transport activity upon reconstitution. J. Biol. Chem. 256, 3685-3689

Baldwin, J. M., Lienhard, G. E. and Baldwin, S. A. (1980) The monosaccharide transport system of the human erythrocyte. Orientation upon reconstitution. Biochim. Biophys. Acta 599, 699-714

Baldwin, S. A., Baldwin, J. M., Gorga, F. R. and Lienhard, G. E. (1979) Purification of the cytochalasin B binding component of the human erythrocyte monosaccharide transport system. Biochim. Biophys. Acta 552, 183-188

Baldwin, S. A. and Henderson, P. J. F. (1989) Homologies between sugar transporters from eukaryotes and prokaryotes. Annu. Rev. Physiol. 51, 459-471

Baldwin, S. A. and Lienhard, G. E. (1980) Immunological identification of the human erythrocyte monosaccharide transporter. Biochem. Biophys. Res. Commun. 94, 1401-1408

Baldwin, S. A. and Lienhard, G. E. (1981) Glucose transport across membrane: Facilitated diffusion systems. Trends Biochem. Sci. 6, 205-208

Baly D.L. and Horuk, R. (1987) Dissociation of insulin-stimulated glucose transport from the translocation of glucose carriers in rat adipose cells. J. Biol. Chem. 262, 21-24

Bang, O. and Ørskov, S. L. (1937) Variations in the permeability of the red blood cell in man. J. Clin. Invest. 16, 179-281

Barnett, J. E. G., Holman, G. D., Chalkley, R. A. and Munday, K. A. (1975) Evidence for two asymmetric conformational states in the human erythrocyte sugar-transport system. Biochem. J. 145, 417-429

Barnett, J. E. G., Holmon, G. D. and Munday, K. A. (1973) Structural requirements for binding to the sugar transport system of the human erythrocyte. Biochem. J. 131, 211-221

Basketter, D. A. and Widdas, W. F. (1977) Competitive inhibition of hexose transfer in human erythrocytes by cytochalasin B. J. Physiol. 265, 39p

Batt, E. R., Abbott, R. E. and Schachter, D. (1976) Impermeant maleimides. Identification of an exofacial component of the human erythrocyte hexose transport mechanism. J. Biol. Chem. 251, 7184-7190

Batt, E. R. and Schachter, D. (1973) Transport of monosaccharides. I. Asymmetry in the human erythrocyte mechanism. J. Clin. Invest. 52, 1686-1697

Beguinot, F., Kahn, C. R., Moses, A. C. and Smith, R. J. (1986) The development of insulin receptors and responsiveness in the muscle cell line L6. Endo. 118, 446-455

Biber, J. W. and Lienhard, G. E. (1986) Isolation of vesicles containing insulin-responsive, intracellular glucose transporters from 3T3-L1 adipocytes. J. Biol. Chem. 261, 16180-16184

Birnbaum, M. J., Haspel, H. C. and Rosen, O. M. (1986) Cloning and characterization of a cDNA encoding the rat brain glucose-transporter protein. Proc. Natl. Acad. Sci. U.S.A. 83, 5784-5788

Bloch, R. (1973) Inhibition of glucose transport in the human erythrocyte by cytochalasin B. Biochemistry 12, 4799-4801

Bohinski, R. C. (1987) Modern Concepts in Biochemistry (Fifth edition), Allyn and Bacon, INC. Newton, Massachusetts. Chapter 11, p.440

Bona, C. A. and Kohler, H. (1984) Anti-idiotypic antibodies and internal images. In: Receptor Biochemistry and Methodology Vol. 4, (Venter, J. C. and Harrison, L. C., ed.), Alan R. Liss, Inc. New York, pp. 141-149

Burn, P. (1988) Amphitropic proteins: a new class of membrane proteins. Trends in Biochem. Sci. 13, 79-83.

Cairns, M. T., Elliot, D. A., Scudder, P. R. and Baldwin, S. A. (1984) Proteolytic and chemical dissection of the human erythrocyte glucose transport proteins. Biochem. J. 221, 179-188

Calderhead, D. M. and Lienhard, G. E. (1988) Labelling of glucose transporters at the cell surface in 3T3-L1 adipocytes. Evidence for both translocation and a second mechanism in the insulin stimulation of transport. J. Biol. Chem. 263, 12171-12174

Carruthers, A. (1986) ATP regulation of the human red cell sugar transporter. J. Biol. Chem. 261, 11028-11037

Carruthers, A. and Melchiors, D. L. (1984) A rapid method of reconstituting human erythrocyte sugar transport proteins. Biochemistry 23, 2712-2718

Carter, J. R., Avruch, J. and Martin, D. B. (1973) Glucose transport by trypsin treated red blood cell ghosts. Biochem. Biophys. Acta 291, 506-518

Carter-Su, C. and Okamoto, K. (1985) Effect of glucocorticoids on hexose transport in rat adipocytes. Evidence for decreased transporters in the plasma membrane. J. Biol. Chem. 260, 11091-11098

Carter-Su, C., Pessin, J. E., Mora, R., Gitomer, W. and Czech, M. P. (1982) Photoaffinity labelling of the human erythrocyte D-glucose transporter. J. Biol. Chem. 257, 5419-

5425

Cates, G. A., Brickenden, A. M. and Sanwal, B. D. (1984) Possible involvement of a cell surface glycoprotein in the differentiation of skeletal myoblasts. J. Biol. Chem. 259, 2646-2650

Cheung, M. O. and Lo, T. C. Y. (1984) Hexose transport in plasma membrane vesicles of rat myoblast L6. Can. J. Biochem. Cell Biol. 62, 1217-1227

Christopher, C. W., Colby, W. W. and Ullrey, D. (1976a) Derepression and carrier turnover: Evidence for two distinct mechanisms of hexose transport regulation in animal cells. J. Cell Physiol. 89, 683-692

Christopher, C. W., Kohlbacher, M. S. and Amos, H. (1976b) Transport of sugars in chick-embryo fibroblasts: Evidence for a low-affinity and high-affinity system for glucose transport. Biochem. J. 158, 439-450

Clark, J. H. and Peck, E. J. Jr. (1979) Steroid receptor characterization and measurement. In:" Female Sex Steroids Receptors and Functions." (Gross, F., Grumbach, M. M., Labhart, A., Lipsett, M. B., Mann, T., Samuels, L. T. and Zander, J. eds.) Springer-Verlag, New York, pp. 4-36

Clarke, E., Nandan, D., Brickenden, A., Cates, G. A., Ball, E. and Sanwal, B. D. (1988) Glycoprotein glycans may not be necessary for the differentiation of skeletal myoblasts. Exptl. Cell Res. 180, 178-188

Cohen, R., Pacifici, M., Rubinstein, N., Biehl, J. and Holtzer, H. (1977) Effects of a tumour promoter on myogenesis. Nature 266, 538-540

Colby, C. and Romano, A. H. (1975) Phosphorylation but not transport of sugars is enhanced in virus-transformed mouse 3T3 cells. J. Cell. Physiol. 85, 15-25

Craik, J. O., Good, H., Gottschalk, R., Jarvis, S. M., Paterson, A. R. P. and Cass, C. E. (1988) Identification of glucose and nucleoside transport proteins in neonatal pig erythrocytes using monoclonal antibodies against band 4.5 polypeptides of adult human and pig erythrocytes. Biochem. Cell Biol. 66, 839-852

Cushman, S. W. and Wardzala, L. J. (1980) Potential mechanism of insulin action on glucose transport in the isolated rat adipose cell. J. Biol. Chem. 255, 4758-4762

Czech, M. P. (1976a) Regulation of the D-glucose transport system in isolated fat cells. Mol. Cell. Biochem. 11, 51-63

Czech, M. P. (1976b) Characterization of [^{3}H]-cytochalasin B binding to the fat cell plasma membrane. J. Biol. Chem. 251, 2905-2910

D'Amore, T. and Lo, T. C. Y. (1986a) Hexose transport in L6 rat myoblasts. I. Rate-limiting step, kinetic properties, and evidence for two systems. J. Cell. Physiol. 127, 95-105

D'Amore, T. and Lo, T. C. Y. (1986b) Hexose transport in L6 rat myoblasts. II. The effects of sulfhydryl reagents. J. Cell. Physiol. 127, 106-113

D'Amore, T. and Lo, T. C. Y. (1986c) Approaches used to examine the mechanism and

regulation of hexose transport in rat myoblasts. Biochem. Cell. Biol. 1081-1091

D'Amore, T. and Lo, T. C. Y. (1988) Properties of hexose transport regulatory mutants isolated from L6 rat myoblasts. Biochem. J. 250, 59-64

D'Amore, T., Cheung, M. O., Duronio, V. and Lo, T. C. Y. (1986a) Stimulation of hexose transport in L6 rat myoblasts by antibody and by glucose starvation. Biochem. J. 238, 831-836

D'Amore, T., Duronio, V., Cheung, M. O., and Lo, T. C. Y. (1986b) Isolation and characterization of hexose transport mutants in L6 rat myoblasts. J. Cell. Physiol. 126, 26-36

Davies, A., Meeran, K., Cairns, M. T. and Baldwin, S. A. (1987) Peptide-specific antibodies as probes of the orientation of the glucose transporter in the human erythrocyte membrane. J. Biol. Chem. 363, 9347-9352

Devlin, R. B. and Emerson, C. P. (1978) Coordinate regulation of contractile protein synthesis during myoblast differentiation. Cell 13, 599-611

Deziel, M. R. and Rothstein, A. (1984) Proteolytic cleavages of cytochalasin B binding components of band 4.5 proteins of the human red blood cell membrane. Biochim. Biophys. Acta 776, 10-20

Dick, A. P. K., Harik, S. I., Klip, A. and Walker, D. M. (1984) Identification and characterization of the glucose transporter of the blood-brain barrier by cytochalasin B binding and immunological reactivity. Proc. Natl. Acad. Sci. U.S.A. 81, 7233-7237

Elbrink, J. and Bihler, I. (1975) Membrane transport: Its relation to cellular meta' olic rates. Science 188, 1177-1184

Ewton D. Z., Spizz, G., Olson, E. N. and Florini, J. R. (1988) Decrease in transforming growth factor binding and action during differentiation in muscle cells. J. Biol. Chem. 263, 4029-4032

Fannin, F. F., Evans, J. O., Gibbs, M. and Diedrich, D. F. (1981) Phloretinyl-3'-benzylazide: A high affinity probe for the sugar transporter in human erythrocytes. Biochim. Biophys. Acta 649, 189-201

Farid, N. R. and Lo, T. C. Y. (1985) Antiidiotypic antibodies as probes for receptor structure and function. Endocrine Rev. 6, 1-23

Ferguson, M. A. J. and Williams, A. F. (1988) Cell surface anchoring of proteins via glycosyl-phosphatidylinositol structures. Annu. Rev. Biochem. 57, 285-320.

Flier, J. S., Mueckler, M., McCall, A. L. and Lodish, H. F. (1987) Distribution of glucose transporter messenger RNA transcripts in tissues of rat and man. J. Clin. Invest. 79, 657-661

Florini, J. R. and Magri, K. A. (1989) Effects of growth factors on myogenic differentiation. Am. J. Physiol. 256 (Cell Physiol. 25), C701-C711

Foley, J. E., Foley, R. and Gliemann, J. (1980) Rate-limiting steps of 2-deoxyglucose

uptake in rat adipocytes. Biochim. Biophys. Acta 599, 689-698

Franchi, A., Silvestre, P. and Pouyssegur, J. (1978) Carrier activation and glucose transport in Chinese hamster fibroblasts. Biochem. Biophys. Res. Commun. 85, 1526-1534

Frost, S. C., Kohanski, R. A. and Lane, M. D. (1987) Effect of phenylarsine oxide on insulin-dependent protein phosphorylation and glucose transport in 3T3-L1 adipocytes. J. Biol. Chem. 262, 9872-9876

Fukumoto, H., Seino, S., Imura, H., Seino, Y., Eddy, R. L., Fukushima, Y., Byers, M. G., Shows, T. B. and Bell, G. I. (1988) Sequence, tissue distribution, and chromosomal localization of mRNA encoding a human glucose transporter-like protein. Proc. Natl. Acad. Sci. U.S.A. 85, 5434-5438

Gargus, J.J., Adelberg, E.A. and Slayman, C.W. (1983) Coordinated changes in potassium fluxes as early events in the differentiation of the human promyelocyte line HL-60. In "Regulation and Development of Membrane Transport Processes" (Graves, J. S. ed.) J. Wiley and Sons, N.Y. 39, 179-191

Garvey, W. T., Olefsky, J. M., Mattaei, S. and Marshall, S. (1987) Glucose and insulin co-regulate the glucose transport system in primary cultured adipocytes. A new mechanism of insulin resistance. J. Biol. Chem. 262, 189-197

Gay, R.J. and Hilf, R. (1980) Density-dependent and adaptive regulation of glucose transport in primary cell cultures of the R3230AC rat mammary adenocarcinoma. J. Cell. Physiol. 102, 155-174

Gibbs, E. M., Allard, W. J. and Lienhard, G. E. (1986) The glucose transporter in 3T3-L1 adipocytes is phosphorylated in response to phorbol ester but not in response to insulin. J. Biol. Chem. 261, 16597-16603

Gliemann, J. and Rees, W. D. (1983) The insulin-sensitive hexose transport system in adipocytes. Curr. Top. Membr. Transp. 18, 339-379

Gorga, F. R., Baldwin, S. A. and Lienhard, G. E. (1979) The monosaccharide transporter from erythrocytes is heterogeneously glycosylated. Biochem. Biophys. Res. Commun. 91, 955-961

Gorter, E. and Grendel, F. (1925) Bimolecular layers of lipoids on the chromocytes of the blood. J. Exp. Med. 41, 439-443

Greenbaum, C. J., Shanahan, M. F., Pillion, D. J. and Czech, M. P. (1977) Selective extraction of an intrinsic fat cell plasma-membrane glycoprotein by Triton X-100: Correlation with [^{3}H]cytochalasin B binding activity. FEBS Lett. 83, 71-75

Griffin, J. F., Rampal, A. L. and Jung, C. Y. (1982) Inhibition of glucose transport in human erythrocytes by cytochalasins: A model based on diffraction studies. Proc. Natl. Acad. Sci. U.S.A. 79, 3759-3763

Guidotti, G. (1972) Membrane proteins. Ann. Rev. Biochem. 41, 731-752

Haspel, H. C., Birnbaum, M. J., Wilk, E. W. and Rosen, O. M. (1985) Biosynthetic precursors and in vitro translation products of the glucose transporter of human hepatocarcinoma cells, human fibroblasts, and murine preadipocytes. J. Biol. Chem.

260, 7219-7225

Haspel, H. C., Rosenfeld, M. G. and Rosen, O. M. (1988) Characterization of antisera to a synthetic carboxyl-terminal peptide of the glucose transporter protein. J. Biol. Chem. 263, 398-403

Haspel, H. G., Wilk, E. W., Birnbaum, M. J., Cushman, S. W. and Rosen, O. M. (1986) Glucose deprivation and hexose transporter polypeptides of murine fibroblasts. J. Biol. Chem. 261, 6778-6789

Herbert, D. N. and Carruthers, A. (1986) Direct evidence for ATP modulation of sugar transport in human erythrocyte ghosts. J. Biol. Chem. 261, 10093-10099

Horner, H. C., Munck, A. and Lienhard, G. E. (1987) Dexamethasone causes translocation of glucose transporter from the plasma membrane to an intracellular site in human fibroblasts. J. Biol. Chem. 262, 17696-17702

Horuk, R., Matthaei, S., Olefsky, J. M., Baly, D. L., Cushman, S. W. and Simpson, I. A. (1986) Biochemical and functional heterogeneity of rat adipocyte glucose transporters. J. Biol. Chem. 261, 1823-1828

Huynh, T. V., Young, R. A. and Davis, R. W. (1985) In: DNA Cloning: A practical approach, Vol. 1, (Glover, D. M. ed.) IRL Press, Oxford. pp. 47-49

Ingerman, R. L., Bissonnette, J. M. and Koch, P. L. (1983) D-glucose sensitive and insensitive cytochalasin B binding proteins from microvillus plasma membranes of human placenta. Identification of the D-glucose transporter. Biochem. Biophys. Acta 730, 57-63

Islam, M., Pepper, B., Briones-Urbina, R. and Farid, N. (1983) Biological activity of anti-thyrotropin anti-idiotypic antibody. Eur. J. Immunol. 13, 57-63

James, D. E., Strube, M. and Mueckler, M. (1989) Molecular cloning and characterization of an insulin-regulatable glucose transporter. Nature 338, 83-87

Jarvis, S. M., Young, J. O., Wu, J. R., Belt, J. A. and Paterson, A. R. P. (1986) Photoaffinity labelling of the human erythrocyte glucose transporter with 8-azidoadenosine. J. Biol. Chem. 261, 11077-11085

Jaynes, J. P., Chamberlain, J. S., Buskin, J. N., Johnson, J. E. and Hauschka, S. D.(1986) Transcriptional regulation of the muscle creatine kinase gene and regulated expression in transfected mouse myoblasts. Mol. Cell. Biol. 6, 2855-2864

Jennings, M. L. (1989) Topography of membrane proteins. Annu. Rev. Biochem. 58, 999-1027

Johnson, L. W. and Smith, C. H. (1982) Identification of the glucose transport protein of the microvillus membrane of human placenta by photoaffinity labelling. Biochem. Biophys. Res. Commun. 109, 408-413

Joost, H. G., Weber, T. M. and Cushman, S. W. (1988) Qualitative and quantitative comparison of glucose transport activity and glucose transporter concentration in plasma membranes from basal and insulin-stimulated rat adipose cells. Biochem. J. 249, 155-161

Joost, H. G., Weber, T. M., Cushman, S. W. and Simpson, I. A. (1986) Insulin-stimulated glucose transport in rat adipose cells. Modulation of transporter intrinsic activity by isoproterenol and adenosine. J. Biol. Chem. 261, 10033-10036

Joost, H. G., Weber, T. M., Cushman, S. W. and Simpson, I. A. (1987) Activity and phosphorylation state of glucose transporters in plasma membranes from insulin-, isoproterenol-, and phorbol ester-treated rat adipose cells. J. Biol. Chem. 262, 11261-11267

Jung, C. Y. (1971) Evidence of high stability of the glucose transport carrier function in human red cell ghosts extensively washed in various media. Arch. Biochem. Biophys. 146, 215-226

Jung, C. Y. (1973) Carrier-mediated glucose transport across human red cell membrane. In "The Red Blood Cell." (Second edition) (Surgenor, D. M., ed.) Academic Press, New York and London. pp. 705-749

Jung, C. Y. and Carlson, L. M. (1975) Glucose transport carrier in human erythrocyte membranes. Dinitrophenylation of a membrane component modified by D-glucose. J. Biol. Chem. 250, 3217-3221

Jung, C. Y. and Rampal, A. L. (1977) Cytochalasin B binding sites and glucose transport carrier in human erythrocyte ghosts. J. Biol. Chem. 252, 5456-5463

Jung, E. K. Y., Chin, J. J. and Jung, C. Y. (1986) Structural basis of human erythrocyte glucose transporter function in reconstituted system. Hydrogen exchange. J. Biol. Chem. 261, 9155-9160

Kaback, H. R. (1973) Bacterial transport mechanism. In "Bacterial Membranes and Walls." (Lieve, L., ed.) Marcel Dekker, Inc., New York. pp. 241-292

Kahn, B. B. and Cushman, S. W. (1987) Mechanism for markedly hyperresponsive insulin-stimulated glucose transport activity in adipose cells from insulin-treated streptozotocin diabetic rats. Evidence for increased glucose transporter intrinsic activity. J. Biol. Chem. 262, 5118-5124

Kalckar, H. M. and Ullrey, D. B. (1984) Hexose uptake regulation mediated through aerobic pathways: schism in a fibroblast mutant. Fed. Proc. 43, 2242-2245

Karnieli, E., Zarnowski, M. J., Hissin, P. J., Simpson, I. A., Salans, L. B. and Cushman, S. W. (1981) Insulin-stimulated translocation of glucose transport systems in the isolated rat adipose cell. Time course, reversal, insulin concentration dependency, and relationship to glucose transport activity. J. Biol. Chem. 256, 4772-4777

Kasahara, M. and Hinkle, P. C. (1976) Reconstitution of D-glucose transport catalyzed by a protein fraction from human erythrocytes in sonicated liposomes. Proc. Natl. Acad. Sci. U.S.A. 73, 396-400

Kasahara, M. and Hinkle, P. C. (1977) Reconstitution and purification of the D-glucose transporter from human erythrocytes. J. Biol. Chem. 253, 7384-7390

Kay, M. M. B. (1985) Glucose transport protein is structurally and immunologically related to band 3 and senescent cell antigen. Proc. Natl. Acad. Sci. U.S.A. 82,

1731-1735

Kayano, T., Fukumoto, H., Eddy, R. L., Fan, Y., Byers, M. G., Shows, T. B. and Bell, G. I. (1988) Evidence for a family of human glucose transporter-like proteins. Sequence and gene localization of a protein expressed in fetal skeletal muscle and other tissues. J. Biol. Chem. 263, 15245-15248

Klip, A., Li, G. and Walker, D. (1983a) Insulin binding to differentiating muscle cells in culture. Can. J. Biochem. 61, 644-649

Klip, A., Logan, W. J. and Li, G. (1982) Hexose transport in L6 muscle cells. Kinetic properties and the number of [^{3}H]-cytochalasin B binding sites. Biochim. Biophys. Acta 687, 265-280

Klip, A. and Walker, D. (1983) The glucose transport system of muscle plasma membranes: Characterization by means of [^{3}H]cytochalasin B binding. Arch. Biochem. Biophys. 221, 175-187

Klip, A., Walker, D., Ransome, K. J., Schroer, O. W. and Lienhard, G. E. (1983b) Identification of the glucose transporter in rat skeletal muscle. Arch. Biochem. Biophys. 226, 198-205

Koepsell, H., Korn, K., Raszeja-Specht, A., Bernotat-Danielowski, S. and Ollig, D. (1988) Monoclonal antibodies against the renal Na^+-D-glucose cotransporter. Identification of antigenic polypeptides and demonstration of functional coupling of different Na^+-cotransport systems. J. Biol. Chem. 263, 18419-18429

Krupka, R. M. and Deves, R. (1986) Access channels in carrier systems: Evidence derived from inhibition studies of the choline and glucose transport systems of erythrocytes. In" Dynamics of Biochemical Systems" (Damjanovich, S., Keleti, T., and Tron, L. eds). Publisher: Akademiai, Kiado pp 537-551

Kurokawa, T., Tillotson, L. G., Chen, C. C. and Isselbacher, K. J. (1986) Solubilization and separation of the human erythrocyte D-glucose transporter covalently and noncovalently photoaffinity-labeled with [^{3}H]cytochalasin B. Proc. Natl. Acad. Sci. U.A.S. 83, 479-482

Laemmli, U. K. (1970) Cleavage of the structural proteins during the assembly of the head of bacteriophage T4. Nature (London) 227, 680-685

Le, A. V. and Doyle, D. (1984) General theory of membrane structure and function. In "Receptor Biochemistry and Methodology." (Craig, J. and Harrison, L. C., eds.) Alan R. Liss, Inc. 1, 1-25

Lee, M. D., Zentella, A., Pekala, P. H. and Cerami, A. (1987) Effect of endotoxin-induced monokines on glucose metabolism in the muscle cell line L6. Proc. Natl. Acad. Sci. USA 84, 2590-2594

LeFevre, P. G. (1948) Evidence of active transfer of certain non-electrolytes across the human red cell membrane. J. Gen. Physiol. 31, 505-527

LeFevre, P. G. (1953) Further characterization of the sugar transfer system in the red cell membrane by the use of phloretin. Fed. Proc. Fed. Am. Soc. Exp. Biol. 12, 84

LeFevre, P. G. (1961) Sugar transport in the red blood cells: Structure-activity relationships in substrates and antagonists. Pharmacol. Rev. 13, 39-45

Levine, R., Goldstein, M., Klein, S. and Huddlestun, B. (1949) The action of insulin on the distribution of galactose in eviscerated nephrectomized dogs. J. Biol. Chem. 179, 985-986

Lienhard, G. E., Gorga, F. R., Orasky, J. E. Jr. and Zoccoli, M. A. (1977) Monosaccharide transport system of the human erythrocyte. Identification of the cytochalasin B binding component. Biochemistry 16, 4921-4926

Lienhard, G. E., Kim, H. H., Ransome, K. J. and Gorge, J. C. (1982) Immunological identification of an insulin-responsive glucose transporter. Biochem. Biophys. Res. Commun. 105, 1150-1156

Lin, S. and Spudich, J. A. (1974) Biochemical studies on the mode of action of cytochalasin B. Cytochalasin B binding to red cell membrane in relation to glucose transport. J. Biol. Chem. 249, 5778-5783

Lindberg, O. L. and Ernster, L. (1956) Determination of organic phosphorus compounds by phosphate analysis. Meth. Biochem. Anal. 3, 1-22

Lo, T. C. Y. (1979) The transfer of a bacterial transmembrane function to eukaryotic cells. J. Biol. Chem. 254, 591-594

Lo, T. C. Y. and Duronio, V. (1984a) Activation of hexose transport by antibody. Can. J. Biochem. Cell Biol. 62, 245-254

Lo, T. C. Y. and Duronio, V. (1984b) Mechanism of antibody stimulation of hexose transport in rat myoblasts. Can. J. Biochem. Cell Biol. 62, 255-265

Lorimer, I. A. J., Mason, M. E. and Sanwal, B. D. (1987) Levels of type I cAMP-dependent protein kinase regulatory subunit are regulated by changes in turnover rate during skeletal myogenesis. J. Biol. Chem. 262, 17200-17205

Lowry, O. H., Rosenbrough, N. J., Farr, A. L. and Randall, R. J. (1951) Protein measurement with the folin reagent. J. Biol. Chem. 193, 265-275

Lundsgaard, E. (1939) On the mode of action of insulin. Uppsala Läk. Fören. Förh. 45, 1-4

Maiden, M. C. J., Davis, E. O., Baldwin, S. A., Moore, D. C. M. and Henderson, P. J. F. (1987) Mammalian and bacterial sugar transport proteins are homologous. Nature 325, 641-643

Malchoff, D. M., Parker, V. G. and Langdon, R. G. (1985) Reconstitution of the glucose transport activity of rat adipocytes. Biochim. Biophys. Acta 817, 271-281

Markwell, M. A. and Fox, C. F. (1978) Surface-specific iodination of membrane proteins of viruses and eucaryotic cells using 1,3,4,6-tetrachloro-3α,6α-diphenylglycoluril. Biochemistry 17, 4807-4817

Martin, J. B. and Doty, D. M. (1949) Determination of inorganic phosphate. Modification

of isobutyl alcohol procedure. Anal. Chem. 21, 965-967

Matthaei, S., Olefsky, J. M. and Karnieli, E. (1988) Cycloheximide decreases glucose transporters in rat adipocyte plasma membranes without affecting insulin-stimulated glucose transport. Biochem. J. 251, 491-497

Medford, R. M., Nguyen, H. T. and Nadal-Ginard, B. (1983) Transcriptional and cell cycle-mediated regulation of myosin heavy chain gene expression during muscle cell differentiation. J. Biol. Chem. 258, 11063-11073

Mesmer, O., Cheung, M. O., D'Amore, T. and Lo, T. C. Y. (1986) Hexose transport in plasma membrane vesicles prepared from L6 rat myoblasts. Biochem. Biophys. Res. Commun. 141, 124-130

Miller, D. M. (1969) Monosaccharide transport in human erythrocytes. In "Red Cell Membrane Structure and Function." (Jamieson, G. A. and Greenwalt, T. J. eds.) Lippincott, Philadelphia. pp. 240-290

Morgan, H. E., Regen, D. M. and Park, C. R. (1964) Identification of a mobile carrier-mediated sugar transport system in muscle. J. Biol. Chem. 239, 369-374

Morris, G. E. and Cole, R. J. (1972) Cell fusion and differentiation ir ıltured chick muscle cells. Exp. Cell Res. 75, 191-199

Mueckler, M., Caruso, C., Baldwin, S. A., Panico, M., Blench, I., Morris, H. R., Allard, W. J., Lienhard, G. E. and Lodish, H. F. (1985) Sequence and structure of a human glucose transporter. Science 229, 941-945

Mullins, R.E. and Langdon, R. G. (1980) Maltosyl isothiocyanate: an affinity label for the glucose transporter of the human erythrocyte membrane 2. Identification of the transporter. Biochemistry 19, 1205-1212

Munck, A. (1976) General aspects of steroid hormone-receptor interaction. In: "Receptors and Mechanism of Action of Steroid Hormone (Pasqualini, J. R., ed.) Marcel-Dekker, New York, pp. 1-40

Neeb, M., Fasold, H. and Koepsell, H. (1985) Identification of the D-glucose binding polypeptide of the renal Na^+-D-glucose cotransporter with a covalently binding D-glucose analog. FEBS 182, 139-144

Neeb, M., Kunz, U. and Koepsell, H. (1987) Identification of D-glucose-binding polypeptides which are components of the renal Na^+-D-glucose cotransporter. J. Biol. Chem. 262, 10718-10727

Oka, Y., Asano, T., Shibasaki, Y., Kasuga, M., Kanazawa, Y. and Takaku, F. (1988) Studies with antipeptide antibody suggest the presence of at least two types of glucose transporter in rat brain and adipocytes. J. Biol. Chem. 263, 13432-13439

Oka, Y. and Czech, M. P. (1984) Photoaffinity labelling of insulin-sensitive hexose transporters in intact rat adipocytes. Direct evidence that latent transporters become exposed to the extracellular space in response to insulin. J. Biol. Chem. 259, 8125-8133

Olefsky, J. M. (1978) Mechanisms of the ability of insulin to activate the glucose

transport system in rat adipocytes. Biochem. J. 172, 137-145

Pearson, M.L. (1981) Muscle differentiation in cell culture: A problem in somatic cell and molecular genetics. In " The Molecular Genetics of Development" (Leighton, T. and Loomis, W.F., Eds.), Academic Press, Orlando, FL. pp. 361-418

Pessin, J. E., Tillotson, L. G., Isselbacher, K. J. and Czech, M. P. (1984) Photoaffinity labelling of the stereospecific D-glucose transport system with cytochalasin B. Fed. Proc. Fed. Am. Soc. Exp. Biol. 43, 2258-2261

Pessin, J. E., Tillotson, L. G., Yamada, K., Gitomer, W., Carter-Su, C., Mora, R., Isselbacher, K. J. and Czech, M. P. (1982) Identification of the stereospecific hexose transporter from starved and fed chicken embryo fibroblasts. Proc. Natl. Acad. Sci. U.S.A. 79, 2286-2290

Phutrakul, S. and Jones, M. N. (1979) The permeability of bilayer lipid membrane on the incorporation of erythrocyte membrane extracts and the identification of the monosaccharide transport proteins. Biochem. Biophys. Acta 551, 188-200

Pinkofsky, H. B., Rampal, A. L., Cowden, M. A. and Jung, C. Y. (1978) Cytochalasin B binding proteins in human erythrocyte membranes. Modulation of glucose sensitivity by site interaction and partial solubilization of binding activities. J. Biol. Chem. 253, 4930-4937

Plagemann, P. G. W., Graff, J. C. and Wohlhueter, R. M. (1977) Binding of [^{3}H] cytochalasin B and its relationship to inhibition of hexose transport in Novikoff rat hepatoma cells. J. Biol. Chem. 252, 4191-4201

Postma, P.W. and Lengeler, J. W. (1985) Phosphoenolpyrurate: Carbohydrate phosphotransferase system of bacteria. Microbiol. Rev. 49, 232-269

Regen, D. M. and Morgan, H. E. (1964) Studies of the glucose transport system in the rabbit erythrocyte. Biochem. Biophys. Acta 79, 151-161

Rogers, J. E., Narindrasorasak, S., Cates, G. A. and Sanwal, B. D. (1985) Regulation of protein kinase and its regulatory subunits during skeletal myogenesis. J. Biol. Chem. 260, 8002-8007

Rogers, J., Ng, S. K., Coulter, M. B. and Sanwal, B. D. (1975) Inhibition of myogenesis in a rat myoblast line by 5-bromo-2-deoxyuridine. Nature 256, 438-440

Rosenberg, J. and Wilbrandt, W. (1957) Uphill transport induced by counterflow. J. Gen. Physiol. 41, 289-296

Rosoff, P.M. and Cantley, L.C. (1983) Ion fluxes and differentiation in transformed cell lines. In "Regulation and Development of Membrane Transport Processes" (Ed. J.S. Graves) J. Wiley and Sons, N.Y. 39, 193-204

Salter, D. W., Baldwin, S. A., Lienhard, G. E. and Weber, M. J. (1982) Proteins antigenically related to the human erythrocyte glucose transporter in normal and Rous Sarcoma virus transformed chicken embryo fibroblasts. Proc. Natl. Acad. Sci. U.S.A. 79, 1540-1544

Sanwal, B.D. (1979) Myoblast differentiation. Trends Biochem. Sci. 4, 155-157

Sarkar, H. K., Thorens, B., Lodish, H. F. and Kaback, H. R. (1988) Expression of the human erythrocyte glucose transporter in Escherichia coli. Proc. Natl. Acad. Sci. U.S.A. 85, 5463-5467

Schreiber, A. B., Couraud, P. Q., Ander, C., Vray, B. and Strosberg, A. (1980) Anti-alprenolol anti-idiotypic antibodies bind to ß-adrenergic receptors and modulate catecholamine-sensitive adenylate cyclase. Proc. Natl. Acad. Sci. U.S.A. 77, 7385-7389

Seamon, K. B., Padgett, W. and Daley, J. W. (1981) Forskolin: Unique diterpene activator of adenylate cyclase in membranes and in intact cells. Proc. Natl. Acad. Sci. U.S.A. 78, 3363-3367

Sege, K. and Peterson, P. A. (1978) Use of anti-idiotypic antibodies as cell-surface receptor probes. Proc. Natl. Acad. Sci. U.S.A. 75, 2443-2447

Semenza, G., Kessler, M. and Schmidt, U. (1985) The small-intestinal sodium-glucose cotransporter(s). Annals New York Academy of Sciences 45, 83-100

Sergeant, S. and Kim, H. D. (1985) Inhibition of 3-O-Methylglucose transport in human erythrocytes by forskolin. J. Biol. Chem. 260, 14677-14682

Shanahan, M. F. (1982) Cytochalasin B. A natural photoaffinity ligand for labelling the human erythrocyte glucose transporter. J. Biol. Chem. 257, 7290-7293

Shanahan, M. F. and Czech, M. P. (1977a) Partial purification of the D-glucose transport system in rat adipocyte plasma membranes. J. Biol. Chem. 252, 6554-6561

Shanahan, M. F. and Czech, M. P. (1977b) Purification and reconstitution of the adipocyte plasma membrane D-glucose transport system. J. Biol. Chem. 252, 8341-8343

Shanahan, M. F. and D'Artel-Ellis, J. (1984) Orientation of the glucose transporter in the human erythrocyte membrane. Investigation by in situ proteolytic dissection. J. Biol. Chem. 259, 13878-13884

Shanahan, M. F. and Jacquez, J. A. (1978) Differential labelling of components in human erythrocyte membranes associated with the transport of glucose. Membr. Biochem. 1, 239-267

Shanahan, M. F., Morris, D. P. and Edwards, B. M. (1987) [^{3}H]-Forskolin. Direct photoaffinity labelling of the erythrocyte D-glucose transporter. J. Biol. Chem. 262, 5978-5984

Shanahan, M. F., Olson, S. A., Weber, M. J., Lienhard, G. E. and Gorge, J. C. (1982) Photolabelling of glucose-sensitive cytochalasin B binding proteins in erythrocyte, fibroblast and adipocyte membranes. Biochem. Biophys. Res. Commun. 107, 38-43

Shanahan, M. F., Wadzinski, B. E., Lowndes, J. M. and Ruoho, A. E. (1985) Photoaffinity labelling of the human erythrocyte monosaccharide transporter with an aryl azide derivative of D-glucose. J. Biol. Chem. 260, 10897-10900

Shelton, R. L. Jr. and Langdon, R. G. (1983) Reconstitution of glucose transport using human erythrocyte Band 3. Biochem. Biophys. Acta 733, 25-33

Simpson, I. B. and Cushman, S. W. (1986) Hormonal regulation of mammalian glucose transport. Ann. Rev. Biochem. 55, 1059-1089

Singer, S. J. (1977) Thermodynamics, the structure of integral membrane proteins, and transport. J. Supramol, Struct. 6, 313-323

Singer, S. J. and Nicolson, G. L. (1972) The fluid mosaic model of the structure of cell membranes. Science 175, 720-731

Smith, U., Kuroda, M. and Simpson, I. A. (1984) Counter-regulation of insulin-stimulated glucose transport by catecholamines in the isolated rat adipose cell. J. Biol. Chem. 259, 8757-8763

Sogin, D. C. and Hinkle, P. C. (1978) Characterization of the glucose transporter from human erythrocytes. J. Supramol. Struct. 8, 447-453

Sogin, D. C. and Hinkle, P. C. (1980) Immunological identification of the human erythrocyte glucose transporter. Proc. Natl. Acad. Sci. U.S.A. 77, 5725-5729

Steck, T. L. and Kant, J. A. (1974) Preparation of impermeable ghosts and inside-out vesicles from human erythrocyte membrane. Methods Enzymol. 31, 172-180

Stryer, L. (1988) Biochemistry (Third edition). W. H. Freeman and Company, San Francisco. Chapter 10, pp. 225-226

Suzuki, K. and Kono, T. (1980) Evidence that insulin causes translocation of glucose transport activity to the plasma membrane from an intracellular storage site. Proc. Natl. Acad. Sci. U.S.A. 77, 2542-2545

Taverna, R. D. and Langdon, R. G. (1973a) Reversible association of cytochalasin B with the human erythrocyte membrane. Inhibition of glucose transport and the stoichiometry of cytochalasin B. Biochem. Biophys. Acta. 323, 207-219

Taverna, R. D. and Langdon, R. G. (1973b) D-glucose isothiocyanate, an affinity label for the glucose transport proteins of the human erythrocyte membrane. Biochem. Biophys. Res. Commun. 54, 593-599

Taylor, N. F. and Gagenja, G. L. (1975) A model for the mode of action of cytochalasin B inhibition of D-glucose transport in the human erythrocyte. Can. J. Biochem. 53, 1078-1084

Thorens, B., Sarkar, H. K., Kaback, H. R. and Lodish, H. F. (1988) Cloning and functional expression in bacteria of a novel glucose transporter present in liver, intestine, kidney, and β-pancreatic islet cells. Cell 55, 281-290

Towbin, H., Staehelin, T. and Gordon, J. (1979) Electrophoretic transfer of proteins from polyacrylamide gels to nitrocellulose sheets: Procedure and some applications. Proc. Natl. Acad. Sci. U.S.A. 76, 4350-4354

Toyoda, N., Flanagan, J. E. and Kono, T. (1987) Reassessment of insulin effects on the Vmax and Km values of hexose transport in isolated rat epididymal adipocytes. J. Biol. Chem. 262, 2737-2745

Ullrich, K. J. (1979) Sugar, amino acid, and Na^+ cotransport in the proximal tubule. Annu. Rev. Physiol. 41, 181-195

Van Putten, J. P. M. and Krans, H. M. J. (1985) Glucose as a regulator of insulin-sensitive hexose transport uptake in 3T3 adipocytes. J. Biol. Chem. 260, 7996-8001

Vidaver, G. A. (1966) Inhibition of parallel flux and augmentation of counter flux shown by transport models not involving a mobile carrier. J. Theor. Biol. 10, 301-306

Wadzinski, B. E., Shanahan, M. F., Clark, R. B. and Ruoho, A. E. (1988) Identification of the glucose transporter in mammalian cell membranes with a ^{125}I-forskolin photoaffinity label. Biochem. J. 255, 983-990

Wadzinski, B. E., Shanahan, M. F. and Ruoho, A. E. (1987) Derivatization of the human erythrocyte glucose transporter using a novel forskolin photoaffinity label. J. Biol. Chem. 262, 17683-17689

Wakelam, M. J. O. (1985) The fusion of myoblasts. Biochem. J. 228, 1-12

Walker, P. S., Ramlal, T., Donovan, J. A., Doering, T. P., Sandra, A., Klip, A. and Pessin, J. E. (1989) Insulin and glucose-dependent regulation of the glucose transport system in the rat L6 skeletal muscle cell line. J. Biol. Chem. 264, 6587-6595

Walmsley, A. R. (1988) The dynamics of the glucose transporter. Trends Biochem. Sci. 13, 226-231

Wang, C. (1987) The D-glucose transporter is tissue-specific. Skeletal muscle and adipose tissues have a unique form of glucose transporter. J. Biol. Chem. 262, 15689-15695

Wardzala, L. J., Cushman, S. W. and Salans, L. B. (1978) Mechanism of insulin action on glucose transport in the isolated rat adipose cell. Enhancement of the number of functional transport systems. J. Biol. Chem. 253,8002-8005

Wardzala, L. J. and Jeanrenaud, B. (1981) Potential mechanism of insulin action on glucose transport in the isolated rat diaphragm. Apparent translocation of intracellular transport units to the plasma membrane. J. Biol. Chem. 256, 7090-7093

Wasserman, N., Penn, A., Cleveland, W. and Erlanger, B. F. (1982) Anti-idiotypic route to anti-acetylcholine receptor antibody and experimental myasthenia gravis. Proc. Natl. Acad. Sci. U.S.A. 79, 4810-4814

Weber, T. M. and Eichholz, A. (1985) Characterization of a photosensitive glucose derivative. A photoaffinity reagent for the erythrocyte hexose transporter. Biochim. Biophys. Acta 812, 503-511

Wheeler, T. J. (1988) Translocation of glucose transporters in response to anoxia in heart. J. Biol. Chem. 263, 19447-19454

Wheeler, T. J. and Hinkle, P. C. (1985) The glucose transporter of mammalian cells. Annu. Rev. Physiol. 47, 503-517

Whitesell, R. R. and Abumrad, N. A. (1985) Increased affinity predominates in insulin

stimulation of glucose transport in the adipocyte. J. Biol. Chem. 260, 2894-2899

Widdas, W. F. (1980) The asymmetry of the hexose transport system in the human red cell membrane. Curr. Top. Membr. Transp. 14, 165-223

Wilbrandt, W. (1954) Secretion and transport of nonelectrolytes. Symp. Soc. Exp. Biol. 8, 136-162

Witters, L. A., Vater, C. A. and Lienhard, G. E. (1985) Phosphorylation of the glucose transporter in vitro and in vivo by protein kinase C. Nature 315, 777-778

Wu, J. -S., Kwong, F. Y. P., Jarvis, S. M. and Young, J. D. (1983) Identification of the erythrocyte nucleoside transporter as a band 4.5 polypeptide. Photoaffinity labelling studies using nitrobenzylthioinosine. J. Biol. Chem. 258, 13745-13751

Wu, J. -S. and Lever, J. E. (1987) Monoclonal antibodies that bind the renal Na^+/glucose symport system. 1. Identification. Biochemistry 26, 5783-5790

Yaffe, D. (1968) Retention of differentiation potentialities during prolonged cultivation of myogenic cells. Proc. Natl. Acad. Sci. U.S.A. 61, 477-483

Yamada, K., Tillotson, L. G. and Isselbacher, K. J. (1983) Regulation of hexose carriers in chicken embryo fibroblasts. Effect of glucose starvation and role of protein synthesis. J. Biol. Chem. 258, 9786-9792

Zoccoli, M. A. and Lienhard, G. E. (1977) Monosaccharide transport in protein-depleted vesicles from erythrocyte membranes. J. Biol. Chem. 252, 3131-3135